ESTCP Project 199902 Demo #3:

GPR UXO Classification Results for

Jefferson Proving Ground V

Dr. Chi-Chih Chen

The Ohio State University ElectroScience Laboratory
1320 Kinnear Rd
Columbus, OH43212

Dr. Kevin O'Neill

US Army Corps of Engineers Research and Development Center (ERDC)
Cold Regions Research and Engineering Laboratory (CRREL)
72 Lyme Road
Hanover, NH 03755

Report Documentation Page

Form Approved
OMB No. 0704-0188

1. REPORT DATE	2. REPORT TYPE	3. DATES COVERED
JUL 2005		**00-00-2005 to 00-00-2005**

4. TITLE AND SUBTITLE	5a. CONTRACT NUMBER
GPR UXO Classification Results for Jefferson Proving Ground V. Demo #3	5b. GRANT NUMBER
	5c. PROGRAM ELEMENT NUMBER
6. AUTHOR(S)	5d. PROJECT NUMBER
	5e. TASK NUMBER
	5f. WORK UNIT NUMBER
7. PERFORMING ORGANIZATION NAME(S) AND ADDRESS(ES) **Ohio State University,Electroscience Laboratory,1320 Kinnear Rd,Columbus,OH,43212**	8. PERFORMING ORGANIZATION REPORT NUMBER
9. SPONSORING/MONITORING AGENCY NAME(S) AND ADDRESS(ES)	10. SPONSOR/MONITOR'S ACRONYM(S)
	11. SPONSOR/MONITOR'S REPORT NUMBER(S)

12. DISTRIBUTION/AVAILABILITY STATEMENT
Approved for public release; distribution unlimited

13. SUPPLEMENTARY NOTES

14. ABSTRACT

15. SUBJECT TERMS

16. SECURITY CLASSIFICATION OF:			17. LIMITATION OF ABSTRACT	18. NUMBER OF PAGES	19a. NAME OF RESPONSIBLE PERSON
a. REPORT	b. ABSTRACT	c. THIS PAGE			
unclassified	**unclassified**	**unclassified**	**Same as Report (SAR)**	**140**	

Table of Contents

List of Figures

List of Tables

`

Chapter 1 Introduction

A broadband, full-polarimetric ground penetrating radar (GPR) operating between 10 MHz to 410 MHz was used at the Jefferson Proving Ground (JPG) UXO site during the June 26 ~ July 2 period. This was the third field demonstration in ESTCP Project 199902, the prior two being at Tyndall AFB, Florida and the Blossom Point (BP) Site, Maryland in 1999 and 2000, respectively [1][2]. The reader is referred to reports on those demos for many details of the technology and approach, beyond what is given here. The objective of these demos is to perform target classification such that UXO-like and non-UXO items can be distinguished: Radar signatures, such as late time natural resonance and polarization sensitivity, are used to separate false alarm objects from UXO-like items, i.e. those that have elongated bodies with length-to-diameter ratios greater than three [1]. Additional features such as length, depth and orientation were also extracted from the data. In some instances, different UXO types could be further classified based on their lengths estimated from the late time resonance. When this technology and approach were applied at the earlier demo sites, important information was obtained from the comparison with the ground truth data provided after the blind test. This resulted in system and processing improvements applied at the JPG site.

The soil type at the Tyndall site is the most accommodating from the point of view of radar, consisting of dry sand. Measurement passes were made by dragging the antenna in linear transects across the presumed target location. However, in this first test such multi-position scans were made only to find the more or less best position from which to get a good single "look." Failure to include spatial (as well as frequency) patterns of signal response resulted in false alarms caused by shallow, non-UXO objects that had position offset and were coupled to one of the four antenna arms more strongly. Also, UXO's that had large inclination angles were more difficult to classify, particularly when the chosen GPR observation point was directly over the target. From that vantage point, a vertical elongated target presents its smallest GPR cross section.

In subsequent demos, the multi-position information in each scan was used to introduce spatial variation of signals into the analysis, to overcome the offset and inclination problems. The BP results showed excellent improvement, relative to the Tyndall results, in correctly classifying the UXO items including a large number of vertically oriented ones. The false alarm rate was also significantly reduced. The survey technique involved multiple passes over each target spot, with some representative positional error purposely introduced by site crew (without communicating this information to the demo crew). The

data were collected along straight lines of approximately 3 meters (or 120 inches). This new approach provided additional position-dependent scattering features in the early-time responses as well as the spatial distributions of the late-time UXO signatures. The combination of these additional features improves the classification of UXO's with large inclination angles because of the additional oblique observation angle with respect to the target. The analysis is able to focus on observations in which the best side views are provided, i.e. transverse to the target's long axis. False alarms caused by offset shallow objects can now be discriminated using the additional positional scattering characteristics. The orientation of the first pass was randomly selected. Overnight processing then estimated the orientations of the items based on any apparent direction of elongation, i.e. on the orientation of any dominant polarization in late time. Two additional passes were performed in the directions parallel and orthogonal to the estimated orientation. For items that failed to show elongation in any predominant direction, only one additional pass transverse to the first pass was performed. Such a process can be made more efficient by utilizing magnetic sensors to estimate the target orientation for the first pass. That approach was adopted during the JPG test and will be discussed in more detail below.

Compared to the Tyndall site's sand soil and BP's sandy clay, JPG contains fine grained, possibly clayey soil, which is much more challenging to GPR. Such soil retains water, tends to absorb more electromagnetic energy, and is more inhomogeneous. At greater depths (but still within the range of target burial depths), natural layering causes the inhomogeneity. At shallower points, on the order of most target burial depths, the inhomogeneity was caused by external disturbance due to emplacement of UXO or earlier use of the site. After rain, the poor drainage properties of the soil and site worsen the inhomogeneous conditions because of patterned water flow and accumulation. Moisture also tends to increase the absorption of the electromagnetic energy. Appendix C includes the electrical properties of the JPG soils in the test areas measured during the demo week. These values were obtained using a soil probe developed at OSU. One can clearly see significant variation in both dielectric constant and conductivity as a function of depth and location. Both the BP site and JPG sites were quite wet at the time of our demos, leading us to expect high soil conductivity and signal losses in both cases. However, the electrical conductivity at JPG was much higher than those obtained at BP, indicating a soil type that absorbs electromagnetic energy more strongly. Specifically, the dielectric constant measured at the JPG test sites during the period of GPR measurement ranged from 20 to 28, with electrical conductivity between about 0.01to 0.05 (S/m) for depths up to 30 inches. In both cases, these are very high values. As described below, we use a processing system designed to take the specific pattern of dielectric constant profile into account. Overall, one gains some notion of the possible error introduced by dielectric constant uncertainty by noting that target depth and length estimations are directly proportional to the

square root of the dielectric constant. That quantity varies here about ±8% about the average of its extreme values, suggesting a maximum error envelope.

During the first two days, the antenna feed (filled with material of dielectric constant 5) was unstable. It was probably due to mechanical failure from stresses during previous measurements. An effort was made to correct the stability problem, without success. The structure was replaced with a new feed filled with dielectric constant of 9 on the third day. The new feed produced slightly higher signal clutter compared to the old one; at the same time, its dielectric fill provided a better match with the ambient soil. This clutter was reduced by calibrating against a long conducting wire laid on the surface. The new feed began to collect data from June 28 to July 2 (five days). Each day, the measurement started at approximately 7:30AM and ended between 5~7 PM, with no stops except for a flat tire on June 28. 112 targets were measured, including 12 known targets, at a rate of approximately 7 passes/hour. Each linear pass contained 41 positions at 3-inch increments.

Chapter 2 below provides a brief discussion of the radar hardware, measurement approach and processing/classification algorithms. Chapter 3 shows the UXO classification results of the blind targets based on GPR signatures. Prioritized dig lists were submitted to ESTCP prior to the release of ground truth. The first "dig list" (prioritized target classification list) utilized GPR signal features only. A revised dig list was subsequently produced by also using information on the target depths estimated from the EMI/MAG sensors, as provided by the site prep and management personnel after our first dig list had been provided. The depth information was utilized as a reference in the selection of late-time responses. This approach was proposed based on lessons learned from the BP demo: particularly for soil conditions that cause substantial signal attenuation, some constraint on probable target depth guides the radar analysis away from specious but stronger shallow returns from ground disturbance/clutter. A 3rd dig list was generated using more accurate depth information released after the submission to ESTCP of the 2nd dig list. Finally, the GPR classification results were compared with the whole ground truth data released after the submission of the 3rd dig list. The classification results clearly demonstrated a good example of improving measurement efficiency and classification performance by combining the features (orientation and depth) estimated from EMI/MAG sensors and those from GPR. The features (length, depth and azimuth orientation) for items classified as UXO-like were found to be reasonably accurate. Most false alarms were from small, shallow items whose co-polarization responses were contaminated by surface clutter that may or may not have linear characteristic. Missed UXO items were found to be either small and shallow or deep with large inclination. The former was improved by selecting a high frequency filter center at 250 MHz. The latter was due to limitations caused by the JPG soil conditions. From the ground

truth, it was found that 9 out of the 42 fragments have length to diameter (L/D) ratios greater or equal to three and 14 out of 42 fragments have L/D ratios between two to three. The majority of these UXO-like fragments are shrapnel that look like curved plates. Our current GPR signal feature processing would classify this kind of clutter as UXO-like. Possible remedies of this limitation will be discussed in Chapter 4. Note that all the GPR data examples presented in this document were plotted with background removal and application of amplification in the later, weaker portions of the signal (gain slope applied). The gain slope is commonly used in displaying GPR data to compensate for signal attenuation at greater depth and to provide a better viewing dynamic range. Such a gain slope is applied only for data display and does not affect the target features. All signal components are plotted using the same scale in the same figure.

Chapter 2 Technology Description

2.1 System Description

The radar system consists of broadband fully-polarimetric horn-fed "bowtie" (HFB) antenna, developed by OSU, towed behind a vehicle as shown in Figure 1. The antenna consists of two sets of perpendicular elements, capable of measuring amplitude and phase of co-polarized ("co-pol") reflections aligned with the pass direction (S_{11}), orthogonal to the pass direction (S_{22}), and the cross polarized return (S_{12} which, by reciprocity, equals S_{21}). A tractor (see Figure 2), used as the towing vehicle, also housed a laptop computer for measurement control. The antenna can be raised during the transportation and lowered to the ground during measurement. Stepped-frequency data were collected along a 120-inch line centered at a “hot spot” (designated target locale) at 3-inch increments manually triggered by the driver using the markers on the front wheel as shown in Figure 3. The frequency range was from 10 MHz to 410 MHz at 2 MHz increments. Notice that data up to 810 MHz were typically collected for soils friendlier to radar penetration. The main radar unit was a commercial RF vector network analyzer (HP8712ET) and a transfer switch for collecting cross-pol and co-pol data. Radar control and data collection were done from a laptop computer via specially developed software. Both frequency-domain and time-domain data were displayed in near real time so that the operator could monitor the status of the operation. Although on-site processing could be performed immediately after each pass, the actual processing was performed overnight to maximize the data collection rate. The radar unit and the antenna were connected via 40-foot RF cables. The length of the cable was increased from the 20 feet used previously in order to delay the multiple reflections between cable terminals beyond 120 ns, thereby separating them from signal content of interest. The cable coils are also shown in Figure 4. Such a long delay should be sufficient for most UXO classification applications.

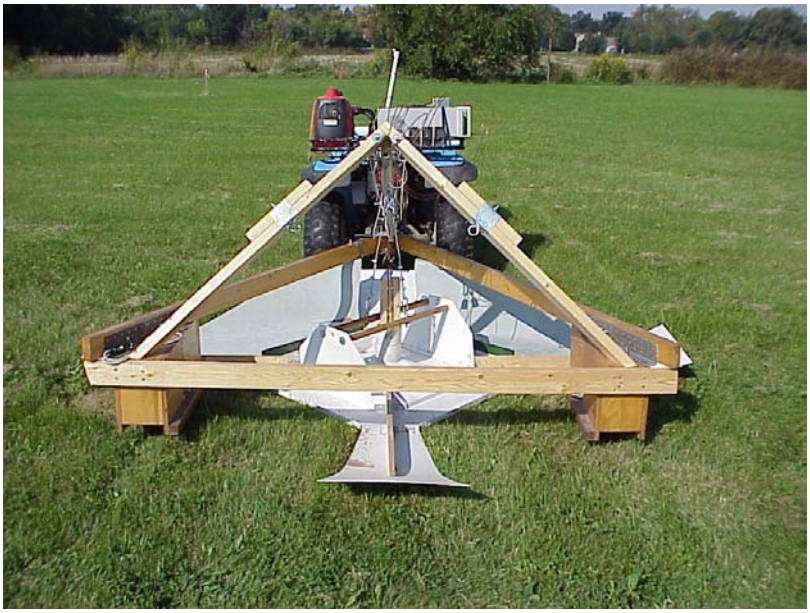

Figure 1 Rear view of the OSU/ESL UWB fully-polarimetric GPR system.

Figure 2 New towing vehicle for the OSU/ESL GPR.

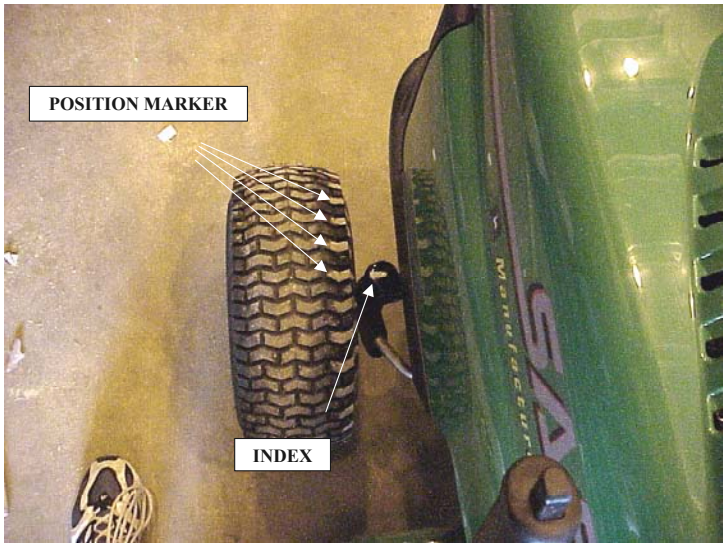

Figure 3 Position markers on the front wheel.

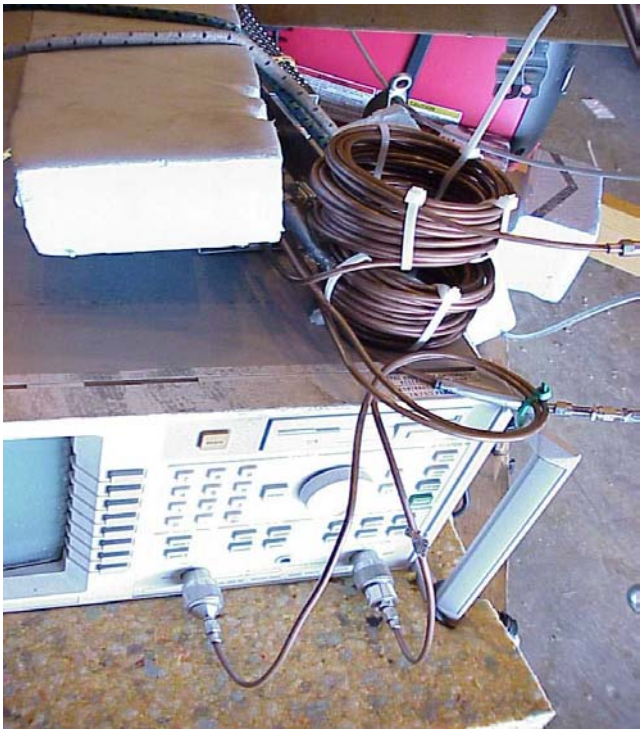

Figure 4 Cable extension.

2.2 Measurement Approach

"Hot spot" locations for each measurement cell were provided by the site prep and management team. That is, based on errors typical of data processing from MAG/EMI data, that team provided flag

locations offset from documented target locations, simulating positional uncertainties such as our GPR team might encounter at a real site. While the position offsets can now be documented from the ground truth, including flag locations, we have no further insight into the method used by the site crew for generating the offsets. For each target (flag) location, up to four passes were made in different orientations. Initially, a conventional Schonstedt metal detector was used to manually survey the target location, by a demo team member preceding the GPR rig. Based on simple guidance (as in the directions accompanying the instrument) the Schonstedt operator simply swept the instrument around the flag location in an attempt to perceive characteristic responses indicative of a dipole pattern. Such a pattern would indicate the approximate azimuthal orientation of an elongated object. If such an orientation was reasonably clear, then the initial radar pass was then oriented in that direction. For targets that did not exhibit unambiguous dipole behavior, an arbitrary orientation was chosen for the initial pass. The radar data collected from the first pass was processed both overnight and on site to determine the approximate orientation of any target that showed orientability in its signal features. If the orientation estimated from radar data was close to what was found from the Schonstedt, the second and third passes were then oriented 90^o and 45^o with respect to the pass-one direction. If the estimated orientation for the radar data was significantly different from the metal-detector orientation, the pass-2, pass-3 and pass-4 orientations were chosen to be parallel, 90^o and 45^o , respectively, with respect to the orientation indicated by the GPR data. In the very least, at minimum cost and effort the Schonstedt measurements served as a "reality check" on the flag locations and a means for detecting unacknowledged clutter.

Notice that the 45^o orientation is an additional pass compared to the BP Demo. This additional orientation would give strongest cross-polarization S_{21} response from a UXO-like target. This property, in conjunction with the fact that S_{21} channel has much lower clutter level, enables one to obtain a better signal to clutter ratio (SCR), in some cases allowing more accurate resonant frequency determination. This is very important for selecting a proper adaptive filter during the feature extraction procedure. If the GPR data collected from pass-1 showed position offset from the flagged center, then the pass-2 center was offset accordingly and the pass oriented transverse to the pass-1 orientation. The target orientation was then re-estimated from the pass-2 data. In such a case, pass-3 and pass-4 data were taken at 90^o and 45^o with respect to the new orientation. A field log included in Appendix D reflects these activities. The reasoning for this approach will be discussed in Chapter 4.

Figure 5 to Figure 7 show all the passes conducted during the JPG demo. Note that the offset of each pass is not shown. That information can be found in Appendix D. Also, much in the design of our

measurement approach is intended to orient the passes parallel and perpendicular to any dominant target directions. Having obtained these best possible renderings of the target response in its principal directions, we can then synthesize the best possible response for an arbitrary incident polarization. Figure 8 plots a histogram of the difference between the magnetic-dipole (Schonstedt) orientation and the principle target orientation inferred from the GPR data, for the UXO-like items. Note that 28 out of 72 have the same orientations and an additional 13 out 72 show about 90^{o} difference. Since both parallel and transverse passes were conducted for each target, this means that the orientations of 41 out 72 UXO-like items predicted from the Schonstedt (magnetic dipole inference) are either parallel or perpendicular to the orientations chosen from the GPR information. This certainly significantly reduced the number of passes required compared to a randomly picked initial pass orientation. The spreading in the histogram is probably due to the error in the orientation estimation associated with signal strength and inclination angle, along with the rather vague patterns often obtained with the Schonstedt. Magnetic-dipole orientation estimated from a more sophisticated MAG/EMI mapping system should be more accurate and efficient then the current waving-by-hand approach.

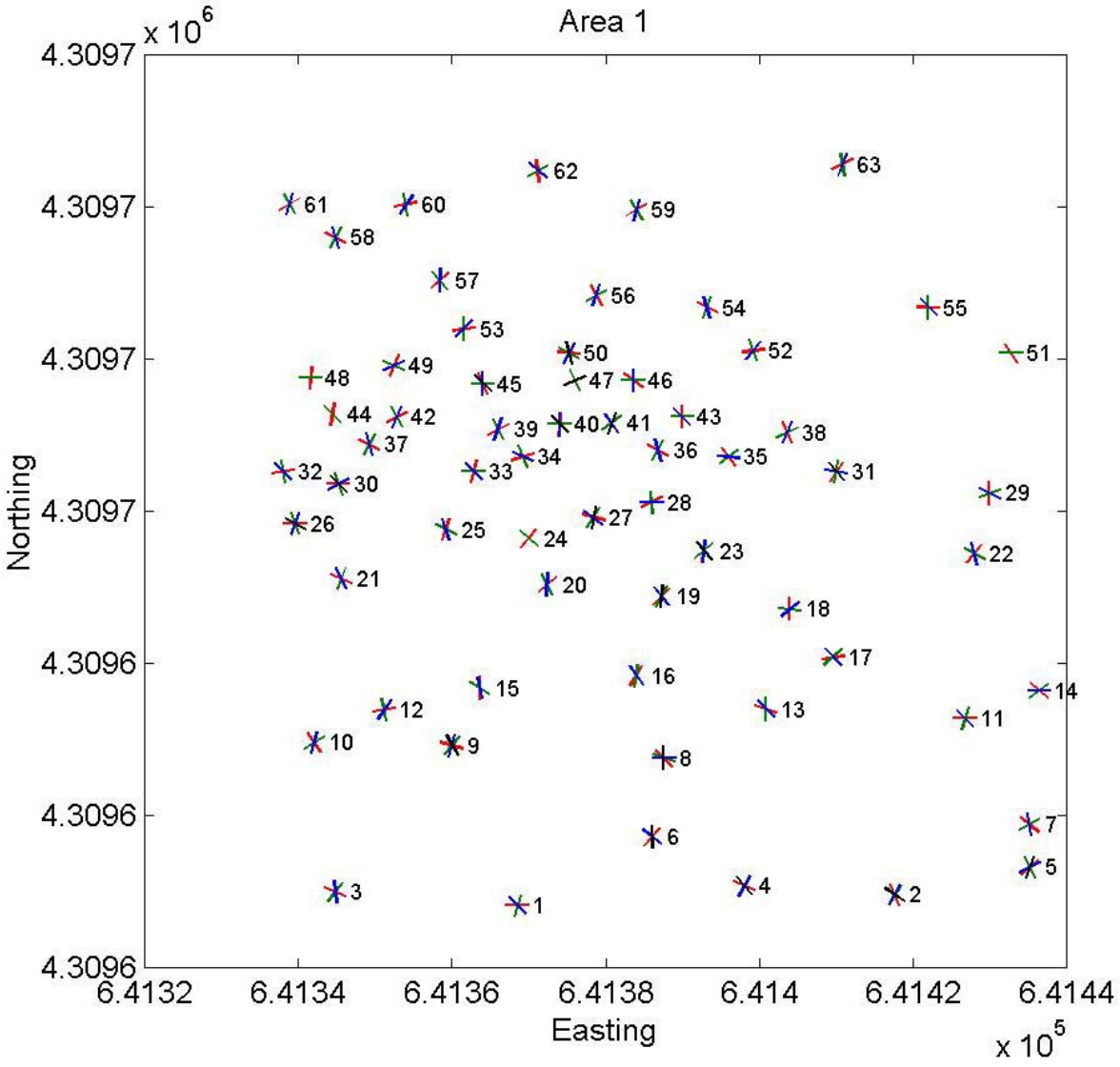

Figure 5 GPR pass orientations for targets in Area 1.

(Red - Pass1; Green- Pass 2; Blue- Pass 3; Black- Pass 4)

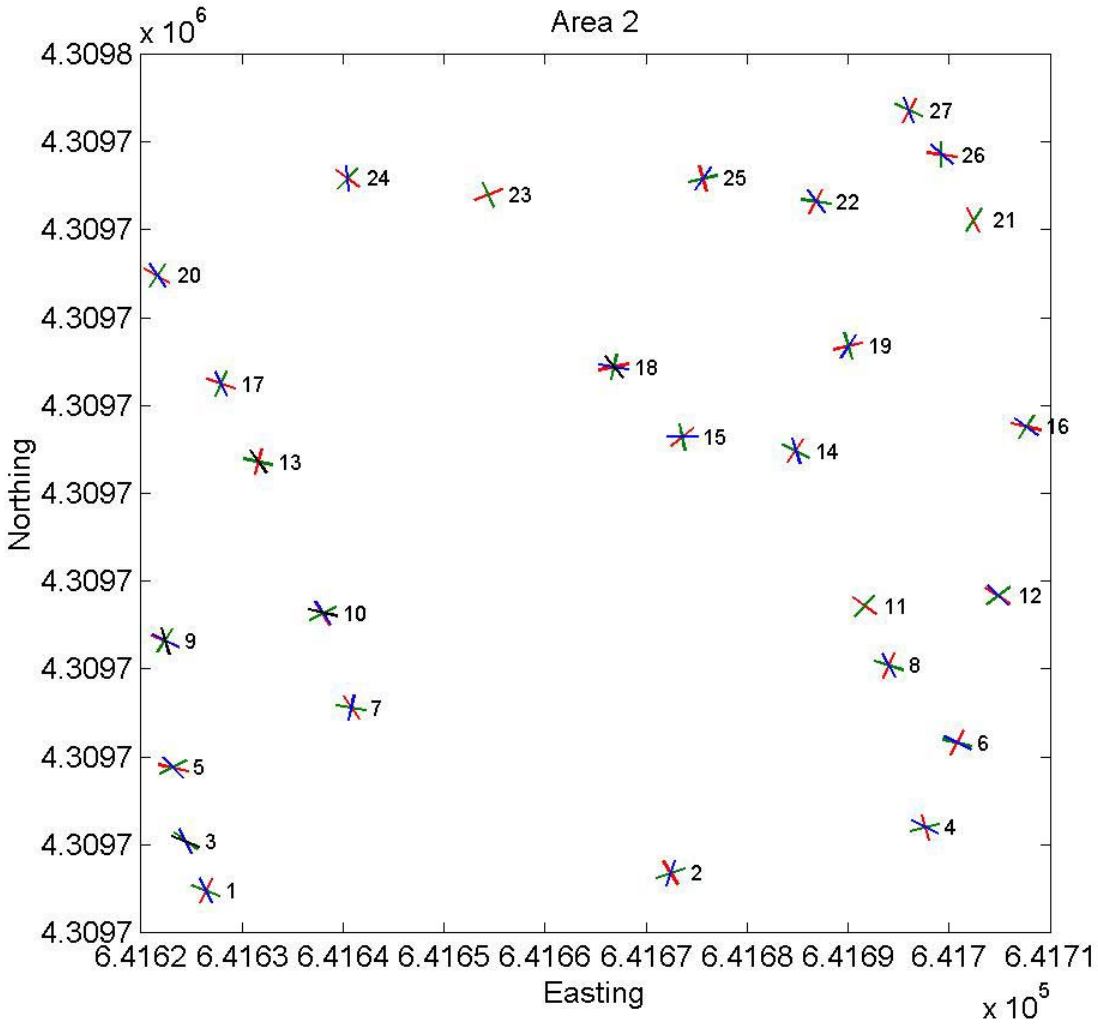

Figure 6 GPR pass orientations for targets in Area 2.

(Red - Pass1; Green- Pass 2; Blue- Pass 3; Black- Pass 4)

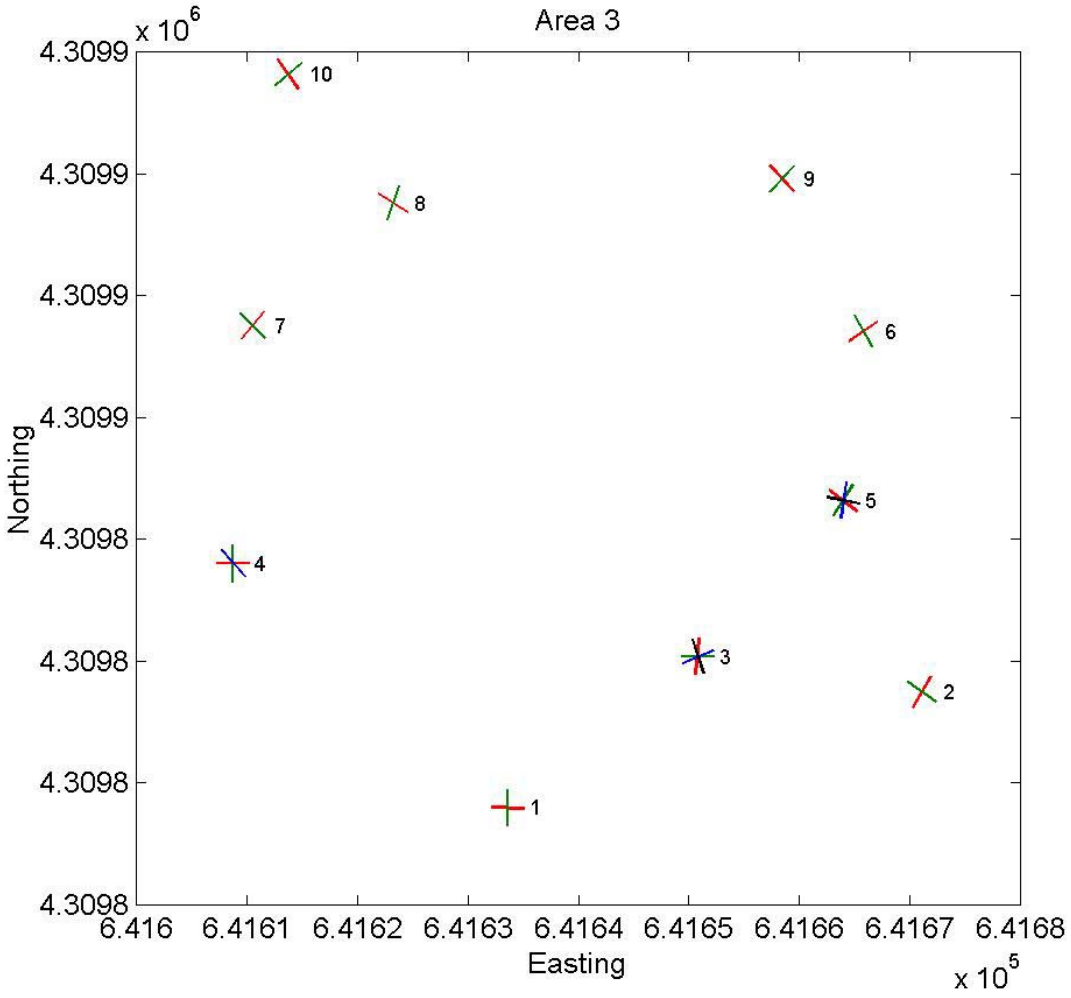

Figure 7 GPR pass orientations for targets in Area 3.

(Red - Pass1; Green- Pass 2; Blue- Pass 3; Black- Pass 4)

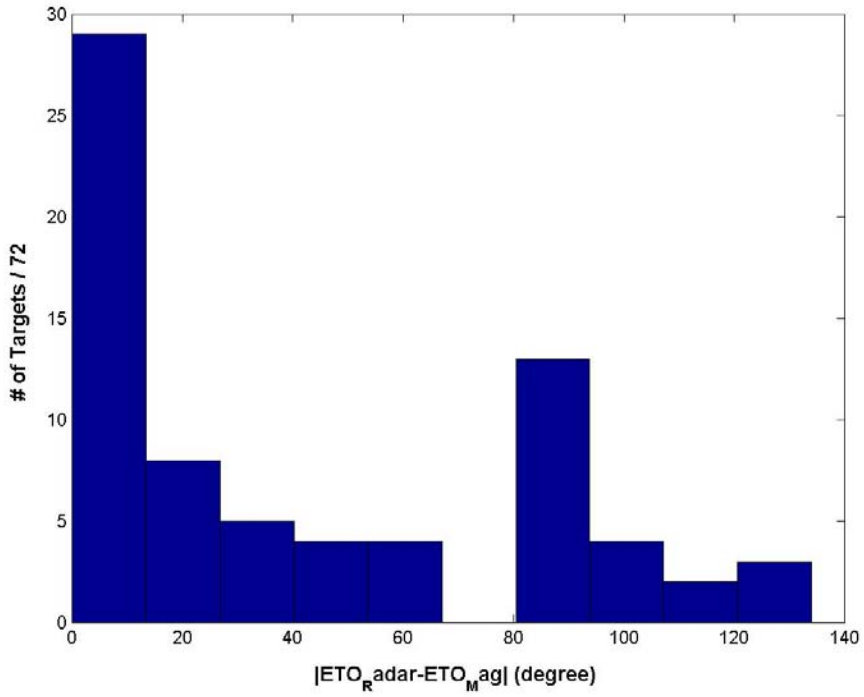

Figure 8 Histogram of the target orientation difference between that estimated from GPR and from Schonstedt metal detector for UXO-like items, as determined without reference to depths estimated from EMI data.

2.3 Antenna Calibration

The system calibration was performed before the input ports of the antenna using some standard cable loads such as short, matched load and thru. The transfer function of the antenna was also calibrated by placing the antenna on top of a long conducting wire laid on the ground surface. The 100 ft long wire was oriented at 45^{o} with respect to the antenna arms, extending far beyond them on each side, so that S_{11}, S_{21} and S_{22} should have similar responses. The background data without the presence of the wire was also taken and removed before the calibration. Because the wire was so long and its ends extended very far beyond the antenna, its resonant frequency (due to finite length) was not stimulated. In general, theory shows that scattering from such a thin, long object will have very little frequency dependence over our frequency band [11]. Thus, any frequency dependent behavior is caused primarily by the antenna's transfer function. The system transfer functions for S_{11}, S_{21} and S_{22} are similar because the sets of antenna arms 1 and 2 have virtually identical characteristics. Such a calibration procedure also includes the effect

of soil near the surface and must be repeated when soil condition change significantly. During the demo, calibration was performed more or less daily, or after any obvious change in conditions (rain). Figure 9 shows the magnitudes of the measured (normalized) transfer functions in Area 3 when the ground surface was dry and when it was soaking wet, respectively. Notice the 30 MHz resonant peak associated with antenna ringing. It was already known that such an undesirable ringing was more pronounced in this new feed, loaded with dielectric constant of 9, compared to the previous feed used during the Tyndall and BP demos. That observation prompted this additional calibration procedure, allowing us to divide the measured data by the transfer function (complex values), frequency by frequency, removing any system bias in the data. Figure 10 and Figure 11 compare the time-domain data with and without applying the antenna calibration for the known target designated as 2-126, a 81mm mortar buried at the depth of 0.35m with a 45^{o} inclination. The target responses are close to the center of the scan at about –25ns position. One can see that the uncalibrated data show less scattering detail due to the low frequency (30MHz) ringing that was convolved with the target responses. The subsurface layers are also more visible in the calibrated data.

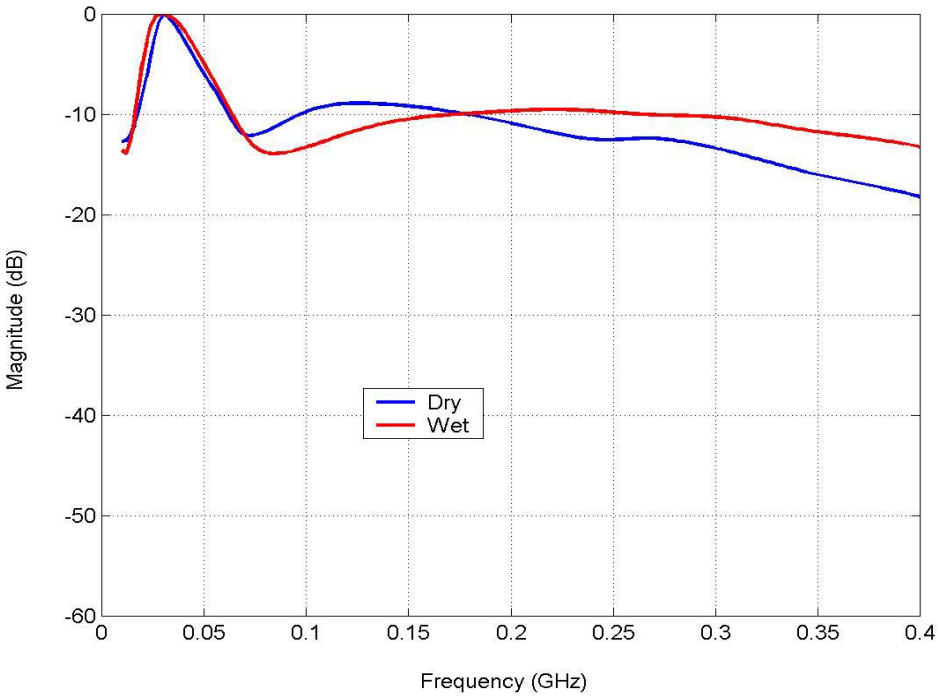

Figure 9 Antenna transfer function for dry and wet soil in Area 3.

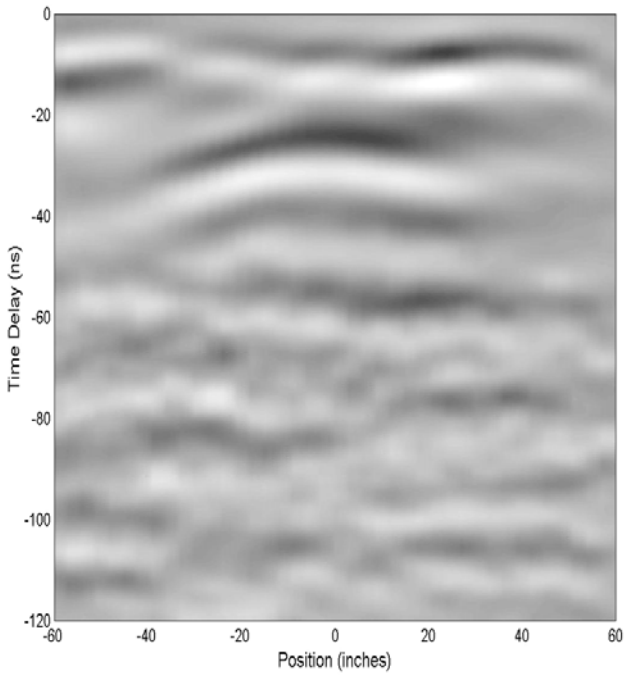

Figure 10 Measured Data for Known Target 2-126 with Antenna Calibration.

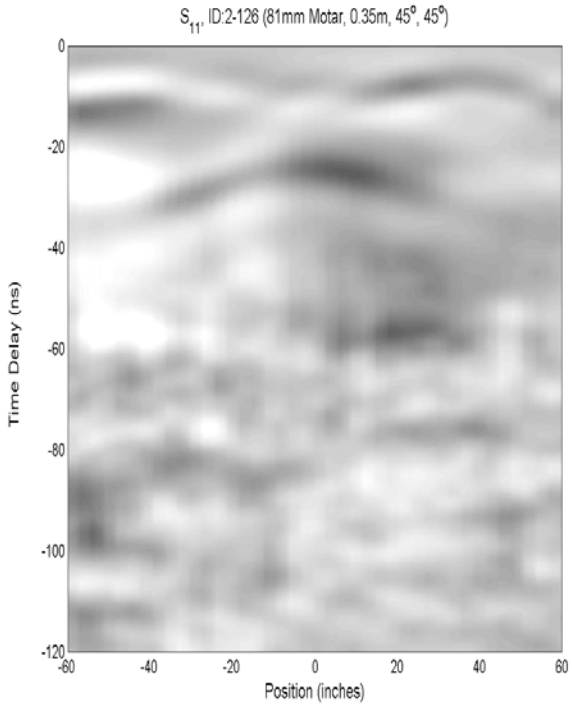

Figure 11 Measured Data for Known Target 2-126 without Antenna Calibration.

2.4 Feature Extraction

2.4.1 Feature Extraction Block Diagram

The procedure for extracting target features is shown in

Figure 12. Detailed algorithms for each block can be found in various publications [3][4][5]. The resultant features include Estimated Linearity Factor (ELF), Estimated Target Orientation (ETO), Complex Natural Resonance (CNR), Angular Density of late time response (DEN), and target depth (DEP). While not repeating here the explanations of these parameters, as they have been presented in above-cited documents, we note generally that angular density measures the extent to which the apparent dominant orientation (ETO) is clustered about any particular direction. Estimated linearity in the late-time signal is a measure of how dominant the signal is in that direction. Both of these are employed to suggest when a target is orientable, i.e. elongated. CNR provides a clue to target length, given an estimate of the soil dielectric constant. Based also on the dielectric constant, the estimated target depth is obtained simply from the delay of the target response in time. As this signal property is not a property of the target

itself, its determination is not indicated explicitly in the flow chart. Many improvements in the feature extraction system and its implementation have been presented in the previous report [5] and will not be repeated here. A new improvement for more accurate depth and length estimations is discussed below. This new algorithm was developed to deal with the JPG soil properties, which vary significantly with depth.

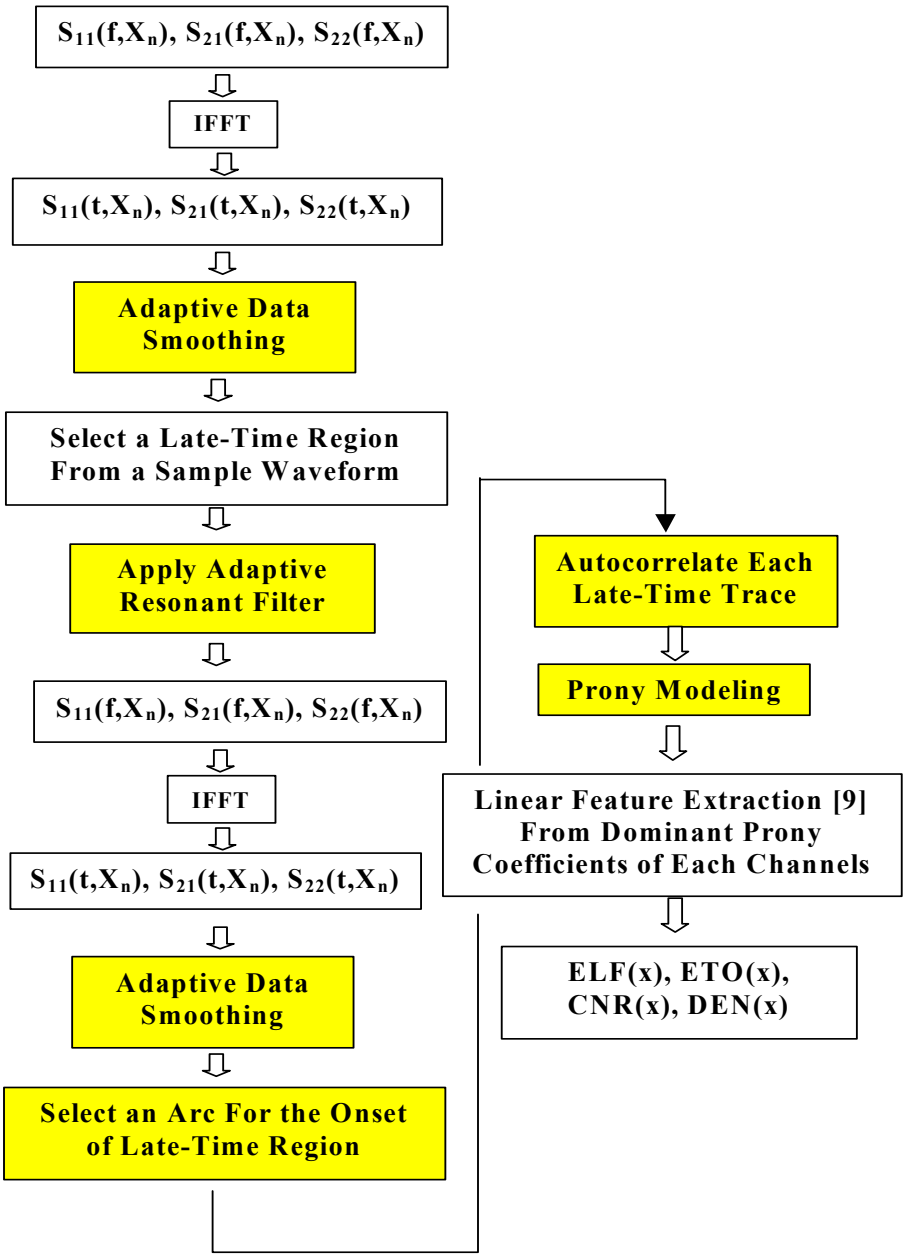

Figure 12 Block diagram of the OSU/ESL UXO feature extraction procedures.

2.4.2 Depth and Length Estimation Improvement Using Soil Property Profile

Prior to the JPG demo, the depth and length of a target were estimated from the time delay and resonant frequency, respectively, based on an average relative dielectric constant estimated from the

probed soil properties, as function of depth, up to approximately 30 inches. That approach was reasonable for relatively homogeneous soil such as that at the Tyndall and BP sites. For JPG soil the dielectric constant varies significantly with depth. A more accurate approach developed to account for such a variation should provide better estimation of the depth and length of a target. First, the soil electrical properties determined using the probe for the site and date of the target were selected automatically by the processing program. Based on the variation of the dielectric constant and conductivity as a function of depth (Figure 13 and Figure 14), the relationship between the delay time and the depth was derived, as shown in Figure 15. The delay time was estimated from the travel time required for electromagnetic waves to propagate through multiple layers with different velocities in different layers. All the soil probe data collected during the JPG demo can be found in Appendix C. The delay time for a given target was determined based on the position of its peak response in time. While inevitable, this timing method introduces a certain ambiguity, in that a geometrically complex, steeply inclined object covers a range of depths and the peak response may be associated with its ends or points in between. Once the delay time has been estimated, target depth is then calculated from Figure 15 using interpolation and extrapolation. The corresponding the dielectric constant and conductivity at that estimated depth were then obtained from Figure 13 and Figure 14. If the estimated depth was greater than the maximum probing depth, the soil properties at the maximum depth were used. This new approach should improve the accuracy of depth and length estimation when soil properties vary significantly with depth. Of course, this is still an approximation since soil properties can vary from location to location and from time to time within the site. The data as used here were based on only a few probe measurements for each area within the site, on each day. In the future, the number of probe measurements will be driven by an estimation of the variability of the soil at the site, based on the initial few measurements.

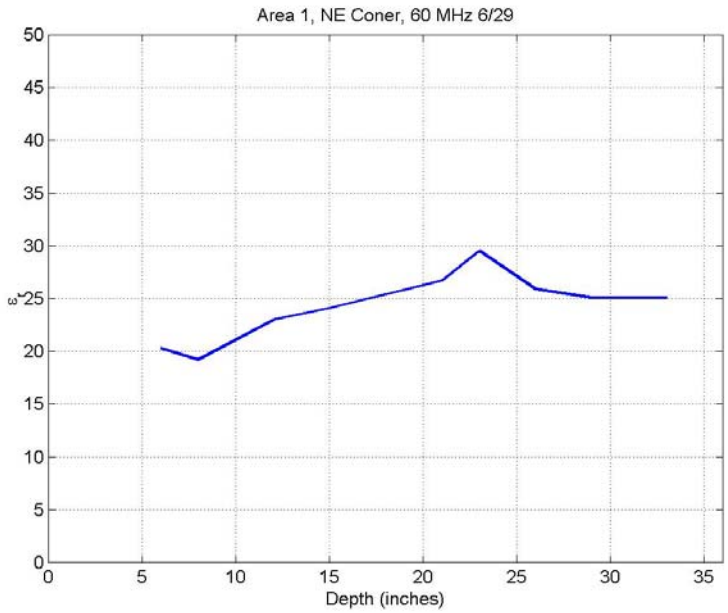

Figure 13 Measured dielectric constant as a function of depth in Area 1 of JPG V on 6/29/01.

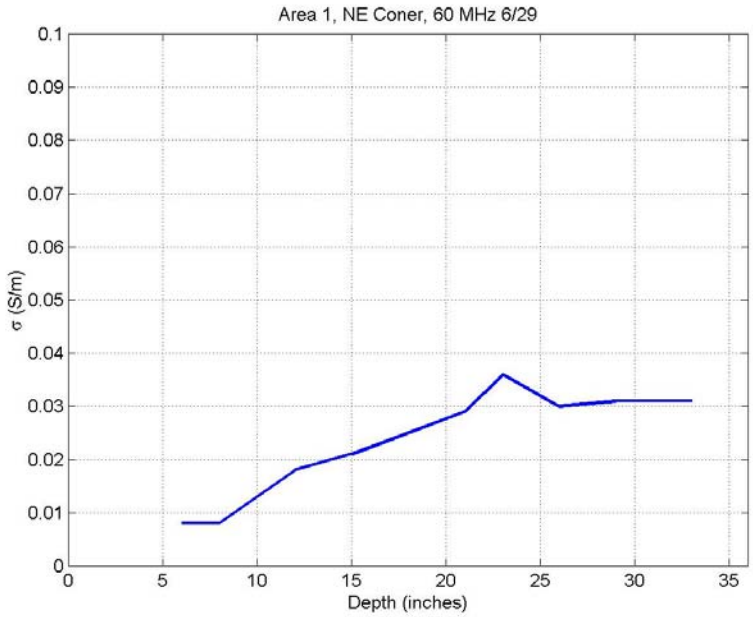

Figure 14 Measured conductivity as a function of depth in Area 1 of JPG V on 6/29/01.

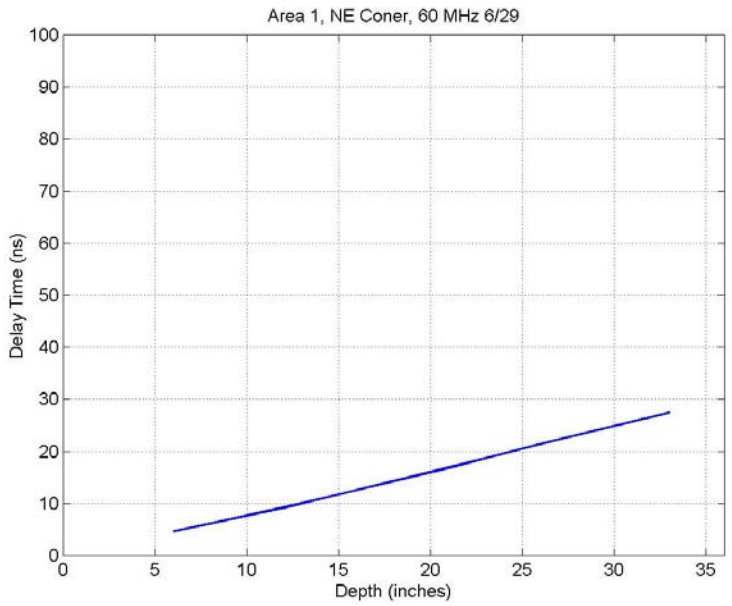

Figure 15 Predicted delay time as a function of depth in Area 1 of JPG V on 6/29/01.

2.5 UXO-Like/Non-UXO Discrimination Criteria

Figure 16 shows the current flow chart for the UXO classification criteria. This flow chart was established and improved using signatures observed for some canonical UXO and non-UXO objects encountered during the previous two demos. The UXO classification procedure starts with inspection of the spatial distributions of the extracted ELF, that is, ELF is plotted as a function of antenna position along the scans. As explained elsewhere, analysis of the pattern suggests how linear or orientable the target is. The overall classification flow chart appears in Figure 16, followed by an explanation with letters corresponding to the different decision steps indicated symbolically on the figure. One can refer to [5] for more examples. "Scattering pattern" or "time-position plots" refers to plots such as Figure 10 (space/antenna position on horizontal axis, signal time on vertical axis), in which the target produces a curve (hyperbola) with peak at the target location.

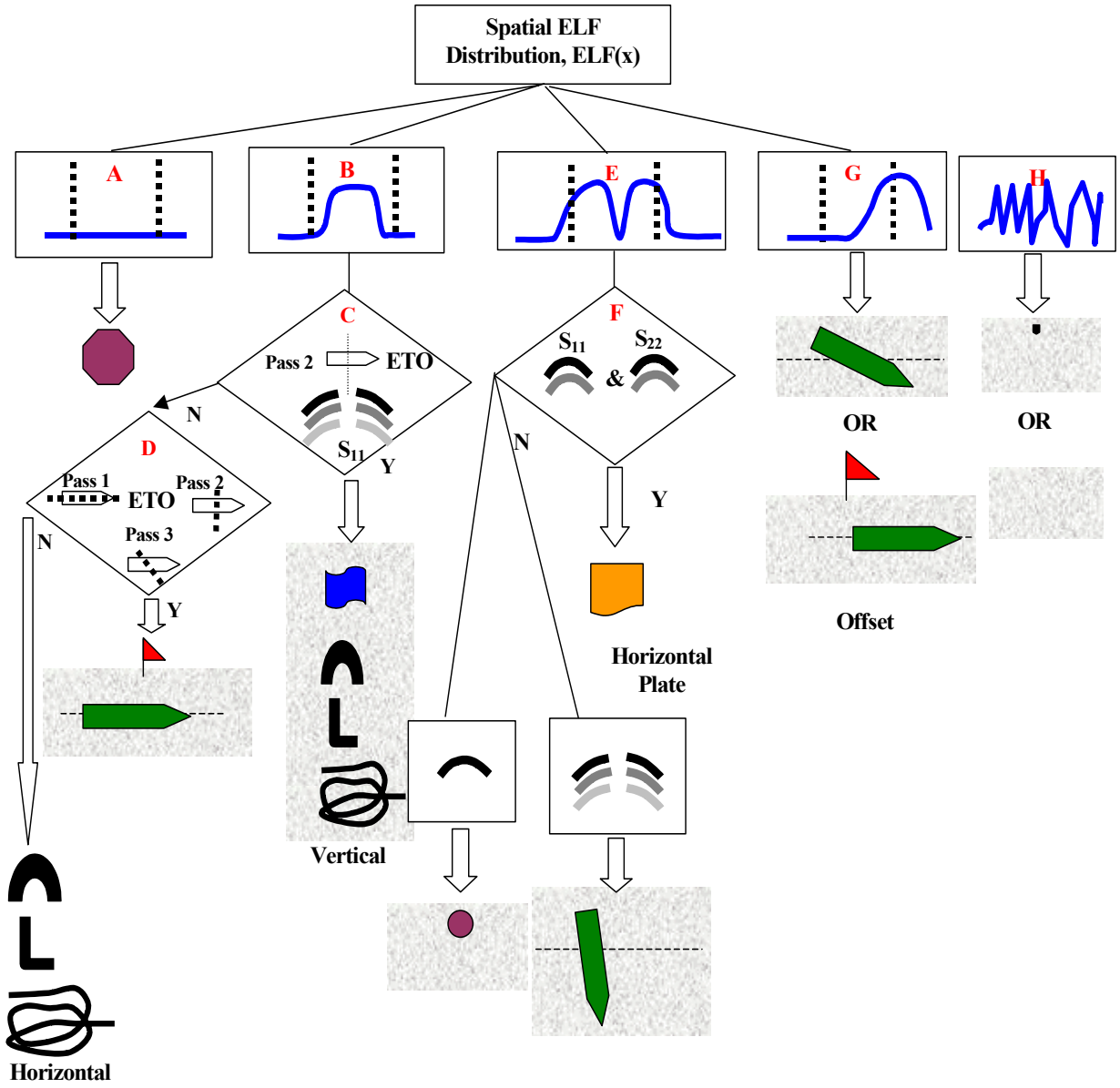

Figure 16 Improved UXO classification flow chart.

A. If the ELF is low over most of the scan region (10 ft transect), it indicates that the target does not have an elongated shape and thus is classified as a non-UXO object.

B. If the ELF values near the target center are high (close to one), the object could be an UXO-like object, vertical plate, or vertically oriented curved object such as a horseshoe. The next thing to check is the scattering pattern, i.e. time-position plots associated with the transverse pass.

C. In the transverse pass, a horizontal UXO would have very weak response in the S_{11} channel. If strong responses are observed in the S_{11} channel at offset positions (F), it would not be an UXO. It could be large vertical plate, vertical horseshoe, vertical bent wire, …, etc.

D. Combine information from all passes: If the object shows good linearity and resonance features in all passes but the ETO or resonant frequency seem to vary in different passes, it is probably from a thin curved shape.

E. If two high-ELF regions next to the target center are observed (double peaks), it could be a vertical UXO or shallow clutter that shows high ELF values when it is very close to either of the antenna arms. In either situation, ETO will indicate an orientation aligned with the scan directions in all passes.

F. Under scenario E, if the scattering pattern in the time-position plot shows strong responses in both S11 and S22 channels at the target center, it is likely a horizontal plate, not an elongated object. If the scattering pattern over space shows response only in S11 channel and is weak at the center (hyperbola peak), the item could be a vertical UXO or a piece small clutter. In the latter case, if significant resonance is present it is considered UXO-like.

G. If the region of high ELF values is offset to one side of target center (single peak), it is probably an inclined UXO or a horizontal UXO with position offset. In these cases, the ETO near the high ELF region should remain unchanged regardless of the scan direction.

H. If ELF values varies drastically between 0 and 1 in a sort of random way, its is either not a target (cluttered/empty cell) or the signal to clutter ratio value is very poor.

The classification criteria discussed above were found to be quite effective in discriminating UXO-like targets for known targets. Each of these criteria may be developed into automatic classification procedures using pattern recognition, image correlation or neural network training techniques. However, at this moment, Figure 16 is implemented by training an operator using a training set and then asking him or her to make classification decisions by following the flow chart. While subjective judgments are required (what is "high" or "low" linearity, etc), these are included in the results by indicating high, low, or medium confidence in the classification.

Chapter 3 Classification Results

3.1 Classification Results for Known Targets

Table 1 shows the processed results including orientation, length, and depth for known targets measured at JPG. The 1st column indicates the item number designated by the site preparation team. The UXO-like items are indicated by the number "1" in the 3rd column. The Confidence Level associated with each classification is listed in the 4th column (H = high, M = medium, L = low, 0 = uninterpretable). This level is currently entered subjectively by the operator based on the signal level and the clarity of the features according to the criteria shown in Figure 16. The estimated (azimuthal) orientation is listed in the 5th column with an ambiguity of +/-180^o while the 6th column lists the target orientation from the ground truth. Column 7 lists the target inclination, from the ground truth; this parameter is not estimated in the processing but is valuable for understanding success/failure in the discrimination. Column 8 shows the estimated target length followed by the ground truth target length in column 9. Columns 10 and 11 show the estimated target depth DEP from the radar data and the ground truth depth, respectively. Three estimated linearity factors (ELF) are listed in 12th, 13th 14th columns. The early-time ELF is a newly introduced parameter based on the magnitude of the target response in the early-time region.

Except for four items, most of the known UXO's showed clear UXO-like features based on our classification rules. Although 1-130 and 2-154 showed UXO-like features, the low signal-to-clutter ratio (SCR) resulted in a certain degree of uncertainty. That is why they both are rated as low confidence. The weak target response from 1-130 resulted in low SCR. The weak target response and high surface clutter level resulted in low SCR for 2-154. The two unidentified cases, 3-106 and 2-142, consist of a modest sized target at about half a meter depth and a larger, more inclined target at almost a meter depth, respectively. Both of these cases produced low magnitude signals, especially under the JPG conditions. Note that a smaller target than 3-106 that is equally inclined but is only at half the depth (3-98) is successfully detected and discriminated.

Table 1 GPR Classification Results on Known UXO's.

Item #	Description	GPR ID	Conf.	ETO (°)	True Azim. (°)	True Incl. (°)	ETL (m)	T.rue Length (m)	DEP (m)	T. Depth (m)	Late-Time ELF(t)	Late-Time ELF(f)	Early-Time ELF
1-86	4.2 inch Mortar	1	M	27	120	45	0.34	0.52	0.19	0.20	0.87	0.94	0.62
1-130	5 inch Projectile	1	L	47	180	30	0.38	0.63	0.78	0.70	0.96	0.89	0.98
1-151	76mm Projectile	1	M	163	150	45	0.45	0.50	0.56	0.25	0.88	0.80	0.62
2-118	60mm Mortar	1	H	0	0	45	0.29	0.18	0.40	0.35	0.89	0.96	0.53
2-126	81mm Mortar	1	H	49	45	45	0.43	0.27	0.30	0.35	0.89	0.92	0.51
2-142	152mm Projectile	0	0		300	45		0.48		0.91			
2-154	57mm Projectile	1	L	253	180	45	0.34	0.12	0.10	0.20	0.76	0.68	0.33
2-161	155mm Projectile	1	H	266	270	30	0.35	0.60	0.68	0.75	0.90	0.89	0.69
3-70	81mm Mortar	1	H	350	0	0	0.33	0.28	0.44	0.25	0.76	0.88	0.97
3-74	60mm Mortar	1	H	219	225	45	0.26	0.18	0.31	0.30	0.85	0.90	0.66
3-98	105mm Projectile	1	H	6	0	-45	0.35	0.37	0.71	0.50	0.88	0.89	0.89
3-106	2.75" Rocket	0	0		120	30		0.41		0.50			

Note: The estimated linearity function (ELF) is a measure of scattering strengths in polarization orientations producing maximum and minimum magnitudes. In general, these correspond to axial or "parallel" (max) and transverse or "perpendicular" (min) orientations of an elongated object, relative to the look angle of the sensor. We express the factor as a ratio in terms of the inferred parallel and perpendicular orientation eigenvalues of the measured scattering matrix, $\lambda_{//}$ and $\lambda_{\perp}$:

$$\mathrm{ELF} = \frac{\left|\,|\lambda_{//}| - |\lambda_{\perp}|\,\right|}{|\lambda_{//}| + |\lambda_{\perp}|}$$

3.2 Blind Target Classification Results

3.2.1 General Performance

A dig list containing target features and UXO-like/non-UXO classification of the blind targets is included in Table 19 of Appendix A. The confidence level is currently entered subjectively by the operator based on the signal level and the clarity of the features according to the criteria shown in Figure

16. The ETO has an inherent ambiguity of $\pm 180^{o}$, which is not a problem. The early-time ELF is a newly introduced parameter based on the magnitude of the target's earliest observable response, indicating the normalized difference between axial to transverse response. Any special comments produced during the processing were entered in the last column.

In general, the target locations observed from GPR data were found to be offset from the flagged location by approximately 10"~20". Some targets appeared to have large offset up to 30"~40" inches. These large offsets are noted in the "Special Note" column. A challenging but realistic flagging approach was suggested by the CRREL/OSU team in an effort to utilize multiple-sensor features since the "hot spots" in a real UXO field will most likely be determined from EMI/Magnetometer survey based on magnetic dipole moments. Such a position offset certainly causes additional difficulty in GPR surveying. Notice that the optimal (strongest) response direction for a GPR system is usually orthogonal to that for EMI/Magnetometer system. This is illustrated in Figure 17. If the offset occurs along the initial pass during the GPR survey, proper adjustment can be applied to obtain the best position for subsequent passes (transverse and 45^{o}) as indicated by the field log shown in Table 32. The offset and orientation of the subsequent pass was determined from the data obtained in the previous pass. The position offset requires the initial estimation of the UXO azimuth angle to be reasonably accurate especially for deeper targets. Otherwise, the subsequent pass could miss the target by a large amount. During our demo, a hand-held magnetometer was used to estimate the magnetic dipole's azimuth angle based on the sign reversal of the response. This response feature becomes increasingly ambiguous when the inclination angle increases and completely disappears in a vertical UXO case. However, the typical position offset also decreases as the inclination angle increases (see Figure 17). In future applications, a bonafide MAG/EMI survey map would be more accurate than the manual approach we used for estimating the magnetic dipole direction. In the next generation of this kind of surveying, with faster data acquisition capability, it may simply be more practical to make three or four passes, uniformly for all targets, in a star shaped pattern around the flagged location (i.e. with equi-angular shifts in azimuthal orientation). In such a scheme the scans and their orientations would not depend on interpretation of previous scans, and there would likely be enough coverage of the target locale to catch essential features in the great majority of cases.

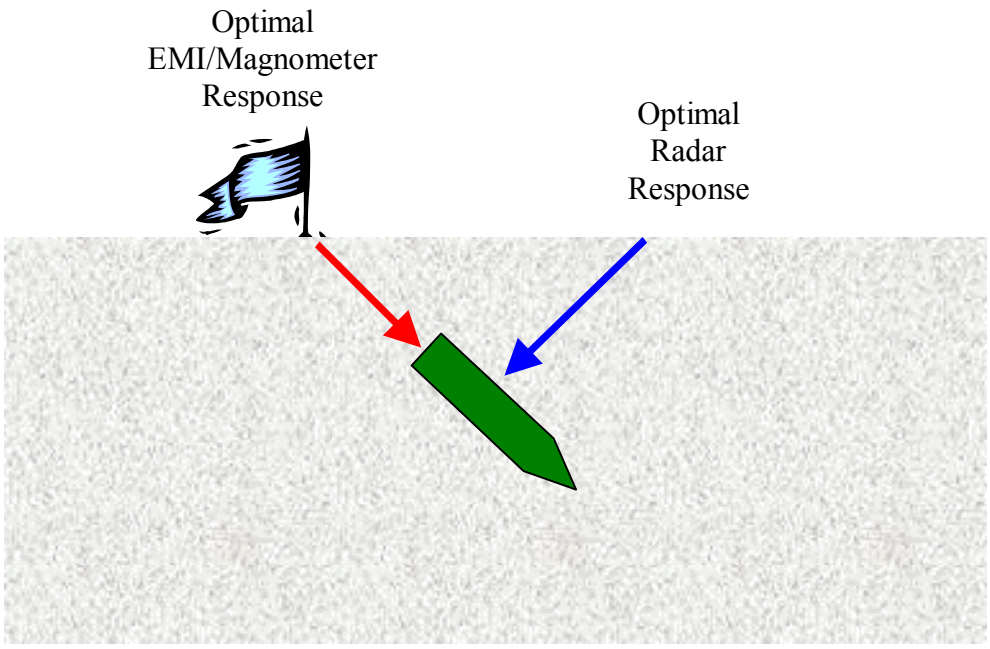

Figure 17 The orthogonal relation between radar and EMI/Magnetometer systems, wherein optimal sensor locations correspond to strongest response.

Table 20 and Table 21 also show the revised dig lists obtained using the EMI based depth estimates (ROUND 2) and more accurate ("true") depth information (ROUND 3), for guidelines in selecting the appropriate signal time region to analyze for each target. In particular, if the estimated depth for a target in Table 19 was very different (>0.2 meter) from the EMI depth or true depth, the data was reprocessed to focus on the time region corresponding to the EMI/true. The changes from ROUND 1 results to ROUND 2 results then to ROUND 3 results are indicated in the tables by the color codes. After the ground truth data was released, the UXO classification performance based on GPR features was evaluated by comparing the reported dig lists with the ground truth data as shown in Table 23 to Table 31 in Appendix A.2. The final statistics are also summarized in

Table **2** through Table 10 below. Figure 18 probably provides the clearest overall summary of performance.

Notice that these results are listed according to three different UXO designations. The first type designates non-UXO/UXO based on the item truth, i.e. only actual UXO were considered to be UXO-like in the ground truth. The second type separates non-UXO/UXO-like items based on whether their length to diameter (L/D) ratio is less than or greater than two. The second type distinguishes non-UXO/UXO-like based on a L/D ratio threshold of three. During the previous demos, the UXO-like items were designated using the $L/D \geq 3$ criteria. However, 57mm ordnance in JPG V has a L/D ratio only slightly greater than two (see Figure 19). In order to include the 57mm's, an additional criteria, $L/D \geq 2$, was also adopted to evaluate the classification performance. Otherwise, the 57mm's would be treated as non-UXO items. Some fragments have L/D ratios greater than two and would be designated as UXO-like based on the $L/D \geq 2$ criterion. For the JPG target set, these "UXO-like" fragments are shown in the Appendix E for reference. Some exploded fragments that still have cylindrical bodies would be very difficult to discriminate from hazardous UXO's. Classification results provided with the ground truth (evidently from EMI) are also plotted for comparison in Figure 18. The eight empty cells and the two magnetic rocks were excluded in obtaining the EMI classification statistics. The number of UXO's detected in the 2nd round is slightly improved over the 1st round, as predicted from the previous demo results. The false alarm rate is also reduced in the 3rd round with a better depth estimation. Clearly, the better the depth information provided to the GPR processing, the better the performance. Even with approximate depth information (Round 2), the GPR results are superior to the EMI performance in that detection rates are comparable while the GPR false alarm rate is less. In every round of processing through which depth information usage was varied, we see the same pattern relative to the object sorting criterion: Detection rates vary only slightly, while false alarm rates decline as we move from use of the true UXO criterion, to the LD3, then to the LD2 criterion.

Since the 3rd round results require true depths that are most likely unavailable in real UXO sites, the analysis of the causes of the missed UXO's and of false alarms as well as the comparison of the features of correctly classified UXO's will be based on 2nd round results using the $L/D \geq 2$ criteria in the following sections. Therefore, the effects of estimation errors for target position and depth obtained from EMI/MAG data are reflected in the analysis.

Table 2 Round One Classification based on GPR data only, with emplaced items sorted into UXO-like/non-UXO categories according to True UXO identity.

Total Number of UXO	50
Total Number of Empty Sites	8
Total Number Fragments (Including one magnetic Rock)	42
Total Number of UXO Classified as UXO	39
Total Number of Clutter Classified as UXO	34
Total Number Missed UXO-Like	11
Detection Rate: $\frac{\text{Number of UXO-like items classified as UXO}}{\text{Total Number of UXO-like items}}$	80.0%
False Alarm Rate: $\frac{\text{Number of clutter items classified as UXO}}{\text{Total number of clutter items}}$	68.0%

Table 3 Round One Classification based on GPR data only, with emplaced items sorted into UXO-like/non-UXO categories according to L/D>=2 Criteria.

Total Number of UXO-Like (L/D >=2)	73
Total Number of Empty Sites	8
Total Number Fragments (Including one magnetic Rock)	19
Total Number of UXO-Like Classified as UXO-Like	57
Total Number of Clutter Classified as UXO-Like	16
Total Number Missed UXO-Like	16
Detection Rate: $\frac{\text{Number of UXO-like items classified as UXO}}{\text{Total Number of UXO-like items}}$	78.1%
False Alarm Rate: $\frac{\text{Number of clutter items classified as UXO}}{\text{Total number of clutter items}}$	59.3%

Table 4 Round One Classification based on GPR data only, with emplaced items sorted into UXO-like/non-UXO categories according to L/D>=3 Criteria.

Total Number of UXO-Like (L/D >=3)	59
Total Number of Empty Sites	8
Total Number Fragments (Including one magnetic Rock)	33
Total Number of UXO-Like Classified as UXO-Like	48
Total Number of Clutter Classified as UXO-Like	25
Total Number Missed UXO-Like	11
Detection Rate: $\frac{\text{Number of UXO-like items classified as UXO}}{\text{Total Number of UXO-like items}}$	81.4%
False Alarm Rate: $\frac{\text{Number of clutter items classified as UXO}}{\text{Total number of clutter items}}$	61.0%

Table 5 Round Two Classification based on GPR data with reference to EMI/Mag depth indications, with emplaced items sorted into UXO-like/non-UXO categories according to True UXO identity.

Total Number of UXO	50
Total Number of Empty Sites	8
Total Number Fragments (Including one magnetic Rock)	42
Total Number of UXO Classified as UXO	42
Total Number of Clutter Classified as UXO	34
Total Number Missed UXO	8
Detection Rate: $\frac{\text{Number of UXO-like items classified as UXO}}{\text{Total Number of UXO-like items}}$	84.0%
False Alarm Rate: $\frac{\text{Number of clutter items classified as UXO}}{\text{Total number of clutter items}}$	68.0%

Table 6 Round Two Classification based on GPR data with reference to EMI/Mag depth indications, with emplaced items sorted into UXO-like/non-UXO categories according to L/D>=2 Criteria

Total Number of UXO-Like (L/D >=2)	73
Total Number of Empty Sites	8
Total Number Fragments (Including one magnetic Rock)	19
Total Number of UXO-Like Classified as UXO-Like	61
Total Number of Clutter Classified as UXO-Like	15
Total Number Missed UXO-Like	12
Detection Rate: $\frac{\text{Number of UXO-like items classified as UXO}}{\text{Total Number of UXO-like items}}$	83.6%
False Alarm Rate: $\frac{\text{Number of clutter items classified as UXO}}{\text{Total number of clutter items}}$	55.6%

Table 7 Round Two Classification based on GPR data with reference to EMI/Mag depth indications, with emplaced items sorted into UXO-like/non-UXO categories according to L/D>=3 Criteria

Total Number of UXO-Like (L/D >=3)	59
Total Number of Empty Sites	8
Total Number Fragments (Including one magnetic Rock)	33
Total Number of UXO-Like Classified as UXO-Like	50
Total Number of Clutter Classified as UXO-Like	26
Total Number Missed UXO-Like	9
Detection Rate: $\frac{\text{Number of UXO-like items classified as UXO}}{\text{Total Number of UXO-like items}}$	84.7%
False Alarm Rate: $\frac{\text{Number of clutter items classified as UXO}}{\text{Total number of clutter items}}$	63.4%

Table 8 Round Three Classification based on GPR data with reference to depths in ground truth, with items sorted into UXO-like/non-UXO categories according to True UXO identity.

Total Number of UXO	50
Total Number of Empty Sites	8
Total Number Fragments (Including one magnetic Rock)	42
Total Number of UXO Classified as UXO	38
Total Number of Clutter Classified as UXO	30
Total Number Missed UXO-Like	12
Detection Rate: $\frac{\text{Number of UXO-like items classified as UXO}}{\text{Total Number of UXO-like items}}$	76.0%
False Alarm Rate: $\frac{\text{Number of clutter items classified as UXO}}{\text{Total number of clutter items}}$	60.0%

Table 9 Round Three Classification based on GPR data with reference to depths in ground truth, with items sorted into UXO-like/non-UXO categories according to L/D>=2 Criteria

Total Number of UXO-Like (L/D >=2)	73
Total Number of Empty Sites	8
Total Number Fragments (Including one magnetic Rock)	19
Total Number of UXO-Like Classified as UXO-Like	57
Total Number of Clutter Classified as UXO-Like	11
Total Number Missed UXO-Like	16
Detection Rate: $\frac{\text{Number of UXO-like items classified as UXO}}{\text{Total Number of UXO-like items}}$	78.1%
False Alarm Rate: $\frac{\text{Number of clutter items classified as UXO}}{\text{Total number of clutter items}}$	40.7%

Table 10 Round Three Classification based on GPR data with reference to depths in ground truth, with items sorted into UXO-like/non-UXO categories according to L/D>=3 Criteria

Total Number of UXO-Like (L/D >=3)	59
Total Number of Empty Sites	8
Total Number Fragments (Including one magnetic Rock)	33
Total Number of UXO-Like Classified as UXO-Like	48
Total Number of Clutter Classified as UXO-Like	20
Total Number Missed UXO-Like	11
Detection Rate: $\frac{\text{Number of UXO-like items classified as UXO}}{\text{Total Number of UXO-like items}}$	81.4%
False Alarm Rate: $\frac{\text{Number of clutter items classified as UXO}}{\text{Total number of clutter items}}$	48.8%

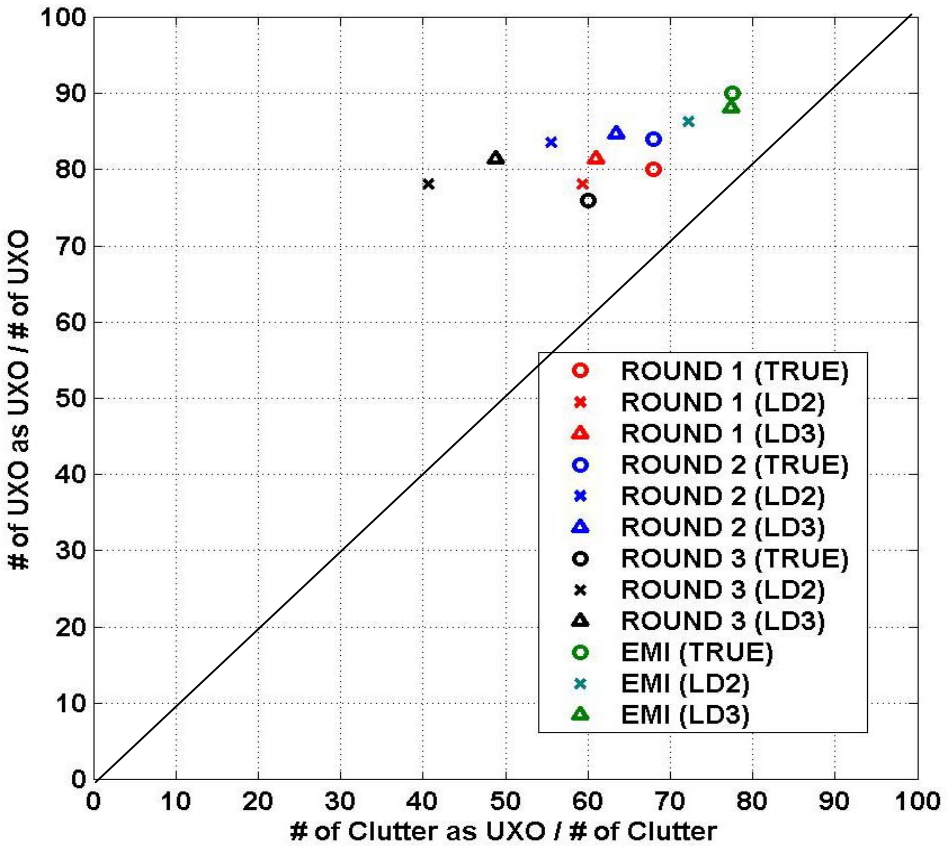

Figure 18. The ROC chart of the GPR UXO classification performed at JPG V. Round 1 = classification based on GPR only; Round 2 = GPR processing + depth estimations from EMI; Round 3 = GPR processing + ground truth depth information; with 45^{o} "line of no discrimination."

Figure 19. 57mm UXO.

3.2.2 Features of Correctly Classified UXO-like Items

For those UXO-like items that were classified correctly (2nd Round, LD2 Criteria), the estimated target lengths are compared with the true lengths in

Figure **20**. The horizontal index corresponds to the target number following the order in Table 27 (Appendix A.2). Note that targets 1~34 have high confidence levels, targets 35~45 have moderate confidence levels and targets 46~61 have low confidence levels. The estimated lengths for the high- and moderate-confidence items are close to true lengths. Larger discrepancies are observed for low-confidence items. The estimated depths for correctly classified UXO-like items are compared with the ground truth depths in Figure 21. As one can see, most of the estimated depths are greater than the true depths. This follows from the inherent ambiguity mentioned above regarding target depth: The true depth is measured from the shallowest point of a target and the radar depth is based on the earliest, strongest scattering point, which depends on the geometry and orientation of the target. Figure 22 compares the estimated depths with the true depths for targets that have inclination angles less than 20 degrees. As expected, better agreement is observed for these items. Overall, these figures give a picture of relative accuracy, for each case. In absolute terms, these figures display specific results from populations in which the mean ETL error was 13 cm, with standard deviation of 23 cm; mean estimate depth error was 14 cm with standard deviation of 18 cm.

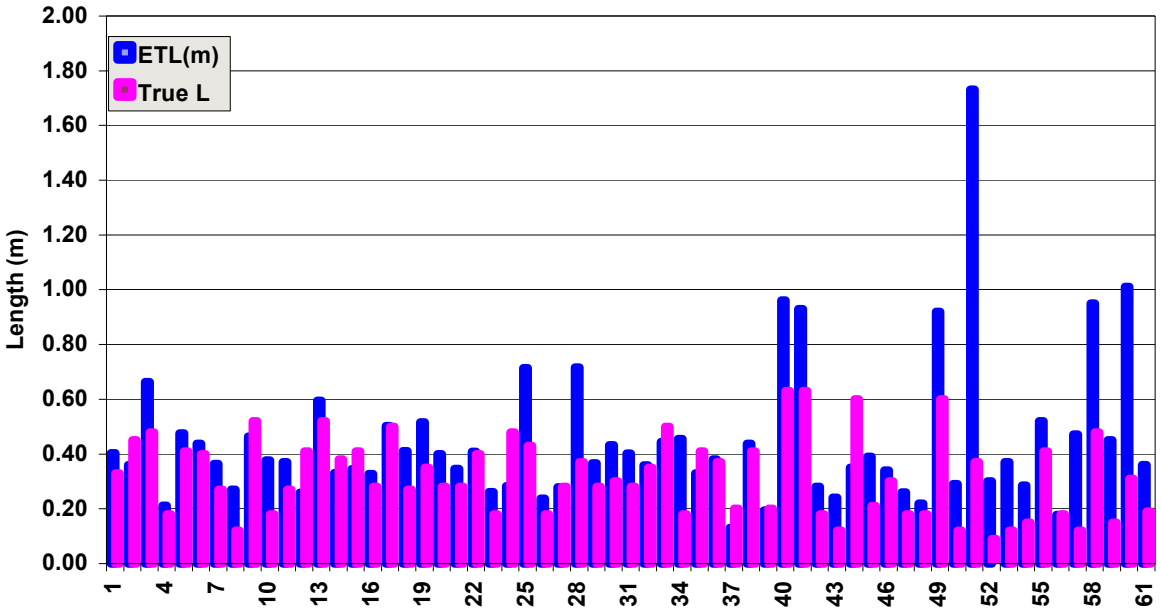

Figure 20 Comparison of ETL and true length for correctly classified UXO-like (LD2) items.

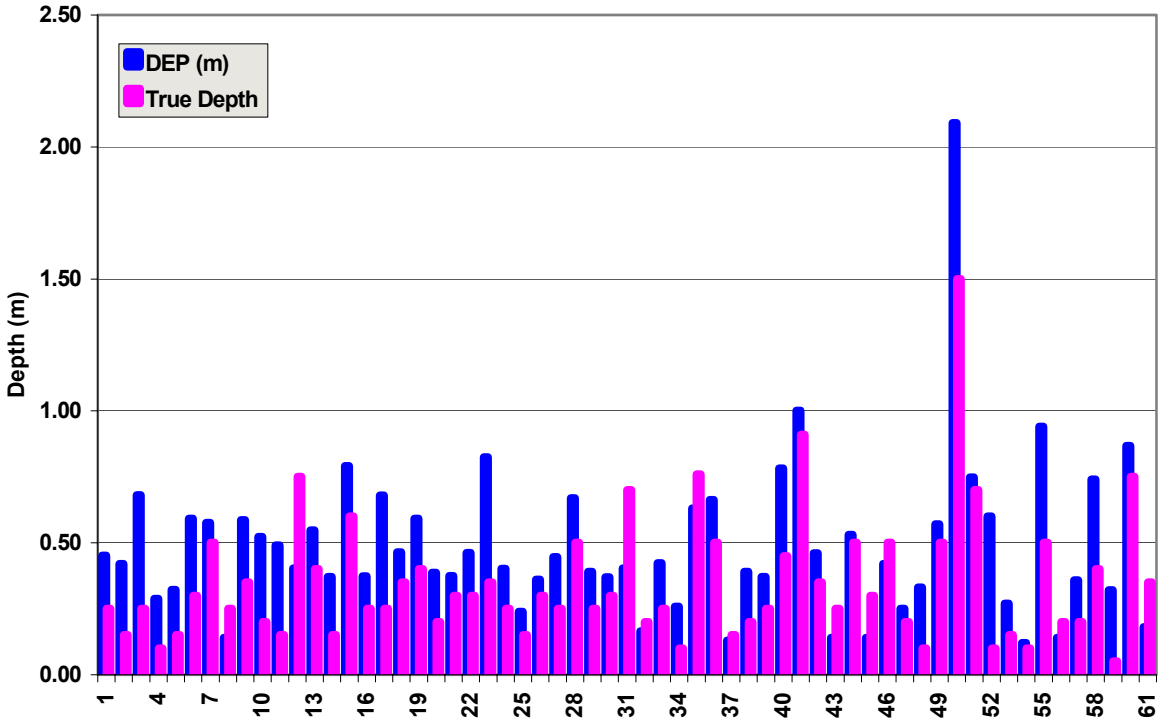

Figure 21 Comparison of estimated depth and true depth for correctly classified UXO-like items (Round Two, LD2 Criteria).

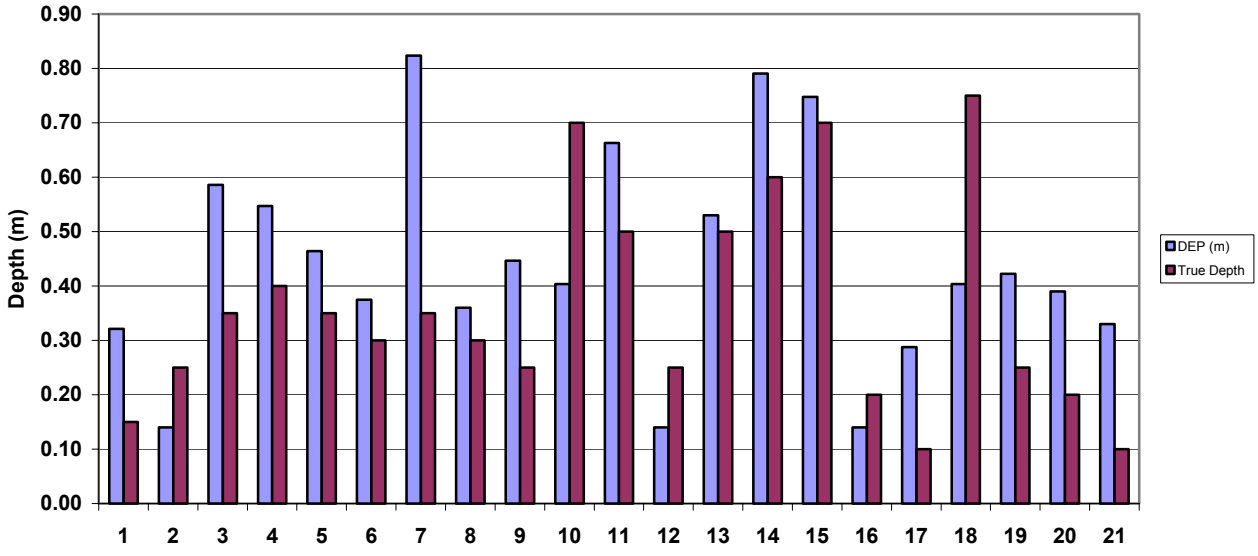

Figure 22 Comparison of estimated depth and true depth for correctly classified UXO-like items (Round Two, LD2 Criteria) with inclination angle less than 30^{o}.

3.2.3 Statistical Analysis of the Estimated Linear Factor

In this section, we examine the distributions of Estimated Linear Factors (ELF), computed in different ways, and the relations of the various ELFs to target identity. Figure 23 and Figure 24 plot histograms of the late-time ELF (LT-ELF) corresponding to the UXO-like and clutter items sorted according to "TRUE-UXO identity" criteria. For the LT-ELF alone to be a good discrimination indicator, we would like to see high bars corresponding to UXO's on the right sides of the plots, and relatively high bars corresponding to clutter towards the left side. The pattern in Figure 24 shows at least some degree of this pattern. Overall, however, since many "clutter" items have elongated bodies with L/D ratios greater than two, these histograms show that the LT-ELF alone appears to have only modest discrimination capability. (Note that in the complete discrimination processing, spatial patterns of ELF values as well as other factors are used together with the ELF values themselves.) If the goal is to isolate elongated objects, e.g. with L/D ratio greater than two, then the LT-ELF alone appears to be a relatively good discriminator, as shown in Figure 25. This figure clearly indicates the effectiveness of the GPR feature extraction algorithms. We note that, under the LD2 criterion, the factor is better at pointing to UXO-like objects than at identifying clutter (suppressing false alarms). It is not surprising to see the same general result in histograms of frequency-domain ELF, extracted from the late-time spectrum near the resonant frequency (RF-ELF), shown in Figure 26 through Figure **28**. The histograms of early-time ELF (ET-ELF) are also shown in Figure 29 through Figure 31. It is interesting to observe that Figure 31 shows that the ET-ELF could also identify the high L/D ratio items reasonably well. Recall that the early-time ET-ELF is calculated from taking the early-time scattering magnitudes of the S_{11}, S_{21} and S_{22} channels to form a 2x2 scattering matrix from which the eigenvalues are determined. Ratios of the extreme eigenvalues correspond to the ratio of strongest to weakest orientation of scatter. Loosely speaking, these early time responses are immediate "bounces" from surfaces or geometrical discontinuities such as tips, edges and corners. They can also be seen as diffractions of the incident wave from the object, on first encounter. In either case, they are fundamentally different from the responses producing the LT-ELF, which are resonating current patterns induced in later time, constrained by the object's overall shape and generally following its orientation. Thus both the LT-ELF and the ET-ELF are related to target geometry, but in different ways. One problem associated with the ET-ELF is the frequent prevalence of early time clutter. Another is that the magnitude of the early time reflection and diffraction terms also depends strongly on the inclination of the target with respect to the incident fields. Therefore, the ET-ELF is less reliable than later time quantities, unless there is some means of inferring the target's disposition.

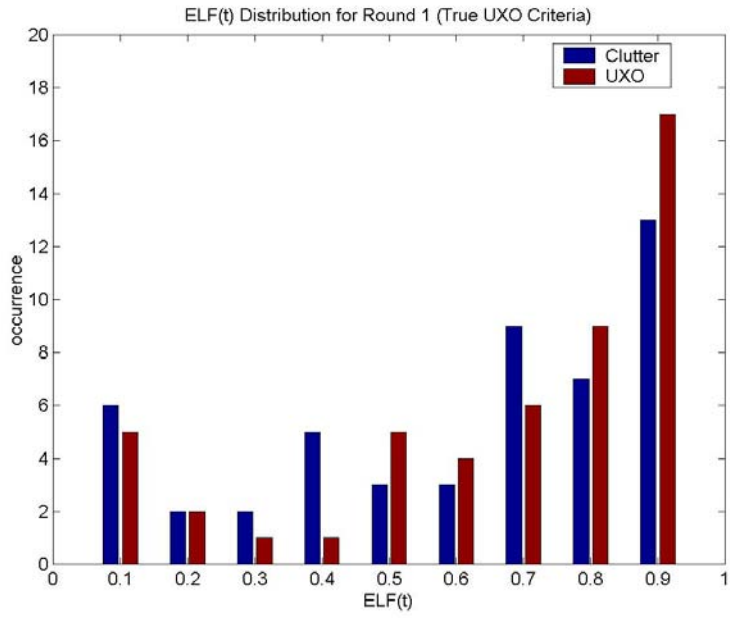

Figure 23 Histogram of LT-ELF from the Round 1 processing based on "TRUE_UXO" criteria

.

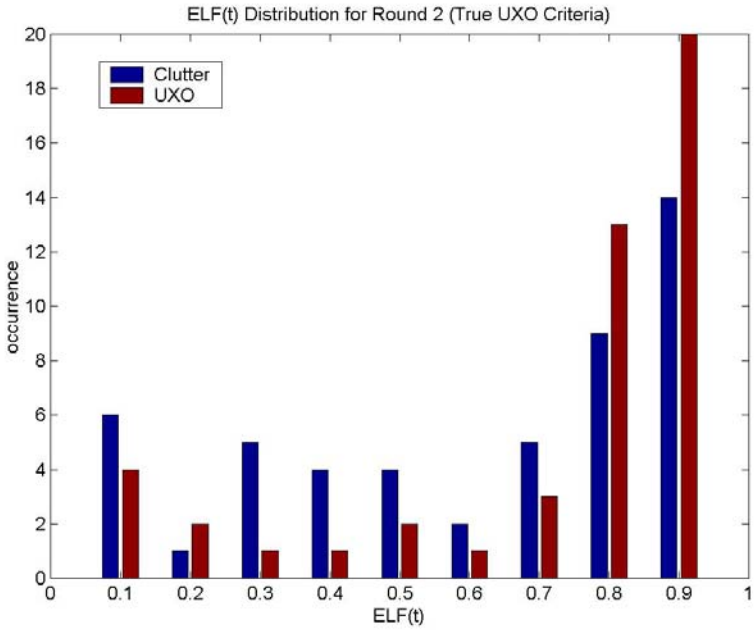

Figure 24 Histogram of LT-ELF from Round 2 processing based on "TRUE_UXO" criteria.

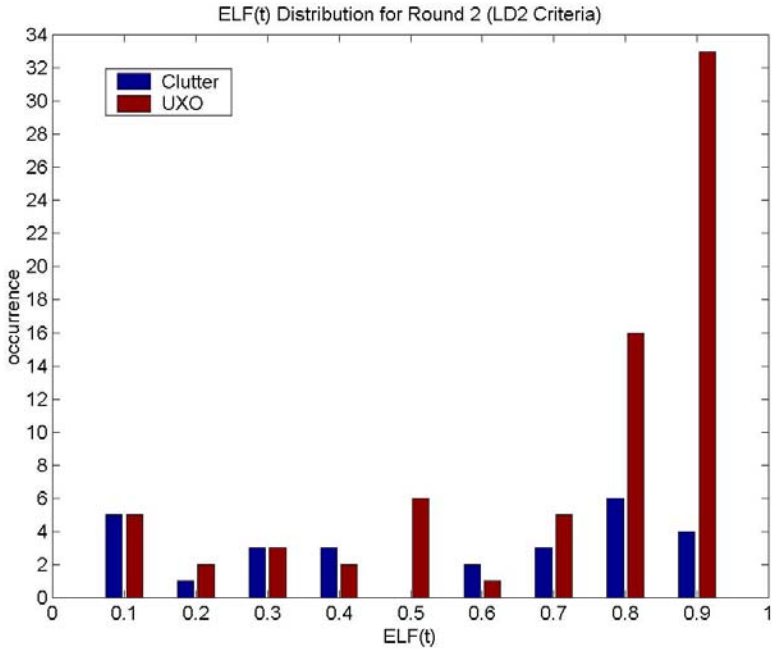

Figure 25 Histogram of LT-ELF from Round 2 processing based on "L/D>2" criteria.

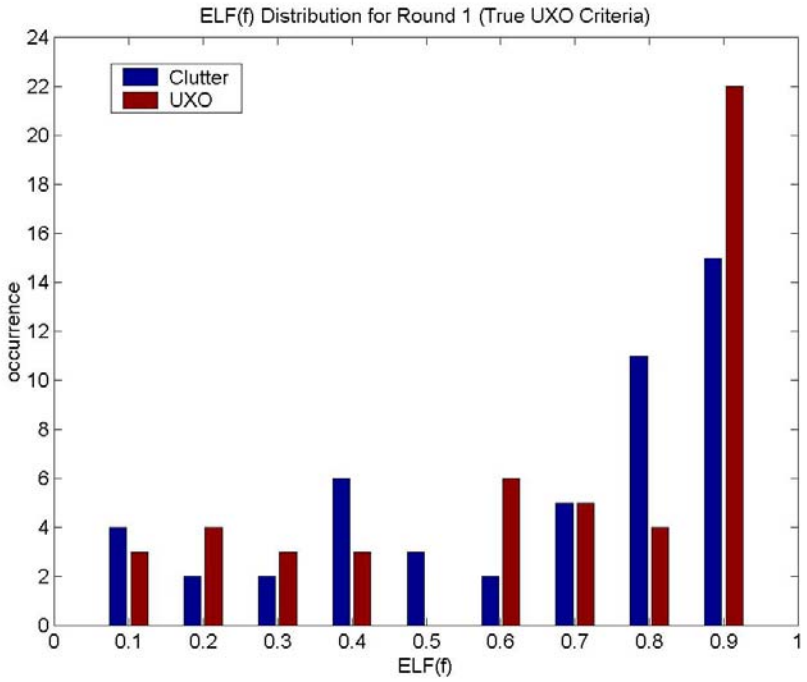

Figure 26 Histogram of RF-ELF from the Round 1 processing based on "TRUE_UXO" criteria.

.

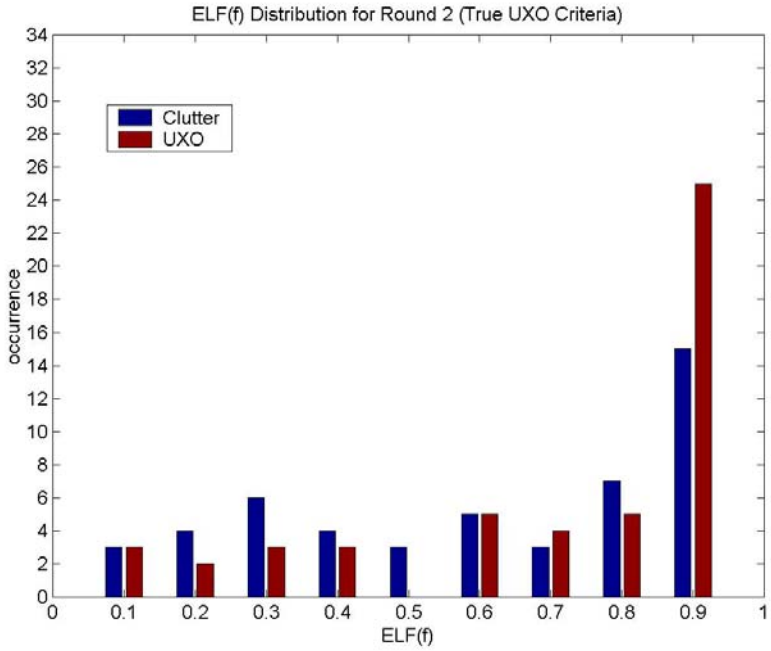

Figure 27 Histogram of RF-ELF from Round 2 processing based on "TRUE_UXO" criteria.

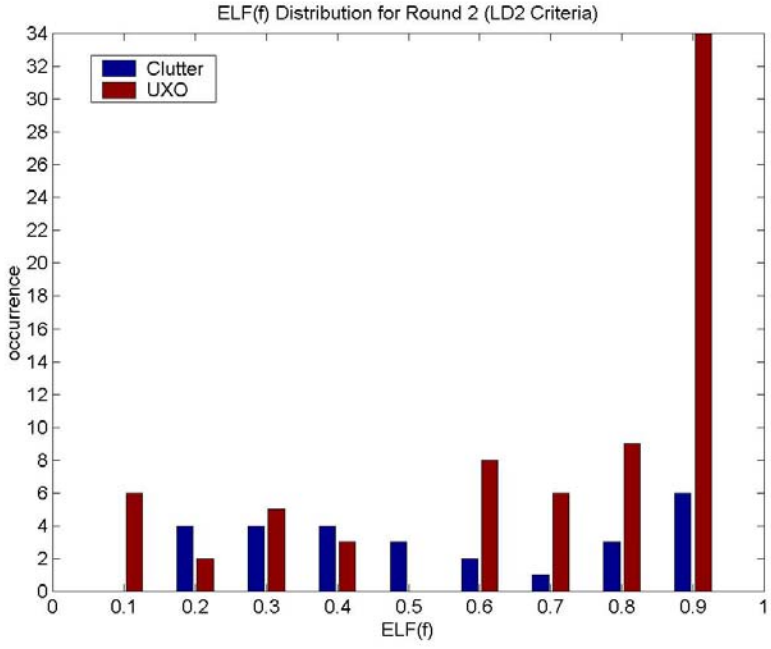

Figure 28 Histogram of RF-ELF from Round 2 processing based on "L/D>2" criteria.

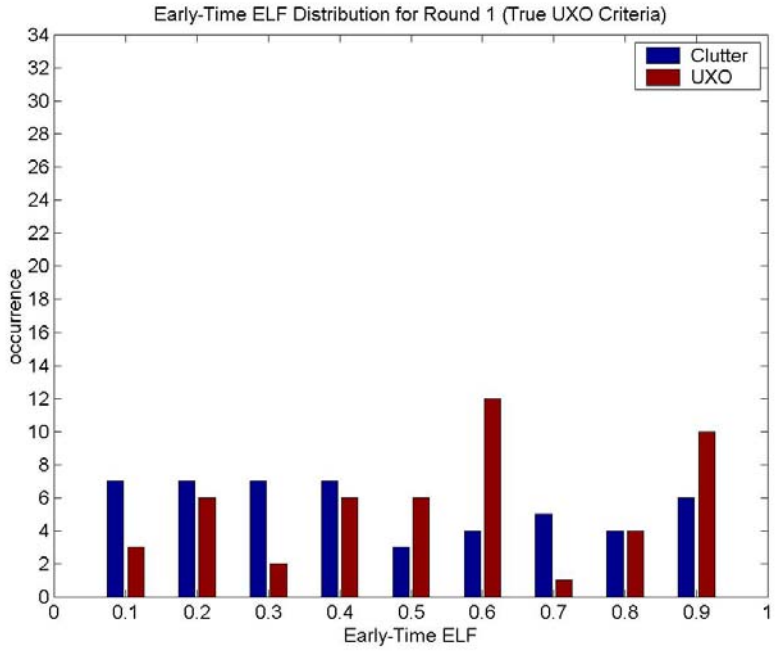

Figure 29 Histogram of ET-ELF from Round 1 processing based on "TRUE_UXO" criteria.

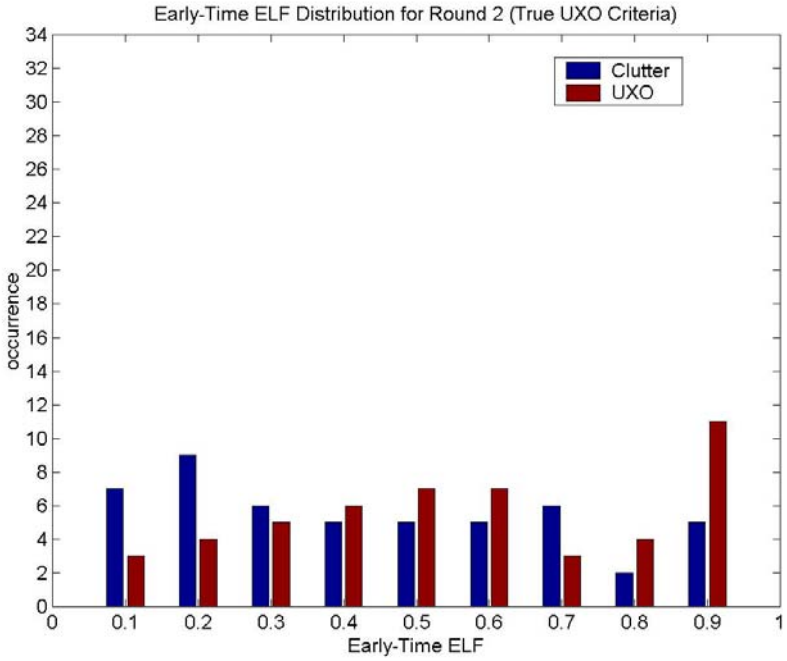

Figure 30 Histogram of ET-ELF from the Round 2 processing based on "TRUE_UXO" criteria.

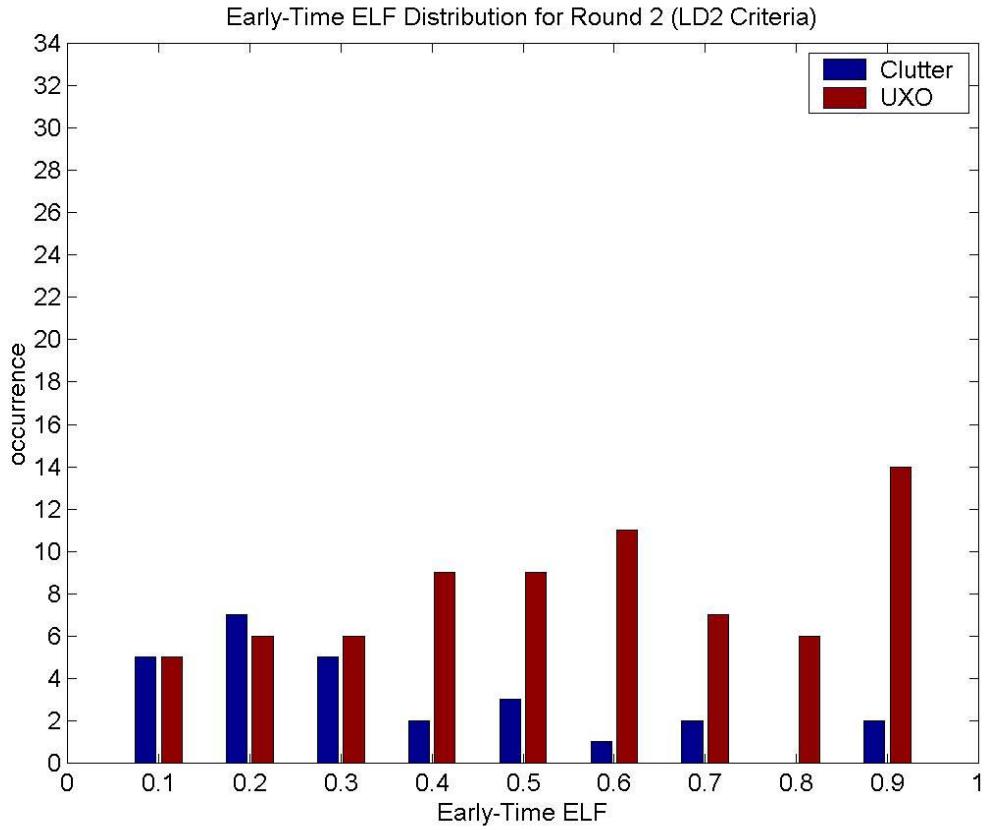

Figure 31 Histogram of ET-ELF from Round 2 processing based "L/D>2" criterion.

3.2.4 Absolute Length Estimation Error

To assess the accuracy of the estimated target length (ETL) compared to the true length, histograms of the length estimation error for Round 1 and Round 2 results are shown in Figure 32 through Figure 35. The horizontal scale is in meters. The tight clustering of the higher values near the center (zero meters error) indicates that the ETL is generally accurate. Overall, we expect more accurate length estimation for the elongated targets. This is because the length is estimated from the fundamental late time resonant frequency. Compact or amorphous objects may hardly resonate at all or may present a more incoherent resonance picture, dying out amidst the clutter of early time returns. All this is reflected, for example, in Figure 35. Under the LD2 criterion, this round and the third round most reliably sorted the emplaced items into elongated and non-elongated classes. Note the very strong peak around zero error for the UXO-like category, while the peak for items classified as clutter lies to the right. Among other things, this is testament to the adequacy of the measurement and processing maneuvers by which the site dielectric constants are obtained and applied. It also emphasizes the basic soundness of the resonance concept and the methods for determining it.

Overall, the distributions shown below are not symmetrical, but are skewed towards the positive values. This means that, when erroneous, the estimated fundamental resonant frequencies are too low. This may be an effect of target inclination. ETL is a useful as a "reality check" and an assessment of the resonance determinations that are fundamental to all our processing. Beyond that the parameter is not used directly here for discrimination per se. It can be, however, when the target set justifies searching for the presence of specific items. See ESTCP report on Tyndall Demo.

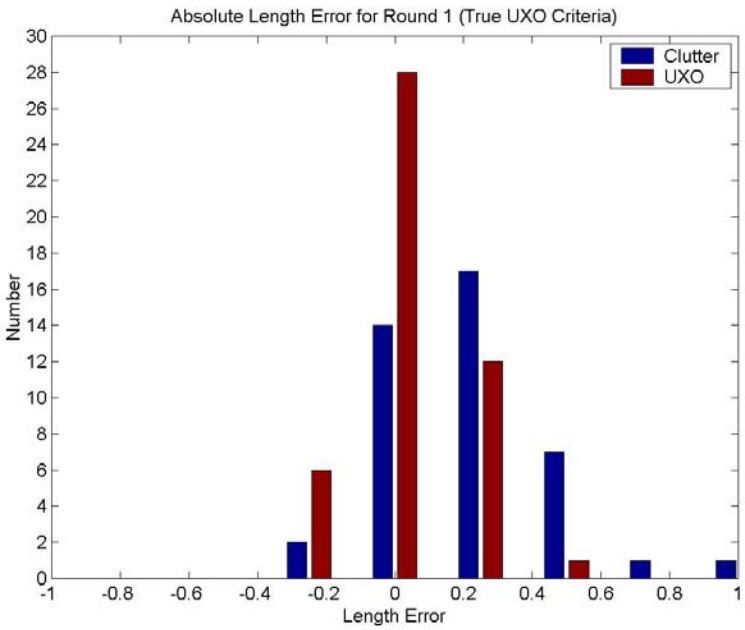

Figure 32 Length estimation errors from the Round 1 processing based on "TRUE UXO" criteria.

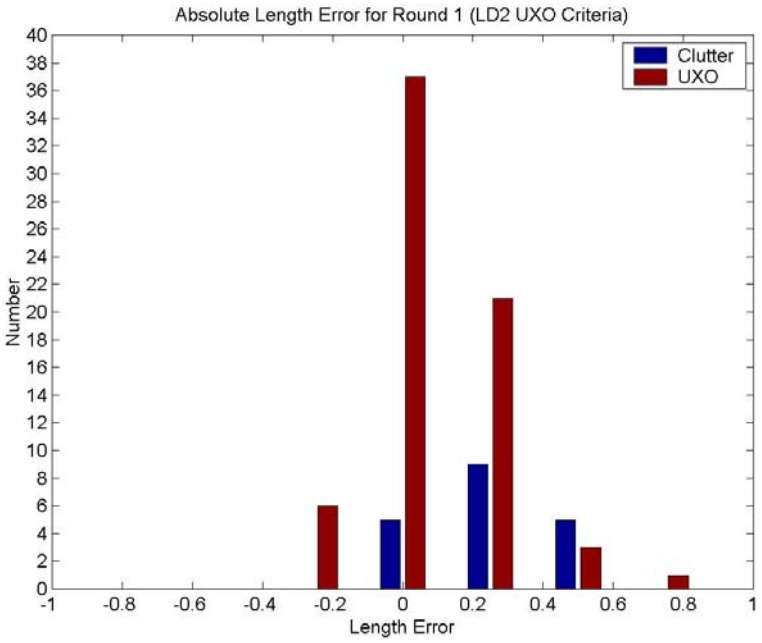

Figure 33 Length estimation errors from the Round 1 processing based on "L/D>2" criteria.

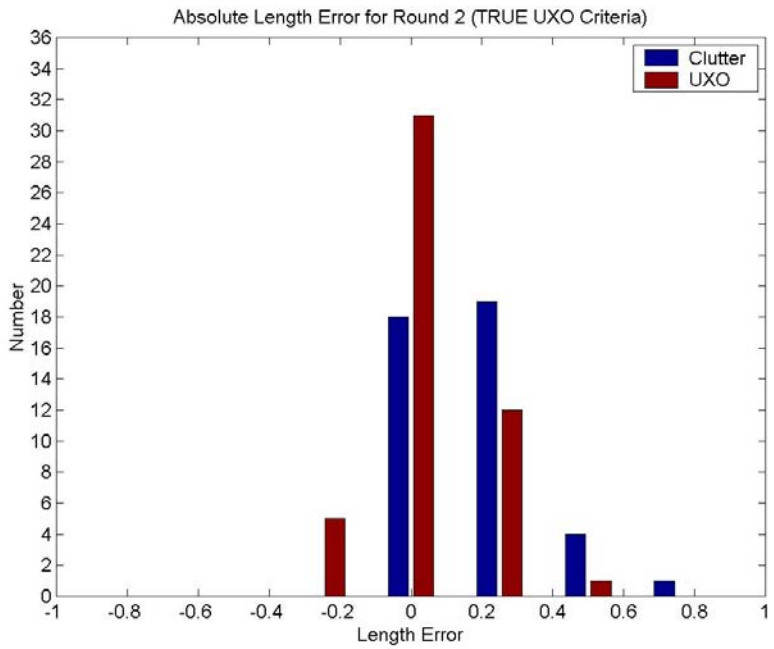

Figure 34 Length estimation errors from the Round 2 processing based on "TRUE UXO" criteria

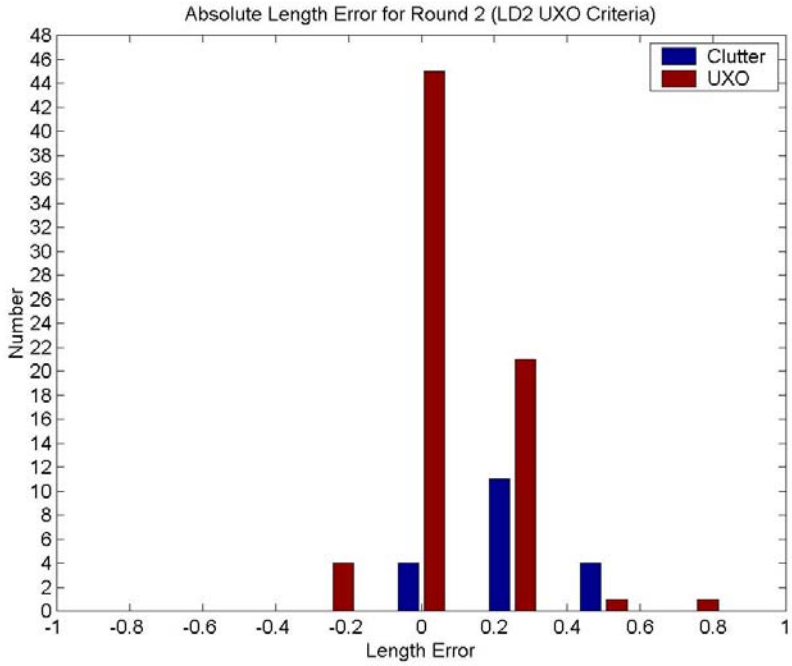

Figure 35 Length estimation errors from the Round 2 processing based on "L/D>2" criteria.

3.2.5 False Alarm Sources

Table 11 summarizes an investigation of the causes of false alarms. The features for items 1-26, 1-42 and 1-45 were extracted from incorrect depths or incorrect positions due to the presence of other scattering anomalies that have linear signal features. An example would be the scattering from an elongated trench. Reprocessing the data near the correct depth and position showed low ELF values, as should appear for most non-UXO like items. The revised features produced by the reprocessing are shown in Table 12. These targets were small items buried at shallow depths. The response from such small targets is weak in the low frequency region and becomes stronger in the high frequency region. The original time domain picture obtained from the Fourier transform of the frequency domain data over the whole frequency band (10~410 MHz) showed little sign of the presence of these small targets. It was found that if the data was filtered first before it was transformed into the time domain using a bandpass filter centered at 250 MHz with a bandwidth of approximately 200 MHz, the target became more visible due to the suppression of the low frequency component of clutter (Figure 36 and Figure 37). Similarly, Figure 38 and Figure 39 show the filtered responses and the corresponding ELF. More detailed discussion of the high frequency filter can be found in Chapter 4.

Items 1-36 and 2-15 showed good UXO-like features as shown in Figure 40 and Figure 41, respectively. Corresponding photos of 1-36 and 2-15 are also included in Figure 42 and Figure 43, respectively, for examination. Although the main body of target 2-15 has an L/D ratio slightly less than two, it has a long curved extended part that make it a good linear resonator, like a UXO. Although the fragment appears to be like a plate from the picture, the radar features do not correspond to a horizontal plate with typical strong responses in both S_{11} and S_{22} channels (see Figure 16 and [5]). The radar data suggested that the fragment was probably oriented vertically, causing strong linearity signal features. Although in principle a vertical plate can be distinguished from a horizontal UXO based on the scattering features from the S_{11} data in the transverse pass (see Figure 16 and [5]), the discrimination capability degrades for small plates and poor SCR.

Some items that were classified as UXO-like with low confidence during the 2nd round were reclassified as non-UXO during the 3rd round, after processing improvement via the above mentioned high frequency bandpass filter during the pre-processing stage. These items are 1-43, 1-59,1-63, 2-17, 2-19 and 2-24 as indicated in

Table 11. Items 2-24 and items 2-26 were entered in the field log as empty sites, as they should be (see Appendix D), based on the lack of apparent target responses in time-position plots compared to what was observed in other cells. Typically, this means that no apparent target arcs were visible other than the scattering from surface and subsurface layers. This is usually not difficult to identify for sandy soil and non-disturbed fine-grained soil. After the fine-grained soil is disturbed by target emplacement and concentration of water flow/accumulation, the picture is not always clear. When a soil disturbance has an elongated shape, the radar data will tend to show elevated ELF values, such as those produced by a UXO. This is apparently what happened with items 2-25, 2-26 and 1-61. Although, this type of soil disturbance scatter should not have strong resonance, the broad range of UXO sizes causes the distinction of early-time response and late-time response to be very ambiguous, impeding resonance identification. In particular, it is difficult to separate a non-resonant response from the highly damped resonance that is expected for small targets and targets in lossy soils. Item 3-2 (magnetic rock) showed mostly non-UXO features. It was selected because of a moderate ELF level near the center position that is assumed to be due to surface clutter. Such magnetic rocks should not be difficult to discriminate from UXO-like items when there is less high ELF clutter.

Table 11 Findings on the Causes of False Alarms.

AREA	TAR #	WES #	Description	Conf.	ETL (m)	True L	DEP (m)	True Depth	Late-Time ELF(t)	Late-Time ELF(f)	Early-Time ELF	Finding
1	26	164	Fragment	M	0.55	0.13	0.56	0.1	0.90	0.98	0.05	**Incorrect Depth** Round 1 Depth = 0.56 EMI Depth = 0.43 (see Figure 38&Figure 39)
1	42	28	Fragment	L	0.74	0.12	2.14	0.15	0.81	0.95	0.52	**Incorrect Depth** Round 1 Depth = 2.14 EMI Depth = 1.82 (see Figure 36&Figure 37)
1	45	26	Fragment	M	0.19	0.20	0.30	0.075	0.77	0.78	0.31	**Incorrect Position**
1	36	42	Fragment	H	0.24	0.15	0.40	0.35	0.94	0.79	0.33	**UXO-Like, good S_{22} responses**
2	15	46	Fragment	M	0.27	0.24	0.37	0.2	0.67	0.75	0.36	**UXO-Like, good responses**
1	59	10	Fragment	L	0.29	0.08	0.11	0.1	0.89	0.16	0.22	**Dropped in Round 3 after reprocessing**
1	63	16	Fragment	L	0.44	0.11	0.17	0.05	0.63	0.64	0.19	**Dropped in Round 3 after reprocessing**

1	43	154	Magnetic Rock	L	0.35	0.21	0.34	0.2	0.62	0.90	0.24	**Dropped in Round 3 after reprocessing**
2	17		Empty	L	0.38		0.76		0.78	0.51	0.62	**Dropped in Round 3 after reprocessing**
2	24		Empty	L	0.57		0.82		0.66	0.54	0.95	**Dropped in Round 3 after reprocessing**
2	19	54	Fragment	L	0.36	0.10	0.24	0.2	0.35	0.41	0.26	**Dropped in Round 3 after reprocessing**
2	25		Empty	L	1.06		1.08		0.28	0.40	0.88	**Near Random ELF**
2	26		Empty	H	0.36		0.73		1.00	0.90	0.71	**No Response In Orthogonal Pass**
1	61	158	Fragment	H	0.36	0.05	0.15	0.05	0.94	0.95	0.74	**Linear Surface Clutter**
3	2	110	Magnetic Rock	L	0.41	0.21	0.20	0.2	0.81	0.80	0.33	**(1) Poor SCR (2) ETO aligned with ATV in all passes**

Table 12 Reprocessed Features from Correct Depths and Positions.

AREA	TAR #	WES #	Description	Conf.	ETL (m)	True L	DEP (m)	True Depth	Late-Time ELF(t)	Late-Time ELF(f)	Early-Time ELF
1	**26**	47	Fragment	M	0.22	0.13	0.35	0.1	0.12	0.11	0.26
1	**42**	28	Fragment	L	0.36	0.12	0.08	0.15	0.55	0.67	0.37
1	**45**	26	Fragment	M	0.37	0.20	0.02	0.08	0.36	0.31	0.15

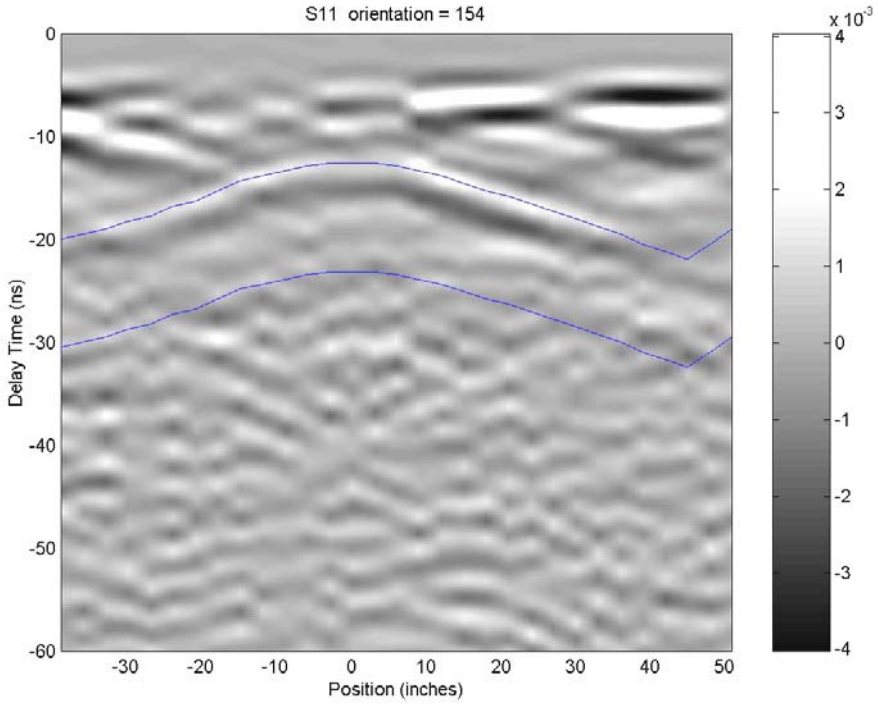

Figure 36a. Filtered S11 Responses

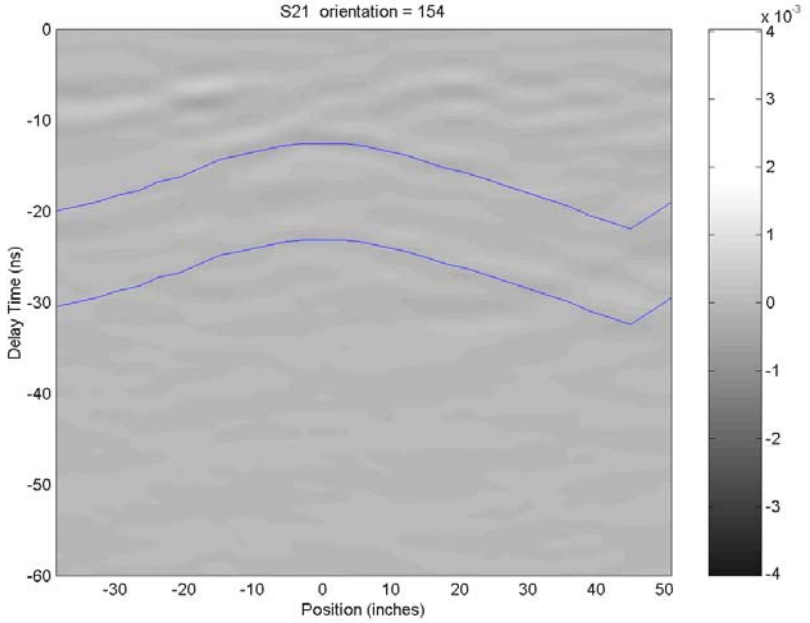

Figure 36b. Filtered S21 Responses

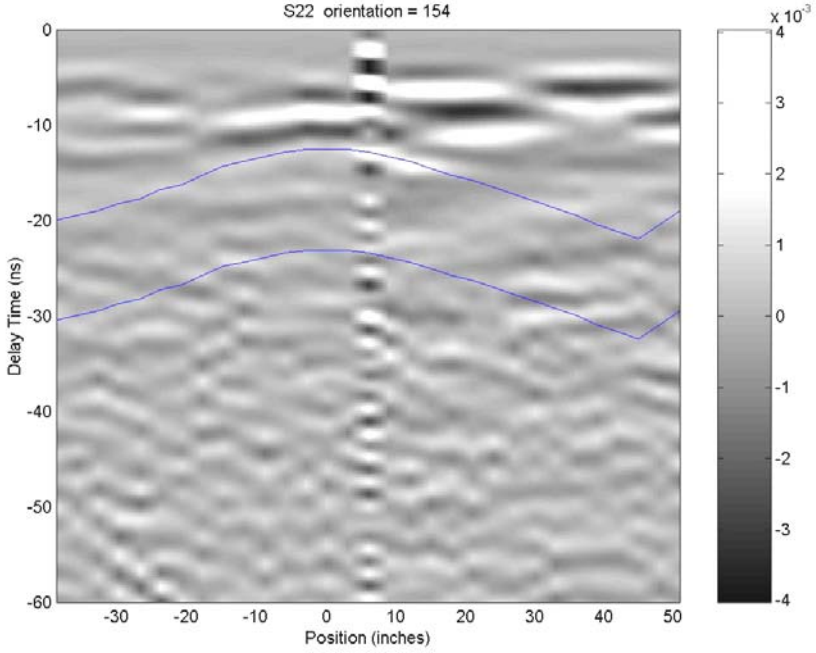

Figure 36c. Filtered S22 Responses

Figure 36. Filtered responses for Item 1-42, with arcs showing region of data analysis.

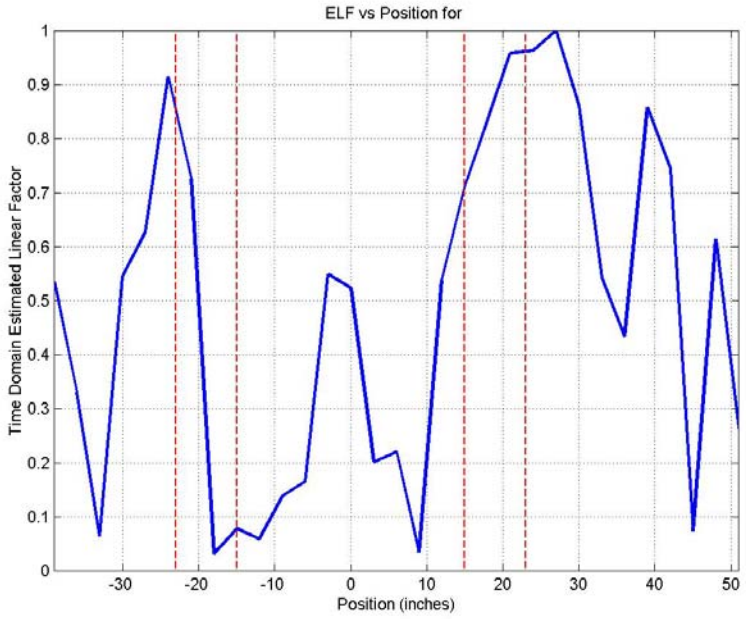

Figure 37 Revised Time-Domain ELF for Item 1-42.

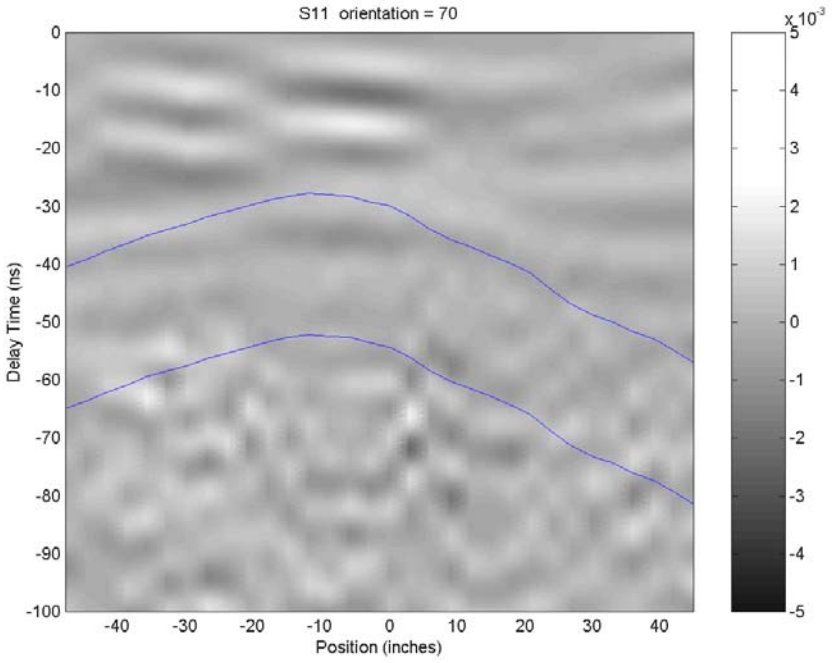

Figure 38 Filtered responses for Item 1-26.: S_{11}

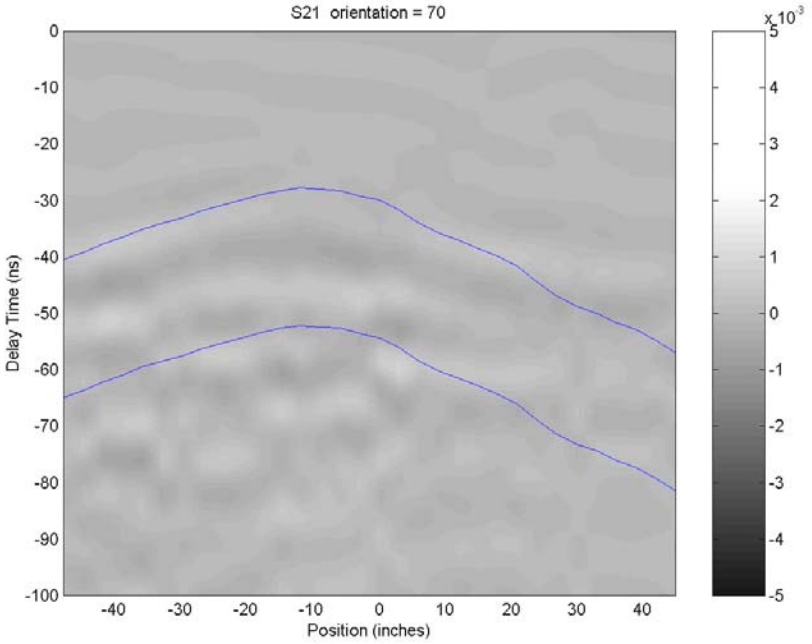

Figure 38 Filtered responses for Item 1-26. S_{21}

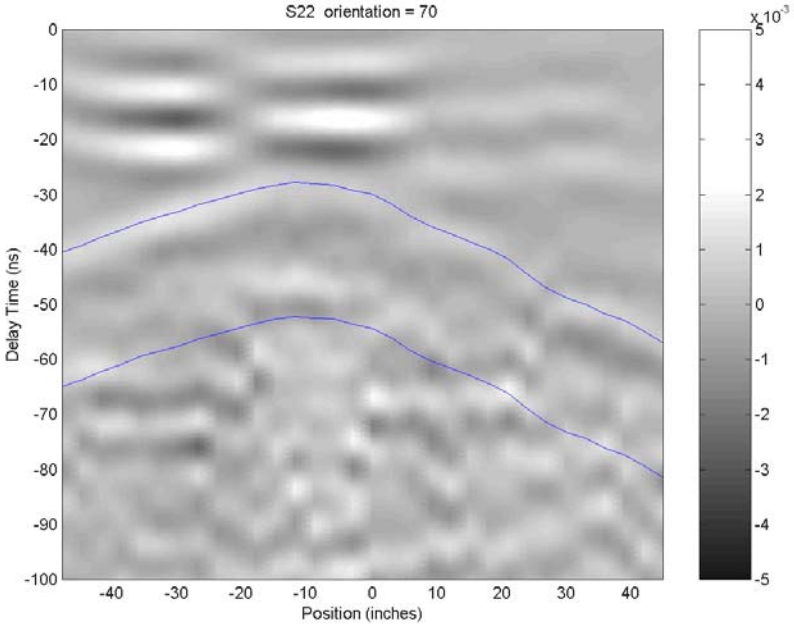

Figure 38 Filtered responses for Item 1-26. S_{22}

Figure 38 Filtered responses for Item 1-26.

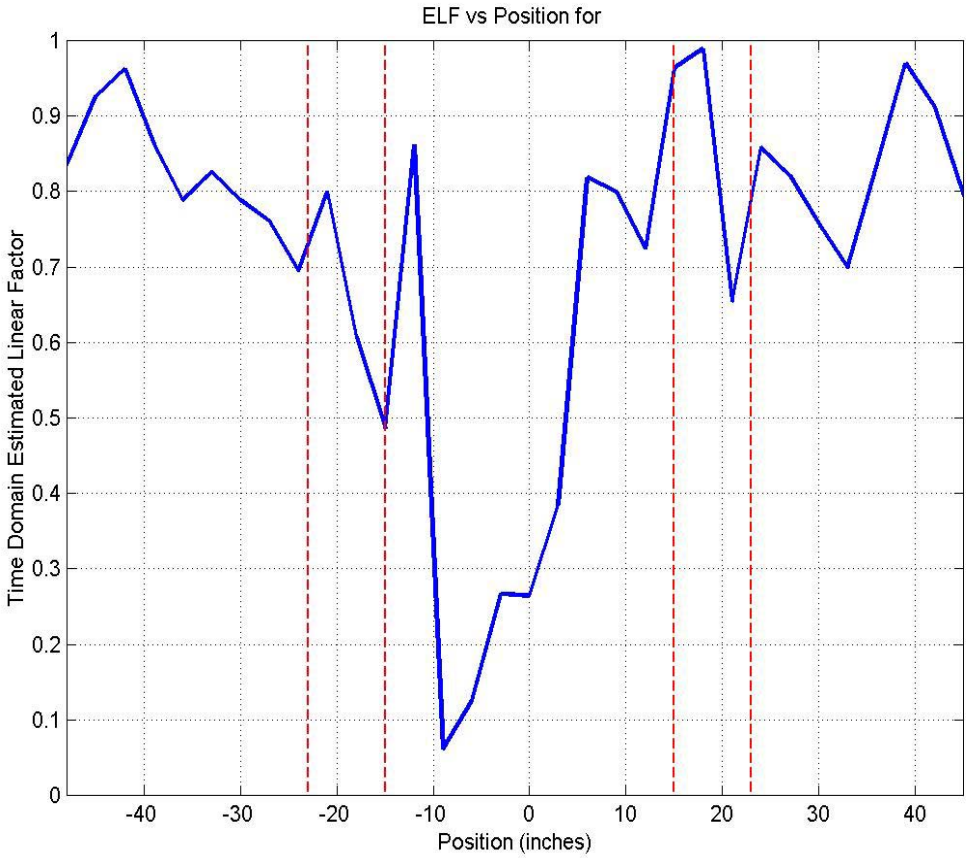

Figure 39 Time-Domain ELF extracted from data for Item 1-26.

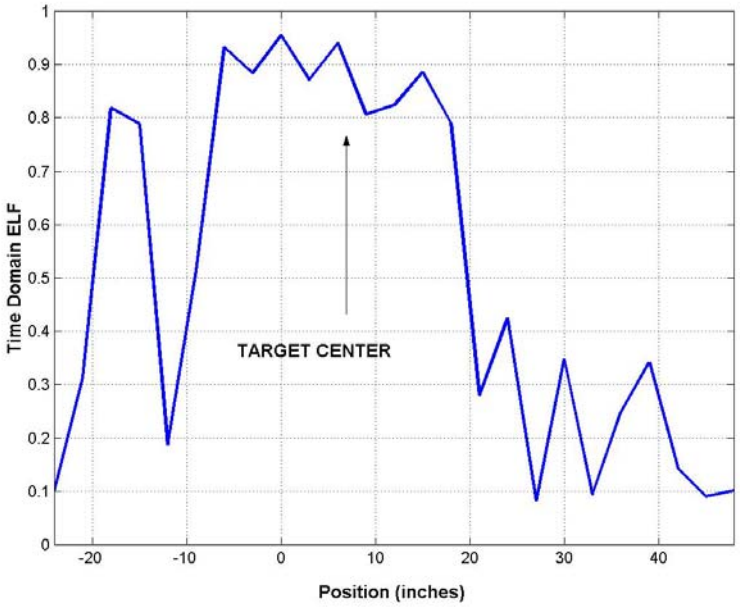

Figure 40. Time-Domain ELF Extracted for Item 1-36.

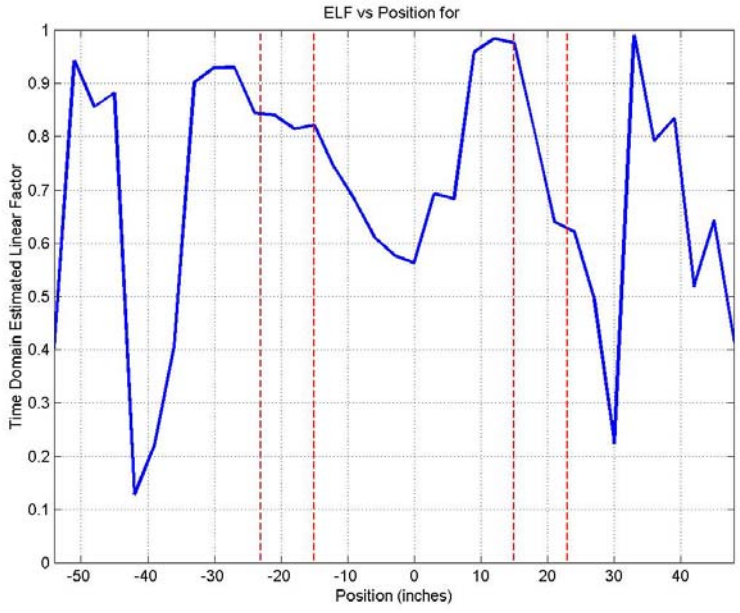

Figure 41. Extracted Time-Domain ELF for Item 2-15 shown below.

Figure 42. Picture of Item 1-36 (WES 1-42).

Figure 43. Picture of Item 2-15 (WES 2-62).

3.2.6 Causes of Missed UXO-Like Items

The causes of missed UXO-like items (2^{nd} Round, LD2 criteria) were investigated and results are summarized in Table 13. These causes can be separated into three types.

The first type includes Items 2-18, 1-48, 1-1 and is related to large depth estimation error. Processing in the 1^{st} round, from the GPR data alone, actually classified Items 2-18 and 1-48 correctly and produced reasonably accurate depth estimates (see Table 14). Subsequently, however, these were reclassified as non-UXO items due the inaccurate depth estimations provided from EMI measurements. The relatively deep Item 1-1 was classified as an empty site during the 1^{st} round because there were no apparent target responses. It was missed again during the 2^{nd} round since the EMI-based depth estimation still did not allow sufficient isolation of the target signal. Although it showed some linearity and was correctly classified during the 3^{rd} round with the true depth information, the confidence was set pretty low level due to weak responses. Item 1-48 was located approximately 0.3m away from a long (>2m) and deep (~1m) trench and only a single pass was usable. According to the ground truth, the EMI position error was also very large (1.75m) for this target. Therefore, the confidence level for the classification of this target was also set to a low level. Overall, the use of the EMI depth estimates increases the correct classification rate, as shown in

Table 15.

The second type of missed UXO-like items has weak or no observable responses compared to the background clutter (low SCR). Item 1-18 showed no observable target responses (arcs). This is likely due to the combination of absorptive soil, large inclination, and great depth.

The remaining misses of UXO-like items were caused by clutter contamination in co-polarization channels (S_{11} and S_{22}). Figure 44 shows the measured responses of Item 2-27 as an example. A strong surface anomaly is located between the –10 and –50 inch positions. From the data log recorded in the file header during the measurement, a ground surface depression was observed 12 inches away from the flag, which agrees with the location of said anomaly. The depression had a length of approximately 12 inches, width of 6 inches and depth of 6 inches. Such a depression also resulted in concentrated water accumulation and water penetration after rain, causing higher clutter level in the late-time region below the depression as observed in Figure 44. The small size and vertical orientation of the target, in addition to the presence of ground depression, resulted in poor signal to clutter ratio and loss of linear features in the signal. Figure 45 shows the GPR responses obtained for Item 3-9, a vertical 152mm projectile buried at a

depth of 0.91m. Although possible target responses were clearly observed in both S_{21} and S_{22} channels, the responses in the S_{11} channel were buried under clutter. Notice that soil disturbance effects due burial of the target are clearly observable near the surface. This is typical for wet, fine-grained soil. Figure 46 to Figure 48 show more examples of clutter contaminated co-polarization data for Items 1-20, 1-56 and 1-22, respectively. The target responses are clearly visible in the S_{21} channel (after filtering), which usually has much less clutter compared to co-polarization channels. This is because most ground scattering features such as layers tend to produce weak cross-polarized responses compared to the co-polarized reflections from those same items. The region between the two lines in the figures indicates the late-time region used for feature extraction. The target responses in either the S_{11} or S_{22} or in both of those channels are severely contaminated by the clutter due to the presence of shallow subsurface layers and disturbance during emplacement. Such poor SCRs resulted in the loss of linear features in the processed signals.

In summary, the main cause for missed UXO-like items is poor SCR in the co-polarization channels, which are more susceptible to subsurface layers and hydrological effects; these in turn are usually more pronounced in fine-grained soil such as that at JPG. The situation gets worse when the terrain elevation varies rapidly such as those in Areas 1 and 2. Figure 49 shows the positions of all items in Area 1 with the missed UXO-like items marked with triangles. It is interesting to find that these missed UXO-like items are concentrated in the lower area where the magnetometer also found high level of background signal (see Figure 51).

Table 13 Analysis of missed UXO-like items (LD2 criteria) in the 2nd Round results.

AREA	TAR #	WES #	Type	ETO (o)	True Azi.	True Inc.	ETL (m)	True L	DEP (m)	True Depth	Finding
2	18	42	Fragment	87	--	--	0.33	0.33	0.07	0.75	Correctly Classified in 1st & 3rd Rounds (See Table 14) Round 2 Mislead by EMI depth (0.23m)
1	48	150	2.75" Rocket	93	275	45	0.47	0.41	0.40	0.7	Correctly Classified in 1st Round (See Table 14) Round 2 Mislead by EMI depth (0.31m)
1	1	196	Fragment	-45	--	--	0.18	0.30	0.05	1.2	Weak Response Correctly Classified in 3rd Round (See Table 14) Round 2 Mislead by EMI depth (0.0514m)
1	18	122	5" Projectile	-177	270	55	0.53	0.63	0.57	0.91	No Target Response
2	27	112	81mm Mortar	-62	--	90	0.30	0.28	0.09	0.1	Strong clutter due to soil disturbance (See Figure 44, Position -30)
3	9	100	152mm Projectile	40	35	90	0.37	0.48	0.56	0.91	Poor SCR in S_{11} (See Figure 45)
2	10	144	152mm Projectile	150	50	30	0.24	0.48	0.37	0.45	Presence of shallower, low ELF clutter item
1	20	106	60mm Mortar	136	75	35	0.48	0.18	0.39	0.25	Poor SCR in S_{11} & S_{22} (See Figure 46)
1	23	142	57mm Projectile	15	265	45	0.18	0.12	0.10	0.15	Poor SCR in S_{11} & S_{22}
1	56	8	Fragment	157	--	--	0.24	0.20	0.42	0.3	Poor SCR in S_{11} & S_{22} (See **Figure 47**)
1	22	176	Fragment	50	--	--	0.16	0.13	0.18	0.15	Poor SCR in S_{22} (See **Figure 48**)
1	25	132	57mm Projectile	-125	180	0	0.21	0.12	0.09	0.25	Poor SCR in S_{11} & S_{22}

Table 14 UXO-like items that were correctly classified during 1st and 3rd rounds but missed during the 2nd round.

AREA	TAR #	WES #	GPR ID	Description	Conf.	ETO (o)	ETL (m)	DEP (m)	Late-Time ELF(t)	Late-Time ELF(f)	Early-Time ELF
2	18	118	1	Fragment	H	-147	0.47	0.89	0.76	0.72	0.83
1	48	150	1	2.75" Rocket	L	91	1.65	0.74	0.98	0.89	0.38
1	1	196	1	Fragment	L	-4	0.18	1.06	0.41	0.55	0.71

Table 15 UXO-like items added in the 2nd Round after incorporating the depth estimation from EMI data.

AREA	TAR #	WES #	Description	Conf.	True Azi.	True Inc.	ETL (m)	True L	DEP (m)	True Depth
1	**5**	147	57mm Projectile	H	0	0	0.27	0.12	0.14	0.25
1	**11**	153	2.75" Rocket	M	0	90	0.33	0.41	0.63	0.76
1	**12**	119	152mm Projectile	L	270	30	0.95	0.48	0.74	0.4
1	**28**	138	57mm Projectile	L	95	45	0.37	0.12	0.27	0.15
1	**29**	54	Fragment	L	--	--	0.34	0.30	0.42	0.5
1	**33**	36	Fragment	M	--	--	0.13	0.20	0.13	0.15
1	**62**	149	2.75" Rocket	L	30	55	0.52	0.41	0.94	0.5

Table 16 UXO-like items dropped in the 2nd Round after incorporating the depth estimation from EMI data.

AREA	TAR #	WES #	Description	Conf.	True Azi.	True Inc.	ETL (m)	True L	DEP (m)	True Depth
2	**18**	42	Fragment	H	--	--	0.47	0.33	0.89	0.75
1	**48**	150	2.75" Rocket	L	275	45	1.65	0.41	0.74	0.7
1	**25**	132	57mm Projectile	L	180	0	0.45	0.12	0.52	0.25

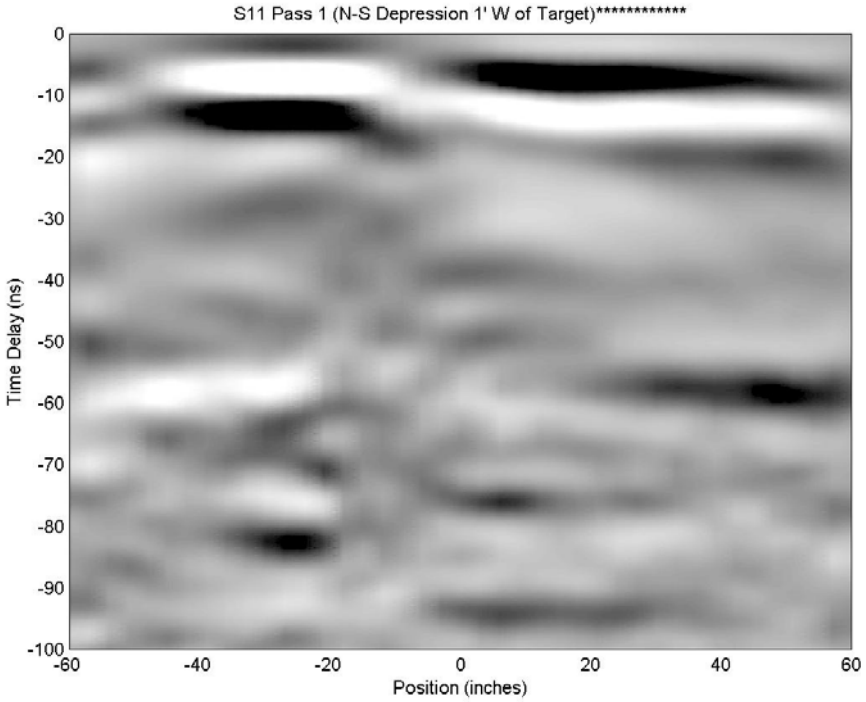

Figure 44a. S_{11}

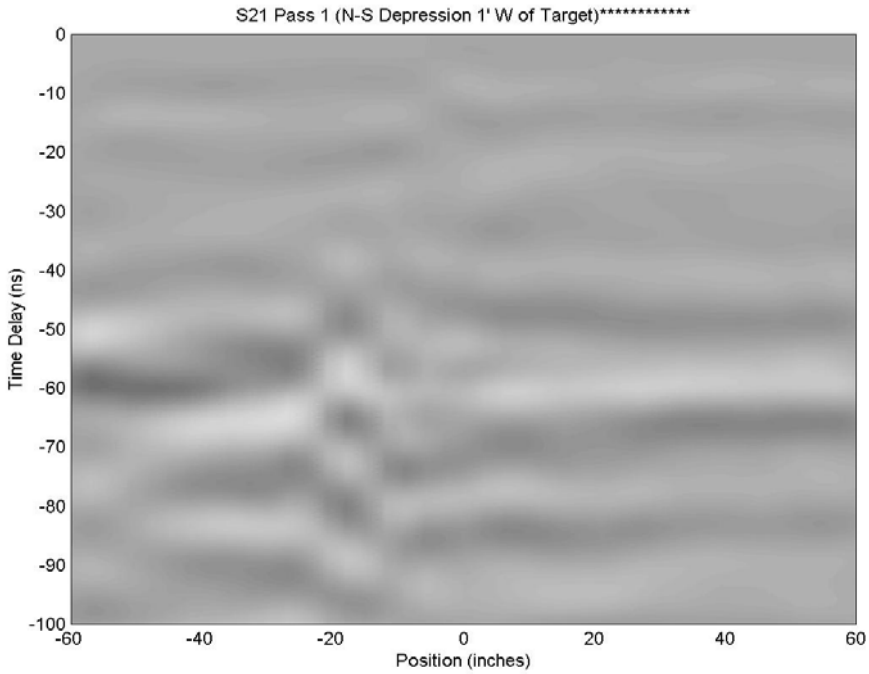

Figure 44b. S_{21}

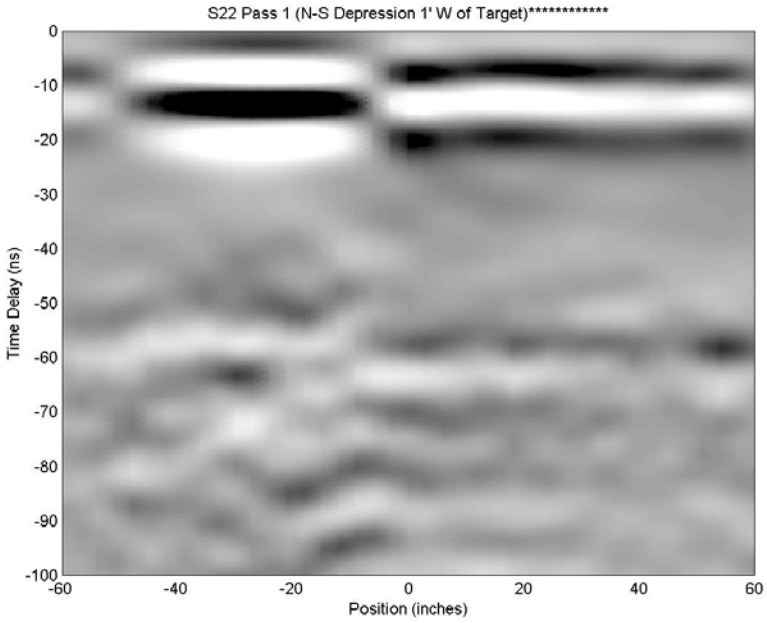

Figure 44c. S_{22}

Figure 44. Responses for Item 2-27 (WES 2-112).

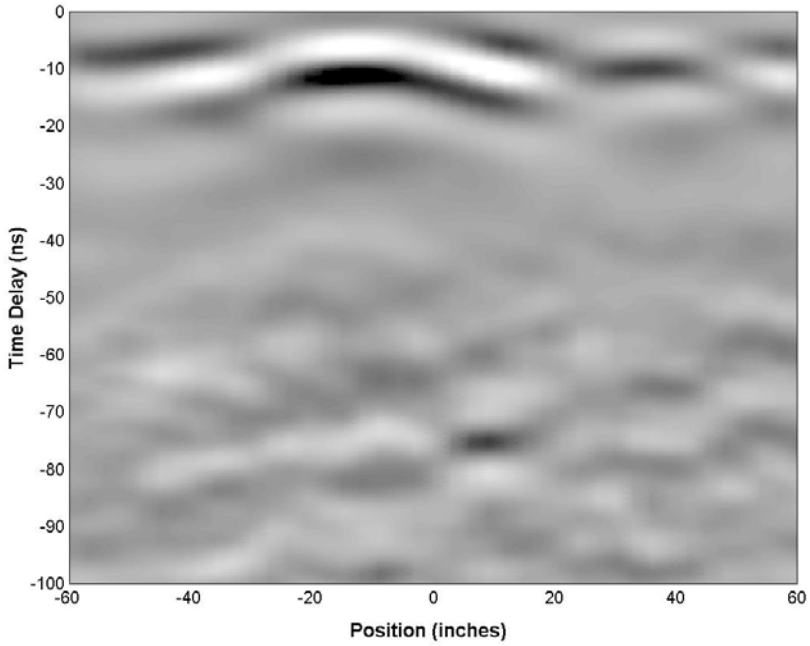

Figure 45a. S_{11} Response for Item 3-9.

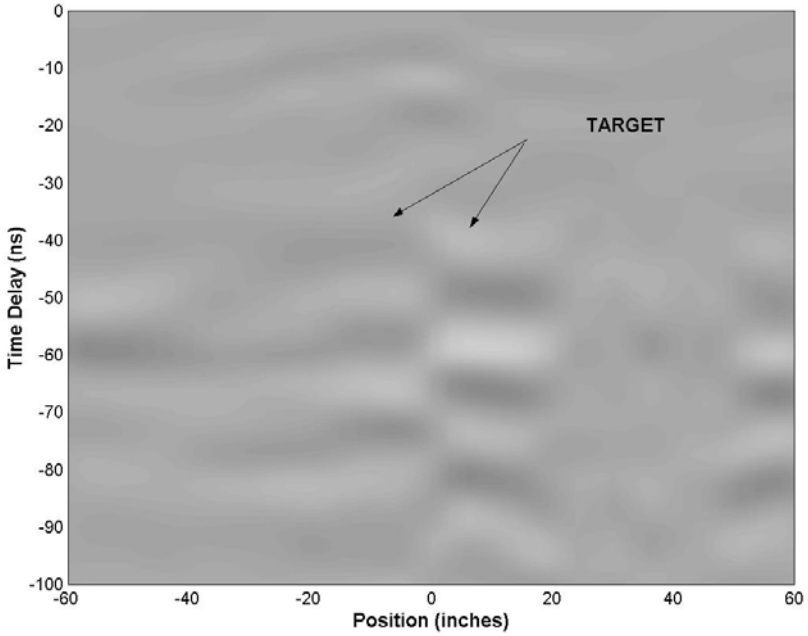

Figure 45b. S_{21} Response for Item 3-9.

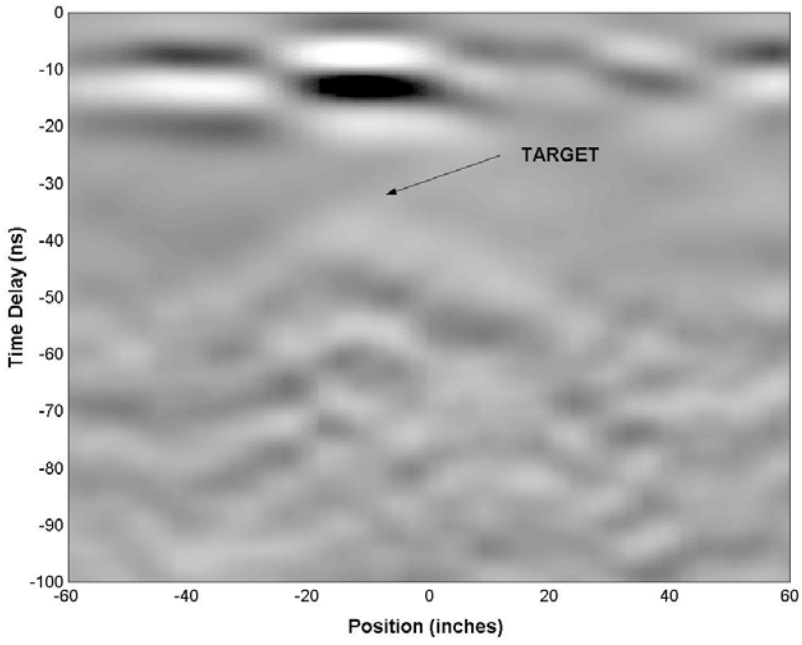

Figure 45c. S_{22} Responses for Item 3-9.

Figure 45 GPR responses for Item 3-9 (WES 3-100).

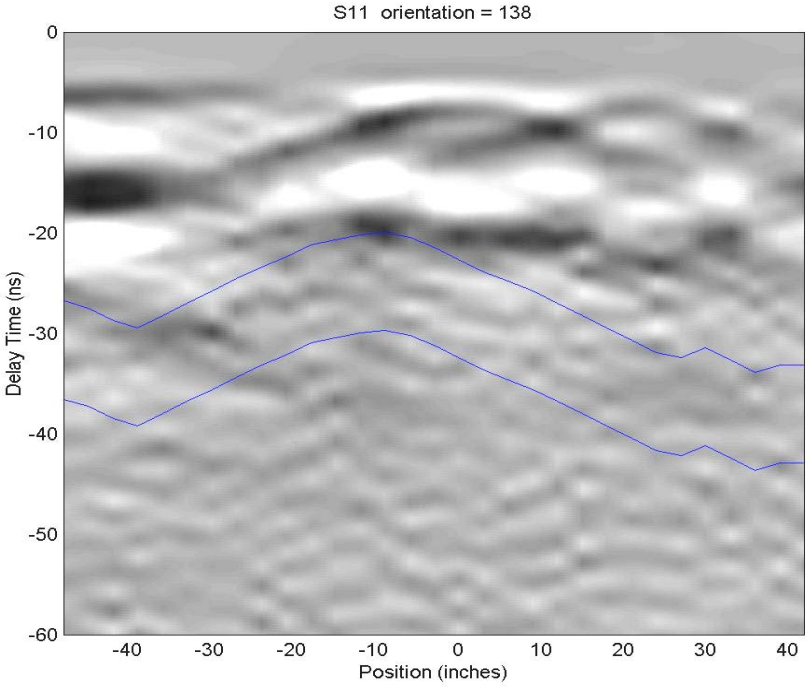

Figure 46a. S_{11} responses for Item 1-20.

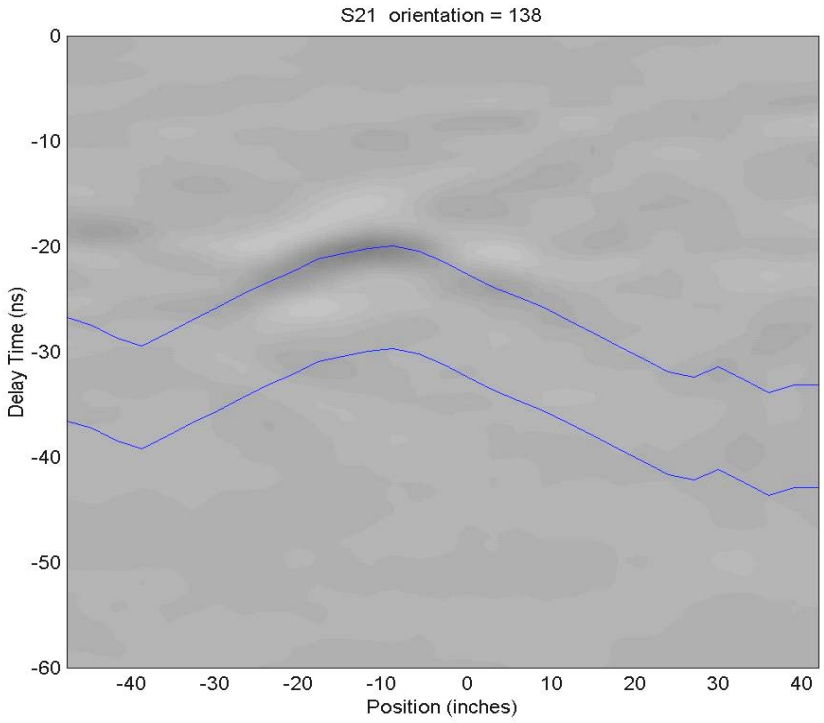

Figure 46b. S_{21} responses for Item 1-20.

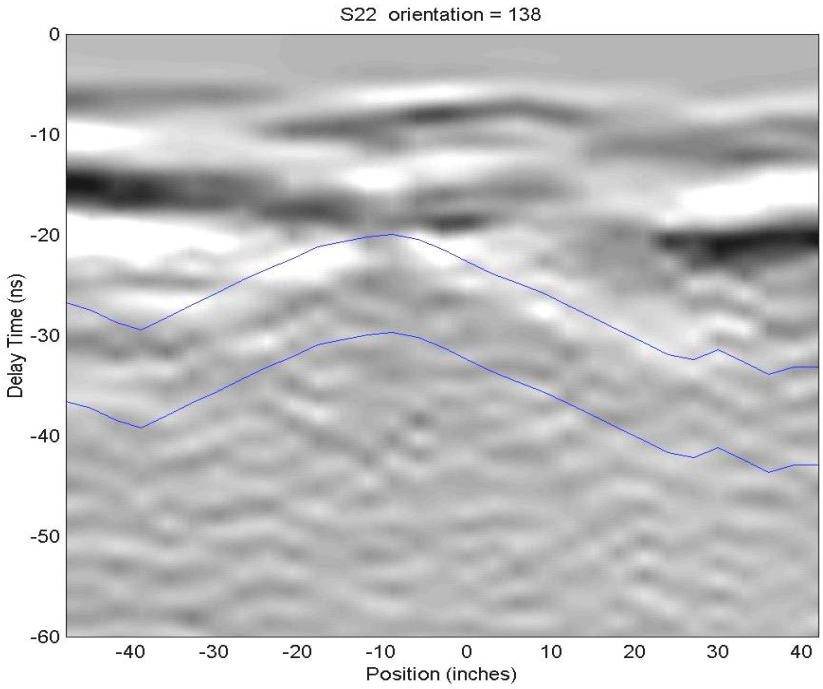

Figure 46c. S_{22} responses for Item 1-20.

Figure 46 GPR responses for Item 1-20 (WES 1-106), showing strong near surface clutter.

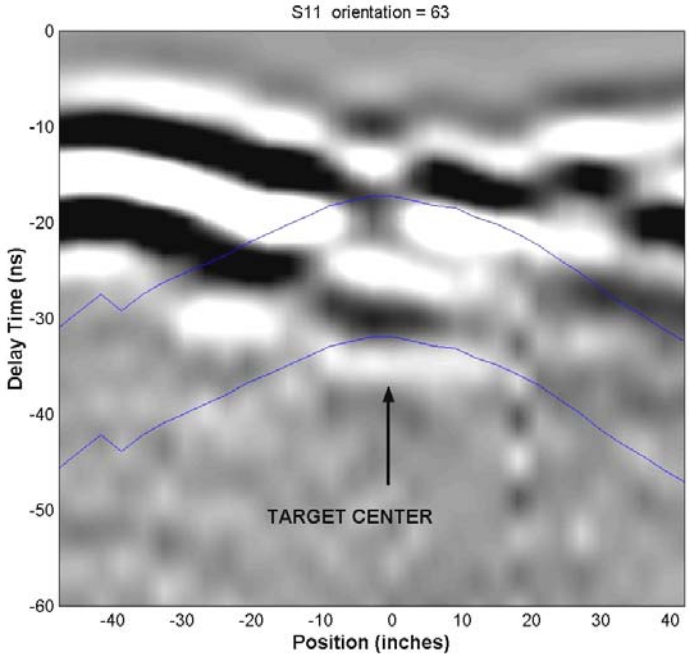

Figure **47**a. S_{11} responses for Item 1-56.

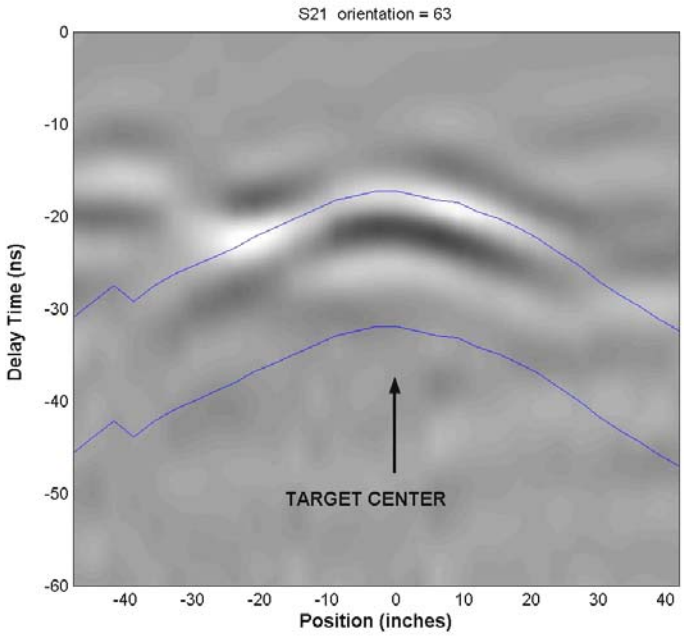

Figure **47**b. S_{21} responses for Item 1-56.

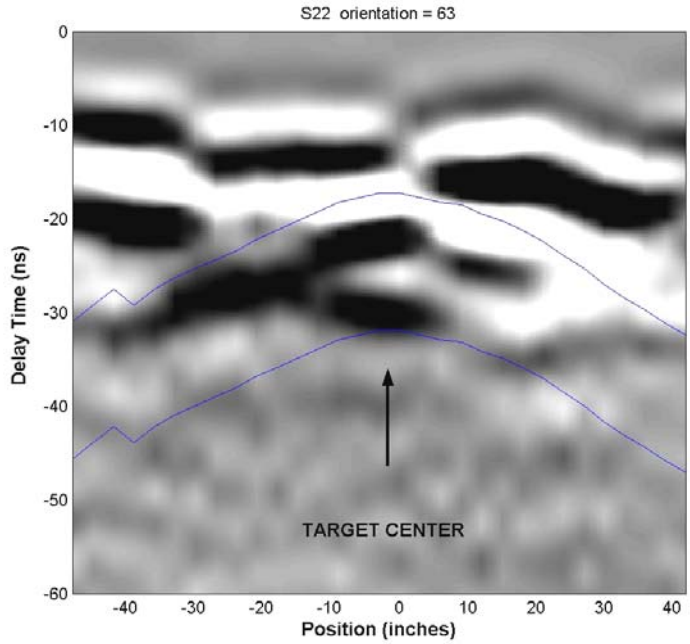

Figure **47**c. S_{22} responses for Item 1-56.

Figure 47. Filtered GPR Responses for Item 1-56 (WES 1-8), showing strong co-polarized clutter and small cross-pol clutter.

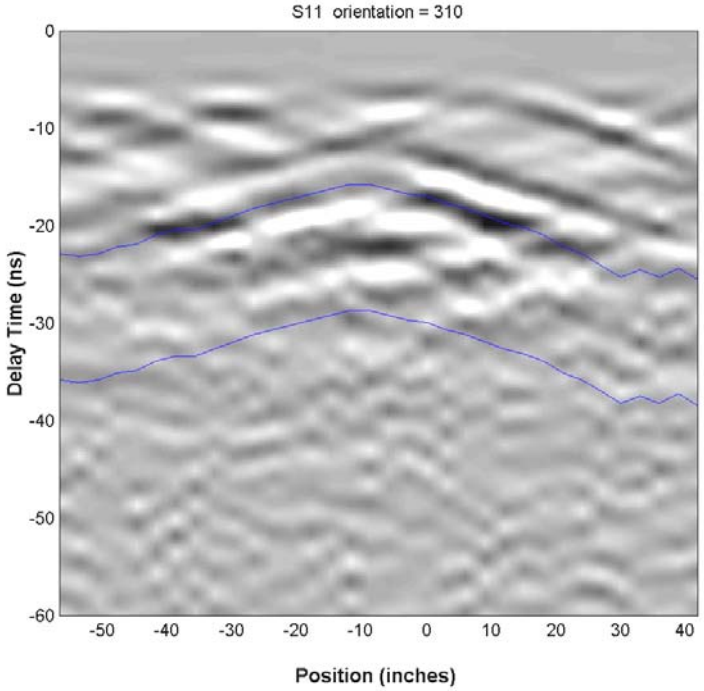

Figure 48a. S_{11} responses for Item 1-22.

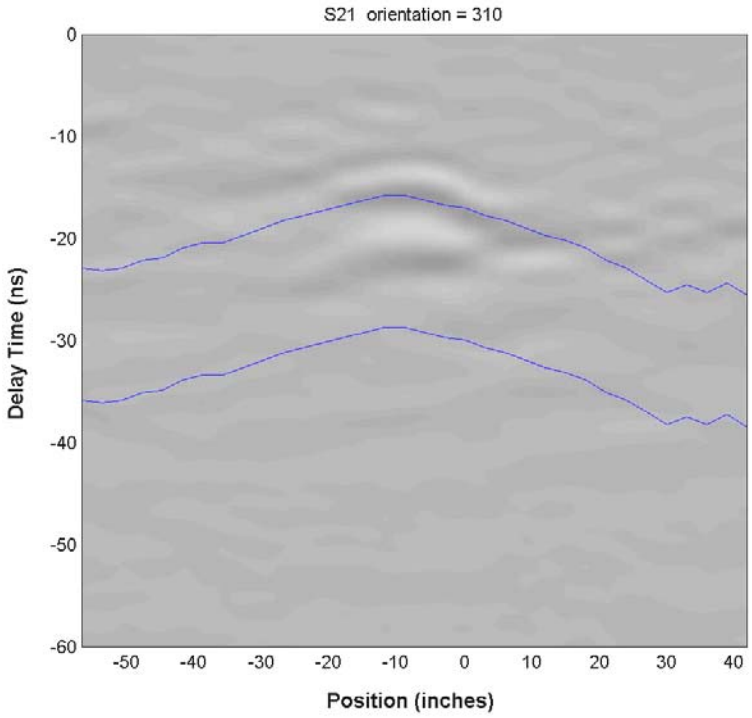

Figure 48b. S_{21} responses for item 1-22

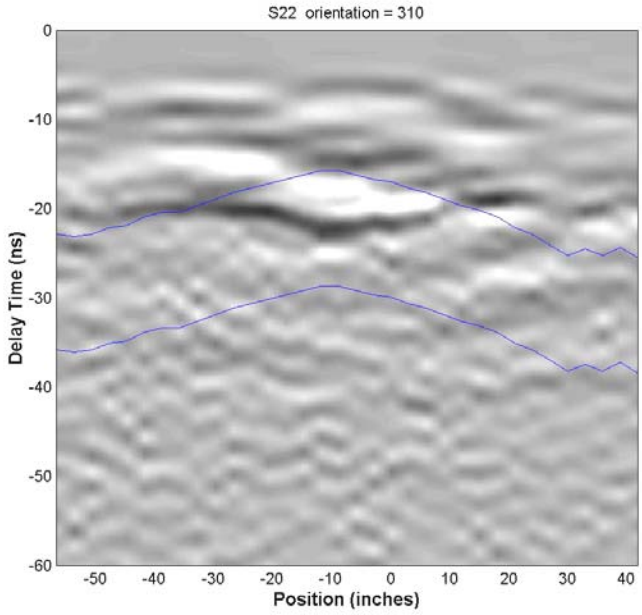

Figure 48c. S_{22} responses for Item 1-22

Figure 48. Filtered GPR responses for Item 1-22 (WES 1-176) , showing strong co-polarized clutter and small cross-pol clutter.

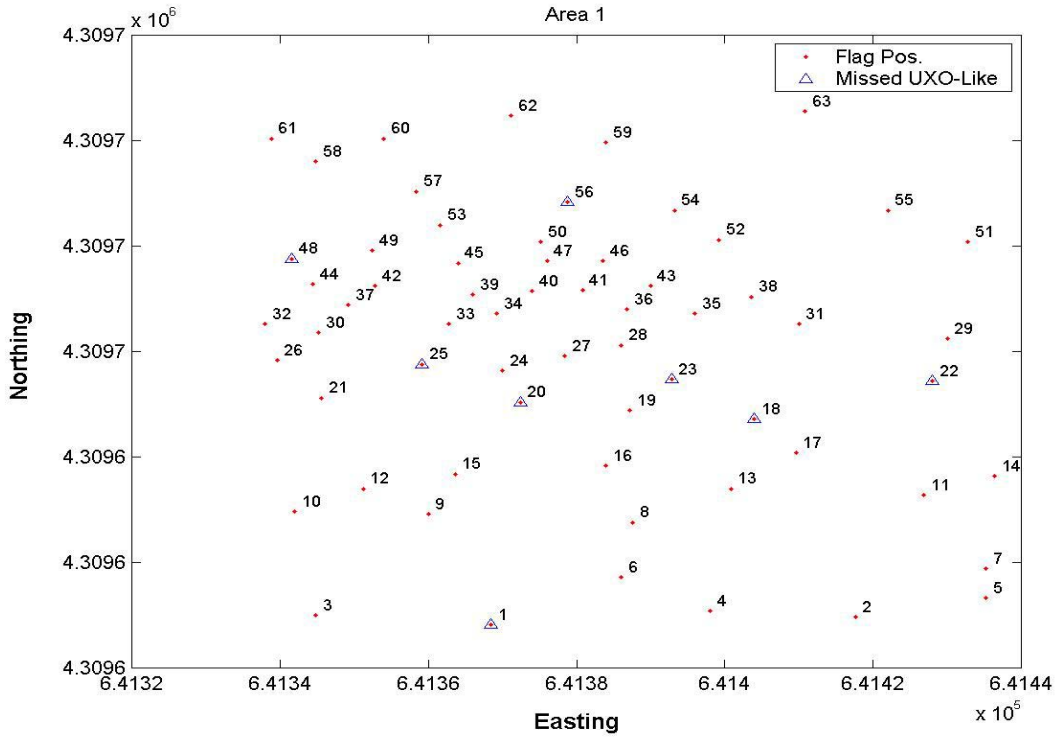

Figure 49 The positions of all items and of missed UXO-like items (LD2 criteria) in Area 1.

.

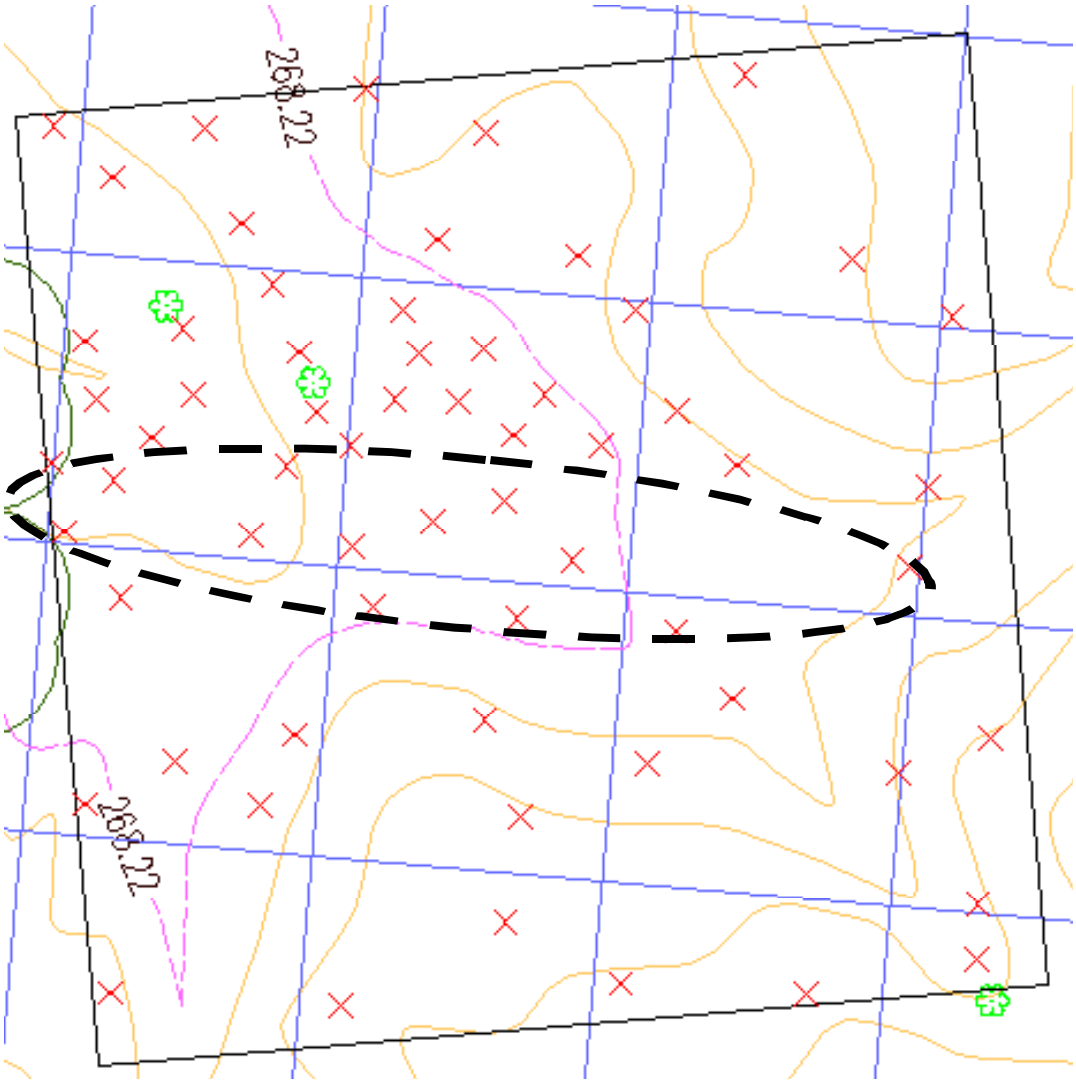

Figure 50. Contour plot of the terrain elevation in Area 1 (From ESTCP Document), showing depression.

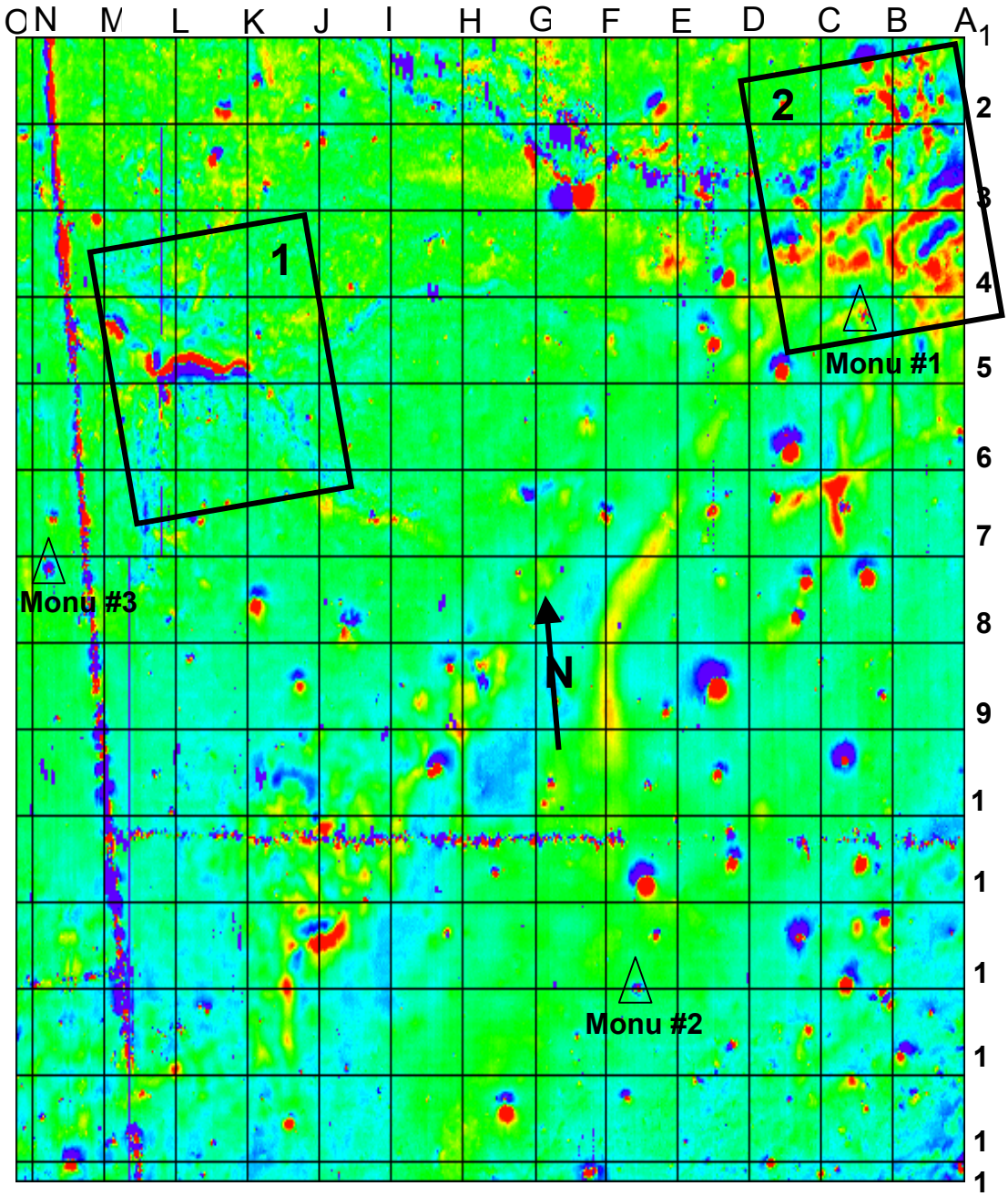

Figure 51. Mapping of the Magnetometer Data (From ESTCP Document).

Chapter 4 Summary and Concluding Discussion

At the outset, one should expect JPG to be a difficult site for GPR applications because of its fine-grained soil. The soil tends to retain water, especially after weather such as preceded our demo; and this causes the soil to absorb electromagnetic energy strongly. For instance, it was found that the current demo was unable to obtain meaningful responses from some items buried greater than 0.7 meters. However, if the only limitation of the site were reduced penetration depth due to signal absorption, this could be overcome by transmitting more power. The greater challenge posed by this kind of soil really lies in 1) its inhomogeneity caused by the presence of subsurface layers and disturbances introduced by humans, animals, or natural forces, and 2) the stronger production of clutter signals from such inhomogeneities in this kind of soil. Conditions are worsened by water flows through variations in surface contour and soil density. Such inhomogeneity results in a higher overall clutter level, complex clutter structures in the data, and increases in both false alarm and missed UXO rates. Nevertheless, the UWB full-polarimetric GPR system showed substantial discrimination capability, particularly relative to that provided with the ground truth, evidently from earlier (EMI) investigations (Figure 18).

The length-to-diameter (L/D) ratio has been used as a criterion to separate UXO-like and non-UXO items in the ground truth target list. In previous demos, the $L/D \geq 3$ criterion was used to designate UXO-like items. The items at JPG contain a type of 57mm projectile that has L/D ratio only about two. Three different criteria were applied for identifying UXO-like objects amongst the emplaced items: true UXO identity, $L/D \geq 3$ (LD3) and $L/D \geq 2$ (LD2). Considering realistic scenarios, the analysis of the causes of false alarms and missed UXO's only focused on results from Round 2 and the $L/D \geq 2$ criterion. Recall that the 1st round processing and classification utilized GPR signal features alone. The 2nd round incorporated the depth estimation from an EMI/MAG system to provide a delay time reference during feature extraction. The 3rd round incorporated the most accurate (ground truth) depth information as a delay time reference during processing. Reference to the EMI/MAG depths was incorporated because of lessons learned in the previous demos. In Section 1.1.1, such additional depth information was shown to improve the classification performance. There were only two cases where the 1st round results correctly classified UXO-like items which were later erroneously reclassified as non-UXO items, because of inaccurate EMI depths. In any case, the trend is quite clear: Particularly for soil conditions such as these, the more accurate the depth information that is drawn upon, the more successful our GPR classifications can be. Round 3 with the $L/D \geq 2$ criterion achieved a detection rate of almost 80% with a false alarm rate of 40%.

Examination of false alarms and missed UXO cases produced the following conclusions:

Causes of False Alarms:

(1) Ground scattering from oriented soil features, such as trenches or directional depressions, which produced elevated ELF values.
(2) Small vertical plate-like frag.
(3) Frag with thin extended parts (curved or non-curved), producing strongly directional response and resonance.

Causes of Missed UXO-like Items:

(1) Co-polarization channels for small, shallow targets were contaminated by the scattering from shallow soil layers and inhomogeneities.
(2) Incorrect depths estimated from EMI
(3) Weak target responses due to large depth, steep target inclination angles, and soil absorption.

A major cause of the classification error was the choice of frequency filter during the preprocessing stage. For a large UXO that resonate strongly, this is not a problem since the resonant peak is usually obvious in the late-time spectrum, i.e. in the frequency response obtained from the late-time region. The difficulty occurs for small items, especially when they are near the surface, where clutter often prevails. Several small UXO's were missed for this reason. Figure 52 and Figure 53 demonstrate how properly selected filters can affect the detection of the target response, which in turn affects the accuracy of the classification. The filter used in Figure 53 was centered at 280 MHz with a width of 260 MHz. Our previous processing approach relied on the visibility of the target "arcs" in the time-position plots generated from the whole band. Once such arcs are identified, an adaptive spatial filter and late-time spectrum are obtained and applied. A small object tends to scatter weakly, primarily in the high frequency region. Such a response then suffers from poor SCR in the time-position plot. The situation is worse for shallow targets, where surface scattering and near surface clutter can very well completely mask out target responses, especially when resolution is restricted by limited bandwidth. A few of possible improvement strategies are:

(1) Utilize the frequency domain data with background removed to select the proper center frequency of a band pass filter. This approach should work well for sandy, relatively undisturbed (homogeneous), and smooth soil.
(2) Utilize the EMI/MAG depth estimation. If the depth is shallow and no obvious target responses are observed in the GPR data, a high frequency bandpass filter should then be applied.

(3) Apply an additional, smaller antenna that operates in a higher frequency band. The advantage of this approach is that the footprint of the antenna can be made much smaller, which in turn reduces the surface clutter and achieves a better SCR.

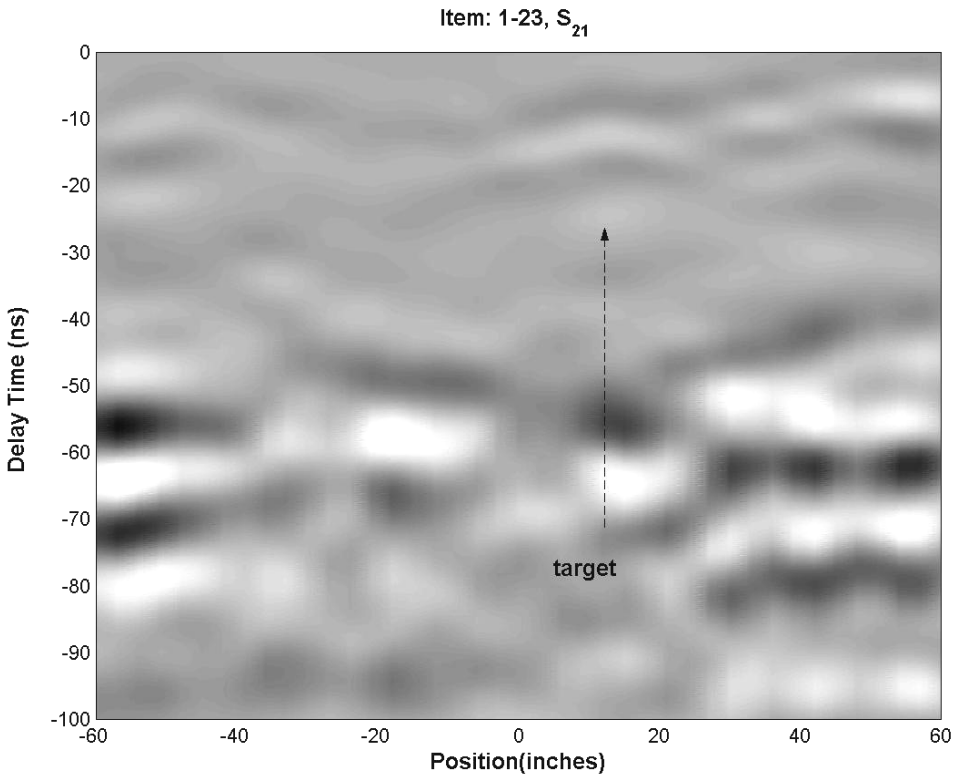

Figure 52. Typical time-position plot using the whole frequency band (10~410 MHz).

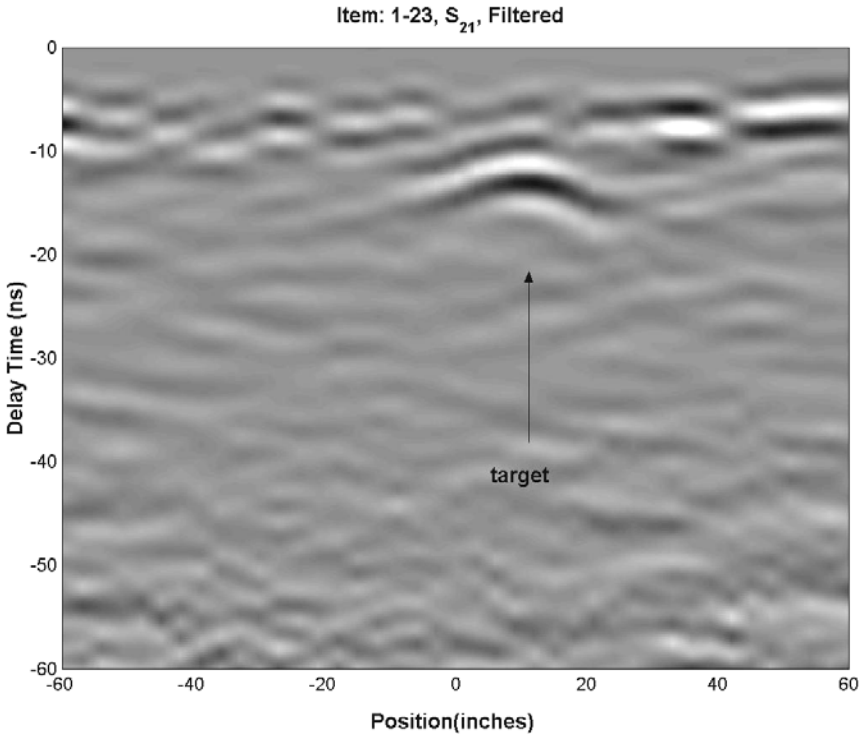

Figure 53. Time-position data after applying a sub-band filter(150~410 MHz).

Based on the above analysis, we estimate the maximum potential improvements that could be made on the performance displayed above, using the strategies suggested. That is, if (a) an effective system is developed for flagging cases that may feature small items requiring an optimized high frequency bandpass filter; and (b) EMI depth estimation is improved to the point where it reliably approximates the ground truth, then the classification performance would be improved as indicated in Table 17 and Figure 54 (refer to Sections 3.2.5 and 3.2.6).

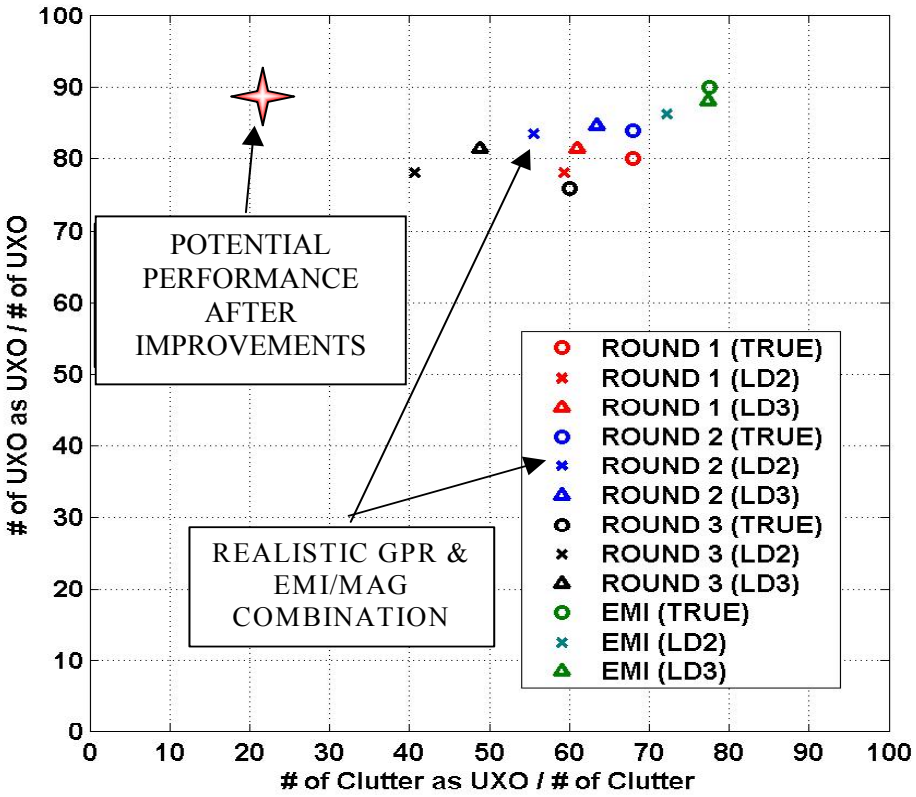

Figure 54 Potential GPR classification performance at JPG, after improvements (LD2 criteria). Table 17 shows the shifts in specific contributing scores that lead to the prediction.

Table 17 Potential GPR UXO classification performance ($L/D \geq 2$ Criteria) after improvements.

Total Number of UXO-Like (L/D >=2)	73
Total Number of Empty Sites	8
Total Number Fragments (Including one magnetic Rock)	19
Total Number of UXO-Like Classified as UXO-Like	61+3
Total Number of Clutter Classified as UXO-Like	15-9
Total Number Missed UXO-Like	12-3
Correctly Classified UXO Rate: $\frac{Number\ of\ UXO\ Classified\ as\ UXO}{Total\ Number\ of\ UXO}$	87.7%
False Classification Rate: $\frac{Number\ of\ Clutter\ Classified\ as\ UXO}{Total\ Number\ of\ Clutter}$	22.2%

The technology and processing we apply in our demos are meant to be used in the discrimination phase of UXO surveying. This means that we survey closely around each anomaly location that has been

provided in prior information. Use of flag locations [such as would be] provided by EMI/MAG surveying, and not by the ground truth, added both an element of actual site realism and a source of classification error, as discussed in Section 3.2.1. If the intent is to evaluate the upper limit of GPR discrimination performance, "other things being equal," then one might redo this test using ground truth position information. That would be tantamount to assuming the best possible (improved) position inference from the other technologies. Doubtless that would result in improved GPR classification performance. At this point, it is probably preferable to remain with the more realistic system of offsets actually or artificially representative of EMI/MAG positioning, while supporting any efforts to improve that positioning. Beyond this, features such as depth, orientation (azimuth and inclination) and “mass” from the EMI/MAG could be combined with GPR during surveying, data processing, and decision stages to obtain an optimal feature level "collaborative" processing. For instance, if an object is estimated to be a certain length by the GPR and has a certain mass according to EMI/MAG, one might be able to use this LENGTH-MASS feature to discriminate elongated frag from a UXO. Many empty cells that cause false alarms in GPR results could also be easily rejected based on EMI/MAG data.

A hint of the possible benefits from combining classification information from GPR and EMI is provided by Table 18. The targets are listed with UXO-like items first, followed by clutter items. The columns are color-coded: yellow = "actual" target type, i.e. according to a sorting of the ground truth by the LD2 criterion; beige = EMI classification; blue = GPR classification. The ultimately "correct" processing result, based on the LD2 criterion, is indicated by the color in the first column. When that color is yellow, both EMI and GPR agree on the correct answer. This covers a large portion of the cases. This in itself constitutes a positive result: When both technologies agree on the UXO-like judgment, one can have a high degree of confidence in the classification. When the first column is colored red, both technologies produced the wrong classification. In this instance, the scoring would not have been affected by this "collaborative" processing. The table also shows that when only one of the technologies correctly indicates that the target is UXO-like, the confidence assigned to that technology's result is generally high. Overall, in the great majority of such cases, the confidence level is at least equal to or greater than that of the erroneous technology. This suggests that, especially with dawning improvements in discrimination processing, guidance by high confidence detection by either technology could significantly reduce the missed UXO rate. The "dawning" improvements in discrimination techniques referred to are those now developing in the PI's SERDP work, entailing both GPR and EMI, as well as those from other sources. The principle flaw in this overall optimistic picture is the performance of both GPR and EMI technologies (Table 18) with reference to clutter items. In a substantial portion of the cases (red first column), both technologies "voted wrong." Regarding the 9 items in which one of the technologies correctly identified clutter correctly, there does not appear to be a clear correlation between

confidence level and which system is correct. Hopefully this picture will be improved in the next few years, as false alarm suppression is a high priority in a number of current UXO related projects.

In summary, considering all the adverse factors at the JPG site, the GPR classification performance achieved is quite encouraging. In the very least, we note that our UWB fully polarimetric GPR shows significant discrimination capability: The results reside securely above the "line of no discrimination" on the ROC chart. Overall, application of GPR technology to UXO classification has been advanced significantly over the sequence of ESTCP demos up to this point. From the perspective of measurement approach, we have moved from single position to multiple positions to multiple passes. From a data processing and feature extraction perspective, various techniques were developed to greatly enhance the signal-to-noise and signal-to-clutter ratios. That in turn improved the accuracy and stability of the extracted features. The set of signal features considered has been extended from a single natural resonance determination to additional polarization and spatial features, leading to comprehensive classification rules that account for many UXO and clutter variations. As far as soil type is concerned, the CRREL/OSU team has collected data in sand (Tyndall AFB), sandy clay (Blossom Point) and fine-grained/clayey soil (JPG).

The data from each demo was first carefully processed to produce "blind" classification, i.e. without reference either to ground truth or information from other sensors. Thereafter, valuable lessons were learned by studying (1) the value added by including extrinsic information, e.g. inferred or actual target depths; and (2) the reasons for false alarms and missed UXO's. Past lessons led to the improvements described above, and lessons learned here will be used to implement further improvements.

Table 18 Comparison of ID Results Between GPR and EMI (LD2 Criterion)

AREA	TAR #	WES #	UXO-Like (LD2)	EMI ID	EMI Conf.	GPR ID	GPR Conf.	Actual Target Description	True Azi.	True Incl.	True L	True Depth
1	60	4	1	1	H	1	L	Fragment	--	--	0.30	0.75
1	1	196	1	1	H	1	L	Fragment	--	--		1.2
1	4	198	1	1	H	1	H	Fragment	--	--		0.3
1	5	147	1	1	H	1	H	57mm Projectile	0	0	0.12	0.25
1	8	121/184	1	1	L	1	M	155mm Projectile	200	0	0.60	0.5
1	9	120	1	1	H	1	H	76mm Projectile	0	20	0.50	0.25
1	11	153	1	1	H	1	M	2.75" Rocket	0	90	0.41	0.76
1	15	62	1	1	H	1	L	Fragment	--	--		0.1
1	16	108	1	1	H	1	M	60mm Mortar	100	45	0.18	0.2
1	24	102	1	1	H	1	H	81mm Mortar	210	45	0.28	0.25
1	27	104	1	1	L	1	H	81mm Mortar	180	0	0.27	0.35
1	29	54	1	1	H	1	L	Fragment	--	--		0.5
1	30	96	1	1	H	1	H	81mm Mortar	330	35	0.27	0.15
1	31	118	1	1	H	1	M	5" Projectile	120	30	0.63	0.45
1	33	36	1	1	L	1	M	Fragment	--	--		0.15
1	35	170	1	1	H	1	H	Fragment	--	--		0.15
1	37	92	1	1	H	1	M	81mm Mortar	30	20	0.41	0.2
1	39	94	1	1	H	1	H	81mm Mortar	75	55	0.48	0.25
1	40	168	1	1	H	1	M	Fragment	--	--		0.25
1	46	40	1	1	H	1	H	Fragment	--	--		0.3
1	49	90	1	1	H	1	H	4.2" Mortar	270	0	0.18	0.35
1	50	100	1	1	H	1	H	60mm Mortar	195	30	0.52	0.2
1	51	162	1	1	L	1	H	Fragment	--	--		0.25
1	52	144	1	1	H	1	M	105mm Projectile	180	0	0.37	0.5
1	54	115	1	1	H	1	H	76mm Projectile	270	30	0.50	0.25
1	55	117/18	1	1	H	1	H	152mm Projectile	--	--	0.48	0.25
1	58	113/2	1	1	L	1	H	105mm Projectile	120	30	0.37	0.5
1	62	149	1	1	H	1	L	2.75" Rocket	30	55	0.41	0.5
2	2	108	1	1	H	1	H	Fragment	--	--		0.4
2	3	98	1	1	H	1	H	Fragment	--	--		0.3
2	5	72	1	1	H	1	H	Fragment	--	--		0.5
2	6	130	1	1	H	1	H	81mm Mortar		0	0.28	0.7
2	7	166/76	1	1	L	1	H	2.75" Rocket	180	20	0.41	0.75
2	8	152	1	1	H	1	M	57mm Projectile	90	0	0.12	0.25
2	9	124	1	1	H	1	L	60mm Mortar	330	10	0.18	0.2
2	11	128	1	1	H	1	H	60mm Mortar	95	20	0.18	0.1
2	12	120/88	1	1	L	1	H	60mm Mortar	270	0	0.18	0.3
2	14	140	1	1	H	1	L	105mm Projectile	330	10	0.37	0.7
2	16	116	1	1	H	1	H	81mm Mortar	45	0	0.28	0.3
2	18	42	1	1	H	1	H	Fragment	--	--		0.75

AREA	TAR #	WES #	UXO-Like (LD2)	EMI ID	EMI Conf.	GPR ID	GPR Conf.	Actual Target Description	True Azi.	True Incl.	True L	True Depth
2	20	164	1	1	H	1	H	2.75" Rocket	90	10	0.41	0.6
2	21	134	1	1	H	1	H	4.2" Mortar	0	0	0.52	0.4
2	22	132	1	1	L	1	M	5" Projectile	0	90	0.63	0.91
2	23	131/16	1	1	H	1	H	81mm Mortar	0	0	0.28	0.25
3	1	62/80	1	1	L	1	H	81mm Mortar	0	180	0.28	0.25
3	3	78	1	1	H	1	M	60mm Mortar	40	330	0.18	0.35
3	5	50/76	1	1	L	1	H	81mm Mortar	-90	--	0.28	0.2
1	12	119	1	1	H	0	L	152mm Projectile	270	30	0.48	0.4
1	18	122	1	1	H	0	H	5" Projectile	270	55	0.63	0.91
1	20	106	1	1	H	0	M	60mm Mortar	75	35	0.18	0.25
1	22	176	1	1	H	0	M	Fragment	--	--		0.15
1	23	142	1	1	H	0	M	57mm Projectile	265	45	0.12	0.15
1	25	132	1	1	H	0	L	57mm Projectile	180	0	0.12	0.25
1	32	30	1	1	H	0	H	Fragment	--	--		0.05
1	34	98	1	1	H	0	M	60mm Mortar	275	20	0.18	0.1
1	44	126	1	1	H	0	L	57mm Projectile	120	30	0.12	0.2
1	48	150	1	1	H	0	M	2.75" Rocket	275	45	0.41	0.7
1	56	8	1	1	H	0	L	Fragment	--	--		0.3
2	1	156	1	1	L	0	L	155mm Projectile	--	90	0.12	1.5
2	10	144	1	1	H	0	H	152mm Projectile	50	30	0.48	0.45
2	27	112	1	1	H	0	H	81mm Mortar	--	90	0.28	0.1
3	9	100	1	1	H	0	M	152mm Projectile	35	90	0.48	0.91

AREA	TAR #	WES #	UXO-Like (LD2)	EMI ID	EMI Conf.	GPR ID	GPR Conf.	Actual Target Description	True Azi.	True Incl.	True L	True Depth
1	7	74	1	0	L	1	H	Fragment	--	--		0.15
1	19	64	1	0	L	1	H	Fragment	--	--		0.2
1	21	152	1	0	L	1	H	2.75" Rocket	30	0	0.41	0.15
1	28	138	1	0	L	1	L	57mm Projectile	95	45	0.12	0.15
1	38	172	1	0	L	1	M	Fragment	--	--		0.3
1	41	136	1	0	H	1	L	155mm Projectile	90	75	0.60	0.5
1	47	38	1	0	L	1	H	Fragment	--	--		0.15
1	53	88	1	0	L	1	H	60mm Mortar	0	0	0.18	0.35
3	8	68/6	1	0	L	1	H	60mm Mortar	--	--	0.18	0.1
1	2	84	1	0	L	0	H	Fragment	--	--		0.1
1	17	66	0	1	L	1	M	Fragment	--	--		0.15
1	36	42	0	1	H	1	H	Fragment	--	--		0.35
1	42	28	0	1	H	1	L	Fragment	--	--		0.15
1	45	26	0	1	L	1	M	Fragment	--	--		0.075
1	61	158	0	1	H	1	H	Fragment	--	--		0.05
2	4	94	0	1	H	1	L	Fragment	--	--		0.35
2	15	46	0	1	H	1	M	Fragment	--	--		0.2
1	6	82	0	1	L	0	H	Fragment	--	--		0.1
1	10	180	0	1	H	0	M	Fragment	--	--		0.1
1	14	72	0	1	L	0	H	Fragment	--	--		0.1
1	26	164	0	1	H	0	H	Fragment	--	--		0.1
1	59	10	0	1	L	0	M	Fragment	--	--		0.1
2	13	36	0	1	H	0	M	Fragment	--	--		0.25
2	19	54	0	1	H	0	L	Fragment	--	--		0.2
1	3	78	0	0	L	1	H	Fragment	--	--		0.1
1	13	186	0	0	L	1	M	Fragment	--	--		0.1
1	57	6	0	0	L	0	H	Fragment	--	--		0.25
1	63	16	0	0	L	0	H	Fragment	--	--		0.05

Appendix A GPR UXO Classification Tables

A.1 Dig List Reported to ESTCP Before Access to Ground Truth

The following dig list include the following fields:

- **Area** – JPG test areas.
- **Item # -** Target number designated for CRREL/OSU GPR test.
- **WES # -** Target number designated by WES.
- **Northing –** GPS position (latitude).
- **Easting** – GPS position (longitude).
- **GPR ID** – UXO-like(1) /non-UXO(0) designation based on GPR features.
- **Confidence Level** – (H) high confidence (M) moderate confidence (L) low confidence.
- **ETO** – Estimated target orientation (azimuth).
- **CNR (NP/ns)** – Damping factor of the complex natural resonance.
- **CNR (GHz)** – Resonant frequency of the complex natural resonance.
- **ETL** – Estimated target length.
- **DEP** – Estimated target depth.
- **Late-Time ELF(t)** – Estimated linear factor extracted from late-time time-domain response.
- **Late-Time ELF(f)** –Estimated linear factor extracted from late-time spectrum.
- **Early-time ELF** – Estimated linear factor extracted form early-time response.
- **Special Comment** – Special notes observed from the processing.

The dig list is prioritized using the following order:

Confidence Level -> Late-time ELF(t) -> Late-time ELF(f) -> Early-time ELF.

Table 19 Extracted Features and Classification Results for Blind Targets in JPGV (First Round).

Area	Item #	WES #	Northing	Easting	GPR ID	Conf.	ETO (o)	CNR (NP/ns)	CNR (GHz)	ETL (m)	DEP (m)	Late-Time ELF(t)	Late-Time ELF(f)	Early-Time ELF	Special Comment
1	21	196	4309651.2	641345.6	1	H	-165	0.07	0.072	0.48	0.32	0.99	0.98	0.95	
1	54	84	4309686.8	641393.2	1	H	110	0.10	0.064	0.50	0.68	0.98	0.91	0.91	
2	5	78	4309668.8	641623.2	1	H	144	0.07	0.082	0.36	0.58	0.97	0.98	0.56	
1	49	198	4309679.2	641352.4	1	H	-67	0.05	0.070	0.46	0.59	0.96	0.98	0.89	
2	2	147	4309656.8	641672.4	1	H	155	0.08	0.058	0.52	0.59	0.95	0.90	0.91	
1	35	82	4309667.2	641396.0	1	H	-127	0.03	0.048	0.71	0.24	0.93	0.82	0.71	
1	4	74	4309610.8	641398.0	1	H	-40	0.06	0.069	0.41	0.46	0.92	0.86	0.76	
2	7	121/184	4309675.6	641640.8	1	H	100	0.13	0.117	0.26	0.40	0.92	0.95	0.44	40" Offset 190 Deg.
1	51	120	4309680.8	641432.8	1	H	-26	0.04	0.076	0.40	0.45	0.92	0.99	0.78	
2	11	180	4309687.2	641691.6	1	H	-60	0.08	0.141	0.21	0.29	0.91	0.99	0.72	
3	10	153	4309878.2	641613.7	1	H	-38	0.02	0.044	0.57	0.04	0.91	0.83	0.18	Deep
1	50	119	4309680.8	641375.2	1	H	3	0.19	0.084	0.38	0.52	0.91	0.98	0.61	
2	12	186	4309688.4	641704.8	1	H	157	0.14	0.126	0.24	0.39	0.91	0.80	1.00	
1	39	72	4309670.8	641366.0	1	H	-88	0.05	0.047	0.66	0.68	0.91	0.99	0.34	
2	26	62	4309738.6	641699.3	1	H	-177	0.03	0.078	0.36	0.73	0.90	1.00	0.71	
1	27	108	4309659.2	641378.4	1	H	33	0.06	0.078	0.41	0.46	0.90	0.91	0.84	Strange? Vertical Plate?
3	1	66	4309818.0	641633.6	1	H	-179	0.06	0.079	0.33	0.37	0.89	0.93	0.92	
3	5	122	4309843.2	641664.0	1	H	-50	0.06	0.064	0.40	0.39	0.88	0.90	0.93	
2	21	64	4309731.2	641702.4	1	H	-115	0.02	0.051	0.60	0.55	0.88	0.94	0.89	
2	23	106	4309734.0	641654.4	1	H	-39	0.14	0.108	0.28	0.45	0.88	0.77	0.37	
2	6	152	4309671.6	641700.8	1	H	-74	0.06	0.074	0.40	0.40	0.86	0.70	0.97	
1	53	176	4309684.0	641361.6	1	H	172	0.17	0.115	0.26	0.82	0.86	0.84	0.58	
3	8	142	4309867.6	641623.2	1	H	17	0.08	0.058	0.46	0.26	0.86	0.88	0.82	
1	36	102	4309668.0	641386.8	1	H	30	0.18	0.134	0.24	0.45	0.83	0.72	0.29	Shallow & Small
1	58	132	4309696.0	641344.8	1	H	-62	0.11	0.045	0.72	0.67	0.83	0.76	0.38	
1	46	164	4309677.2	641383.6	1	H	180	0.09	0.078	0.43	0.37	0.83	0.71	0.69	
2	3	104	4309660.4	641624.4	1	H	-175	0.05	0.068	0.44	0.59	0.78	0.98	0.72	
2	20	138	4309724.8	641621.6	1	H	-172	0.06	0.086	0.34	0.79	0.78	0.93	0.57	30" Offset, 33 Deg.
2	16	54	4309707.6	641707.6	1	H	-140	0.06	0.088	0.35	0.37	0.77	0.87	0.51	
1	7	96	4309618.8	641435.2	1	H	-112	0.08	0.084	0.33	0.37	0.77	0.93	0.86	
2	18	118	4309714.4	641666.8	1	H	-147	0.05	0.064	0.47	0.89	0.76	0.72	0.83	
1	55	30	4309686.8	641422.0	1	H	101	0.11	0.114	0.28	0.40	0.75	0.83	0.37	
1	24	36	4309656.4	641370.0	1	H	41	0.08	0.084	0.37	0.39	0.72	0.75	0.53	
1	19	98	4309648.8	641387.2	1	H	-148	0.04	0.094	0.36	0.16	0.70	0.46	0.45	
1	47	170	4309677.2	641376.0	1	H	-109	0.05	0.056	0.50	0.40	0.66	0.70	0.87	30" Mag. Offset 155Deg.
1	9	42	4309629.2	641360.0	1	H	16	0.05	0.063	0.44	0.42	0.59	0.43	0.87	
2	22	92	4309733.2	641686.8	1	H	69	0.08	0.074	0.41	1.10	0.36	0.65	0.65	
1	26	172	4309658.4	641339.6	1	M	171	0.10	0.059	0.55	0.56	0.98	0.90	0.05	
1	37	94	4309668.8	641349.2	1	M	-153	0.05	0.070	0.44	0.39	0.96	0.91	0.57	
1	40	168	4309671.4	641374.0	1	M	-95	0.21	0.143	0.19	0.37	0.94	0.89	0.75	35" Offset, 0 Deg.
1	52	136	4309681.2	641399.2	1	M	164	0.15	0.088	0.38	0.66	0.91	0.97	0.21	
1	3	28	4309610.0	641344.8	1	M	115	0.09	0.104	0.31	0.73	0.91	1.00	0.89	
2	8	154	4309680.4	641694.0	1	M	20	0.14	0.123	0.24	0.40	0.88	0.79	0.79	Near Surface

Area	Item #	WES #	Northing	Easting	GPR ID	Conf.	ETO (o)	CNR (NP/ns)	CNR (GHz)	ETL (m)	DEP (m)	Late-Time ELF(t)	Late-Time ELF(f)	Early-Time ELF	Special Comment
1	15	126	4309636.8	641363.6	1	M	73	0.12	0.120	0.28	0.38	0.80	0.82	0.50	Small, Near Surface
1	45	26	4309676.8	641364.0	1	M	-171	0.08	0.146	0.19	0.30	0.78	0.77	0.31	
1	31	40	4309665.2	641410.0	1	M	168	0.06	0.033	0.96	0.78	0.77	0.84	0.52	
2	15	38	4309706.4	641673.6	1	M	-47	0.10	0.112	0.27	0.37	0.75	0.67	0.36	
2	4	150	4309662.0	641697.6	1	M	167	0.26	0.080	0.38	0.42	0.69	0.59	0.31	Shallow
1	38	90	4309670.4	641403.6	1	M	-112	0.04	0.087	0.37	0.57	0.61	0.70	0.35	
3	3	100	4309830.4	641650.8	1	M	-28	0.10	0.095	0.28	0.46	0.60	0.81	0.85	
1	8	162	4309627.6	641387.6	1	M	-173	0.10	0.105	0.31	0.68	0.32	0.70	0.65	
1	48	144	4309677.6	641341.6	1	L	91	0.01	0.019	1.65	0.74	0.98	0.89	0.38	Ditch
2	14	88	4309704.8	641684.8	1	L	-61	0.06	0.017	1.73	0.75	0.95	0.85	0.86	
1	32	115	4309665.2	641338.0	1	L	79	0.03	0.046	0.68	0.30	0.93	0.93	0.60	Deep
1	2	117/18	4309609.6	641417.6	1	L	56	0.05	0.044	0.68	0.92	0.92	0.89	0.78	Deep
1	60	8	4309700.4	641354.0	1	L	-101	0.08	0.031	1.01	0.87	0.91	0.54	0.42	
1	43	6	4309672.5	641390.0	1	L	93	0.04	0.099	0.35	0.34	0.90	0.62	0.24	
3	7	113/2	4309857.5	641610.5	1	L	-68	0.02	0.110	0.22	0.95	0.83	0.16	0.41	deep
1	59	10	4309699.6	641384.0	1	L	153	0.01	0.048	0.63	1.08	0.82	1.00	0.40	
3	2	4	4309827.5	641671.1	1	L	123	0.06	0.064	0.41	0.20	0.80	0.81	0.33	
1	41	158	4309671.6	641380.8	1	L	-145	0.03	0.059	0.51	0.42	0.73	0.63	0.65	
1	42	149	4309672.4	641352.8	1	L	154	0.13	0.178	0.17	0.36	0.73	0.38	0.39	
2	1	16	4309654.8	641626.4	1	L	-156	0.02	0.063	0.47	0.80	0.70	0.54	0.38	Poor SCR
1	30	156	4309663.6	641345.2	1	L	-9	0.05	0.072	0.45	0.45	0.69	0.47	0.63	
2	9	108	4309683.2	641622.4	1	L	32	0.27	0.172	0.18	0.39	0.62	0.71	0.47	Near Surface
1	16	98	4309638.4	641384.0	1	L	-59	0.20	0.117	0.28	0.69	0.60	0.73	0.52	
1	34	94	4309667.2	641369.2	1	L	116	0.05	0.080	0.37	0.80	0.56	0.73	0.62	Weak
2	24	72	4309735.9	641640.4	1	L	21	0.07	0.053	0.57	0.82	0.54	0.66	0.95	
1	63	130	4309705.6	641410.8	1	L	21	0.09	0.050	0.64	1.98	0.53	0.85	0.22	Deep
1	44	166/76	4309672.8	641344.4	1	L	136	0.11	0.073	0.47	0.36	0.43	0.59	0.47	Near Tree, Corrected Site
2	19	152	4309716.8	641690.0	1	L	118	0.10	0.083	0.36	0.24	0.41	0.35	0.26	
2	17	124	4309712.5	641627.9	1	L	110	0.08	0.061	0.49	0.78	0.39	0.73	0.55	Poor SCR
1	25	144	4309657.6	641359.2	1	L	27	0.06	0.066	0.45	0.52	0.18	0.47	0.61	Subsurface Dip
2	25	128	4309735.9	641675.6	0	L	-106	0.01	0.028	1.06	1.08	0.40	0.28	0.88	Deep, 20" offset 256 deg.
1	12	120/88	4309634.0	641351.2	0	L	163	0.04	0.040	0.80	0.93	0.86	0.61	0.59	
3	6	36	4309857.1	641665.8	0	L	-100	0.05	0.082	0.32	0.74	0.61	0.43	0.58	
1	33	140	4309665.2	641362.8	0	L	-155	0.01	0.022	1.54	1.07	0.10	0.10	0.58	deep
1	56	46	4309688.4	641378.8	0	L	157	0.13	0.129	0.24	0.42	0.33	0.40	0.47	
2	13	116	4309703.6	641631.6	0	L	-167	0.13	0.122	0.26	0.11	0.39	0.25	0.33	
1	61		4309700.4	641338.8	0	L	155	0.07	0.097	0.32	1.69	0.13	0.52	0.24	Sursurface Water Accum.
1	62	42	4309704.8	641371.2	0	L	-96	0.06	0.086	0.38	0.26	0.61	0.49	0.20	Shallow (-10)
1	29	54	4309662.4	641430.0	0	L	-179	0.23	0.268	0.13	0.21	0.82	0.74	0.18	
1	23	164	4309654.8	641392.8	0	M	15	0.24	0.188	0.18	0.10	0.22	0.08	0.64	Near Surface (+10)
3	9	134	4309869.6	641658.4	0	M	40	0.05	0.067	0.37	0.56	0.20	0.48	0.34	
1	11	132	4309632.8	641426.8	0	M	96	0.05	0.076	0.41	0.35	0.19	0.15	0.20	
1	14	131/16	4309636.4	641436.4	0	M	90	0.16	0.068	0.50	0.15	0.46	0.60	0.20	
1	20		4309650.4	641372.4	0	M	136	0.05	0.064	0.48	0.39	0.32	0.26	0.19	
1	17		4309640.8	641409.6	0	M	-42	0.07	0.099	0.35	0.48	0.41	0.39	0.15	Shallow
1	10		4309629.6	641342.0	0	M	56	0.25	0.053	0.61	0.27	0.19	0.01	0.08	
1	13	112	4309634.0	641400.8	0	M	-60	0.13	0.069	0.40	0.35	0.90	0.85	0.02	

Area	Item #	WES #	Northing	Easting	GPR ID	Conf.	ETO (o)	CNR (NP/ns)	CNR (GHz)	ETL (m)	DEP (m)	Late-Time ELF(t)	Late-Time ELF(f)	Early-Time ELF	Special Comment
1	1	62/80	4309608.1	641368.5	0	M	0	0.00	0.000	0.00	0.00	0.00	0.00	0.00	Refilled Trench
1	22	110	4309654.4	641428.0	0	H	-105	0.12	0.100	0.27	0.83	0.41	0.36	0.13	
2	27	78	4309743.6	641696.0	0	H	-62	0.09	0.100	0.30	0.09	0.40	0.23	0.09	Shallow Plate
2	10		4309686.4	641638.0	0	H	150	0.14	0.126	0.24	0.37	0.35	0.10	0.18	
1	6	50/76	4309617.2	641386.0	0	H	132	0.18	0.096	0.33	0.67	0.31	0.01	0.19	
1	57		4309690.4	641358.4	0	H	137	0.18	0.125	0.26	0.09	0.23	0.11	0.38	Near Surface, Deep Anomaly
1	18		4309647.2	641404.0	0	H	-177	0.14	0.054	0.53	0.57	0.11	0.03	0.15	plate
1	5	68/6	4309613.2	641435.2	0	H	48	0.07	0.060	0.56	0.69	0.02	0.24	0.20	
1	28	100	4309661.2	641386.0	0	H	0	0.00	0.000	0.00	0.00	0.00	0.00	0.00	Empty
3	4		4309838.0	641608.7	0	H	0	0.00	0.000	0.00	0.00	0.00	0.00	0.00	Empty

Table 20 Extracted Features and Classification Results for Blind Targets in JPGV Incorporating Depth Estimation from Magnetic Sensors (Round 2).

GREEN - Changed from First Round Using EMI Feedback

Yello - Changed Without Using EMI Feedback

Red - Believed To Be An Additional Target

Gray - Responses Are Extremely Weak or Buried Under Clutter

Item #	GPR ID	Conf.	ETO (°)	CNR (NP/ns)	CNR (GHz)	ETL (m)	DEP (m)	Late-Time ELF(t)	Late-Time ELF(f)	Early-Time ELF	EMI Depth Estimate
2-26	1	H	-177	0.03	0.078	0.36	0.73	1.00	0.90	0.71	0.35
1-51	1	H	-26	0.04	0.076	0.40	0.45	0.99	0.92	0.78	0.213
1-47	1	H	66	0.04	0.083	0.36	0.42	0.99	1.00	0.95	0
1-39	1	H	-88	0.05	0.047	0.66	0.68	0.99	0.91	0.34	0.399
2-11	1	H	-60	0.08	0.141	0.21	0.29	0.99	0.91	0.72	0.215
1-21	1	H	-165	0.07	0.072	0.48	0.32	0.98	0.99	0.95	0.0141
2-3	1	H	-175	0.05	0.068	0.44	0.59	0.98	0.78	0.72	0.262
2-5	1	H	144	0.07	0.082	0.36	0.58	0.98	0.97	0.56	0.417
1-5	1	H	49	0.09	0.127	0.27	0.14	0.98	0.92	0.68	0.197
1-49	1	H	-67	0.05	0.070	0.46	0.59	0.98	0.96	0.89	0.315
1-50	1	H	3	0.19	0.084	0.38	0.52	0.98	0.91	0.61	0.237
1-30	1	H	179	0.08	0.075	0.37	0.49	0.96	0.92	0.46	0.209
2-7	1	H	100	0.13	0.117	0.26	0.40	0.95	0.92	0.44	0.401
2-21	1	H	-115	0.02	0.051	0.60	0.55	0.94	0.88	0.89	0.317
1-61	1	H	-120	0.07	0.087	0.36	0.15	0.94	0.95	0.74	0.187
1-7	1	H	-112	0.08	0.084	0.33	0.37	0.93	0.77	0.86	0.341
2-20	1	H	-172	0.06	0.086	0.34	0.79	0.93	0.78	0.57	0.408
3-1	1	H	-179	0.06	0.079	0.33	0.37	0.93	0.89	0.92	0.21
1-54	1	H	110	0.10	0.064	0.50	0.68	0.91	0.98	0.91	0.372
1-27	1	H	33	0.06	0.078	0.41	0.46	0.91	0.90	0.84	0.163
2-2	1	H	155	0.08	0.058	0.52	0.59	0.90	0.95	0.91	0.294
3-5	1	H	-50	0.06	0.064	0.40	0.39	0.90	0.88	0.93	0.195
3-8	1	H	17	0.08	0.058	0.46	0.26	0.88	0.86	0.82	0.0432

Item #	GPR ID	Conf.	ETO (°)	CNR (NP/ns)	CNR (GHz)	ETL (m)	DEP (m)	Late-Time ELF(t)	Late-Time ELF(f)	Early-Time ELF	EMI Depth Estimate
2-16	1	H	-140	0.06	0.088	0.35	0.37	0.87	0.77	0.51	0.135
1-4	1	H	-40	0.06	0.069	0.41	0.46	0.86	0.92	0.76	0.193
1-53	1	H	172	0.17	0.115	0.26	0.82	0.84	0.86	0.58	0
1-55	1	H	101	0.11	0.114	0.28	0.40	0.83	0.75	0.37	0.292
1-35	1	H	-127	0.03	0.048	0.71	0.24	0.82	0.93	0.71	0.0895
2-12	1	H	157	0.14	0.126	0.24	0.36	0.80	0.91	1.00	0.0922
2-23	1	H	-39	0.14	0.108	0.28	0.45	0.77	0.88	0.37	0.284
1-58	1	H	-62	0.11	0.045	0.72	0.67	0.76	0.83	0.38	0.359
1-24	1	H	41	0.08	0.084	0.37	0.39	0.75	0.72	0.53	0.215
1-36	1	H	30	0.18	0.134	0.24	0.45	0.72	0.83	0.29	0.293
2-18b	1	H	-147	0.05	0.064	0.47	0.89	0.72	0.76	0.83	0.0473
1-46	1	H	180	0.09	0.078	0.43	0.37	0.71	0.83	0.69	0.2
2-6	1	H	-74	0.06	0.074	0.40	0.40	0.70	0.86	0.97	0.169
1-19	1	H	-148	0.04	0.094	0.36	0.16	0.46	0.70	0.45	0.0116
1-9	1	H	16	0.05	0.063	0.44	0.42	0.43	0.59	0.87	0.246
1-11	1	M	-3	0.11	0.093	0.33	0.63	0.99	0.98	0.57	0.601
1-52	1	M	164	0.15	0.088	0.38	0.66	0.97	0.91	0.21	0.408
1-33	1	M	-166	0.18	0.177	0.13	0.13	0.94	0.93	0.56	0
1-37	1	M	-153	0.05	0.070	0.44	0.39	0.91	0.96	0.57	0.299
1-26	1	M	171	0.10	0.059	0.55	0.56	0.90	0.98	0.05	0.425
1-40	1	M	-95	0.21	0.143	0.19	0.37	0.89	0.94	0.75	0.147
1-31	1	M	168	0.06	0.033	0.96	0.78	0.84	0.77	0.52	0.444
2-22	1	M	-31	0.04	0.035	0.93	1.00	0.82	0.75	0.93	0.681
3-3	1	M	-28	0.10	0.095	0.28	0.46	0.81	0.60	0.85	0.236
2-8	1	M	20	0.14	0.123	0.24	0.14	0.79	0.88	0.79	0.0624
1-8	1	M	-173	0.09	0.086	0.35	0.53	0.78	0.39	0.49	0.424
1-45	1	M	-171	0.08	0.146	0.19	0.30	0.77	0.78	0.31	0
2-15	1	M	-47	0.10	0.112	0.27	0.37	0.67	0.75	0.36	0.228
1-38	1	M	-112	0.03	0.088	0.39	0.14	0.66	0.56	0.37	0.291
1-29	1	L	-174	0.09	0.090	0.34	0.42	0.98	0.72	0.56	0.557
1-16	1	L	-59	0.07	0.130	0.26	0.25	0.91	0.93	0.43	0.169
1-2b	1	L	56	0.05	0.044	0.68	0.92	0.89	0.92	0.78	0.341
1-59	1	L	61	0.03	0.117	0.29	0.11	0.89	0.16	0.22	0
1-34	1	L	160	0.18	0.143	0.22	0.33	0.87	0.95	0.28	0.211
1-41	1	L	-8	0.07	0.032	0.92	0.57	0.86	0.69	0.27	0.777
2-1	1	L	67	0.01	0.104	0.29	2.09	0.86	0.34	0.23	1.5
2-14	1	L	-61	0.06	0.017	1.73	0.75	0.85	0.95	0.86	0.65
1-2	1	L	39	0.03	0.101	0.30	0.60	0.84	0.14	0.65	0.341
1-28	1	L	-110	0.05	0.088	0.37	0.27	0.82	0.58	0.30	0.319
1-15	1	L	73	0.12	0.120	0.28	0.12	0.82	0.80	0.50	0.128
3-2	1	L	123	0.06	0.064	0.41	0.20	0.81	0.80	0.33	0.15
1-42	1	L	-121	0.12	0.043	0.74	2.14	0.81	0.95	0.52	1.82
2-17	1	L	110	0.12	0.078	0.38	0.76	0.78	0.51	0.62	0.5
1-62	1	L	-103	0.04	0.058	0.52	0.94	0.77	0.83	0.68	0.635
2-9	1	L	32	0.27	0.172	0.18	0.14	0.71	0.62	0.47	0
2-24	1	L	21	0.07	0.053	0.57	0.82	0.66	0.54	0.95	1.5
1-63	1	L	-10	0.06	0.069	0.44	0.17	0.63	0.64	0.19	0.227

Item #	GPR ID	Conf.	ETO (°)	CNR (NP/ns)	CNR (GHz)	ETL (m)	DEP (m)	Late-Time ELF(t)	Late-Time ELF(f)	Early-Time ELF	EMI Depth Estimate
1-43	1	L	93	0.04	0.099	0.35	0.34	0.62	0.90	0.24	0.25
1-44	1	L	136	0.11	0.073	0.47	0.36	0.59	0.43	0.47	0.305
1-12	1	L	-100	0.02	0.032	0.95	0.74	0.55	0.61	0.62	0.469
1-32	1	L	80	0.07	0.072	0.45	0.32	0.55	0.58	0.11	0.179
1-60	1	L	-101	0.08	0.031	1.01	0.87	0.54	0.91	0.42	0.623
2-4	1	L	171	0.15	0.090	0.36	0.18	0.52	0.61	0.30	0.141
2-19	1	L	118	0.10	0.083	0.36	0.24	0.35	0.41	0.26	0.0841
3-7b	1	L	60	0.03	0.080	0.31	0.95	0.30	0.08	0.75	0.55
2-25	1	L	-106	0.01	0.028	1.06	1.08	0.28	0.40	0.88	0.55
3-10	0	L	-38	0.35	0.190	0.13	0.54	0.83	0.55	0.18	0.25
1-56	0	L	157	0.13	0.129	0.24	0.42	0.40	0.33	0.47	0.304
1-14	0	L	130	0.07	0.065	0.47	0.36	0.39	0.58	0.17	0.39
3-7	0	L	45	0.12	0.083	0.31	0.59	0.30	0.21	0.19	0.55
1-22	0	L	126	0.23	0.180	0.19	0.48	0.28	0.27	0.23	0.38
2-13	0	L	-167	0.13	0.122	0.26	0.11	0.25	0.39	0.33	0.182
1-25	0	L	-125	0.32	0.138	0.21	0.09	0.17	0.09	0.15	0.0987
3-4	0	L	90	0.07	0.071	0.35	0.82	0.12	0.26	0.50	1.15
3-6	0	L	58	0.09	0.072	0.40	0.19	0.07	0.35	0.14	0.25
1-13	0	M	-60	0.13	0.069	0.40	0.35	0.85	0.90	0.02	0.435
3-9	0	M	40	0.05	0.067	0.37	0.56	0.48	0.20	0.34	0.631
1-17	0	M	-42	0.07	0.099	0.35	0.48	0.39	0.41	0.15	0.503
1-20	0	M	136	0.05	0.064	0.48	0.39	0.26	0.32	0.19	0.335
1-1	0	M	-45	0.31	0.170	0.18	0.05	0.10	0.14	0.04	0.0514
1-23	0	M	15	0.24	0.188	0.18	0.10	0.08	0.22	0.64	0.0944
1-48	0	M	93	0.02	0.067	0.47	0.40	0.03	0.10	0.38	0.433
1-10	0	M	56	0.25	0.053	0.61	0.08	0.01	0.19	0.08	0
1-3	0	H	-155	0.44	0.125	0.25	0.36	0.38	0.29	0.48	0.154
2-18	0	H	87	0.27	0.080	0.33	0.07	0.28	0.02	0.21	0.0473
2-27	0	H	-62	0.09	0.100	0.30	0.09	0.23	0.40	0.09	0.228
1-57	0	H	137	0.18	0.125	0.26	0.09	0.11	0.23	0.38	0
2-10	0	H	150	0.14	0.126	0.24	0.37	0.10	0.35	0.18	0.506
1-18	0	H	-177	0.14	0.054	0.53	0.57	0.03	0.11	0.15	0.616
1-6	0	H	132	0.18	0.096	0.33	0.67	0.01	0.31	0.19	0.67

Table 21 Extracted Features and Classification Results for Blind Targets in JPGV Incorporating True Depth (Round 3).

BLUE - Feature & Priority Revise+A13d After Incorporating True Depth
PINK - UXO-Like <-> Non-UXO

Item ID	UXO	Conf.	ETO (°)	CNR (damping)	CNR (GHz)	ETL (m)	DEP(m)	True Depth	Late-Time ELF(t)	Late-Time ELF(f)	Early-Time ELF	Special Note
2-26	1	H	-177	0.03	0.078	0.36	0.73	0.35	1.00	0.90	0.71	
1-51	1	H	-26	0.04	0.076	0.40	0.45	0.25	0.99	0.92	0.78	
1-47	1	H	66	0.04	0.083	0.36	0.42	0.15	0.99	1.00	0.95	30" Mag. Offset 155Deg.
1-39	1	H	-88	0.05	0.047	0.66	0.68	0.25	0.99	0.91	0.34	
2-11	1	H	-60	0.08	0.141	0.21	0.29	0.10	0.99	0.91	0.72	
1-21	1	H	-165	0.07	0.072	0.48	0.32	0.15	0.98	0.99	0.95	
2-3	1	H	-175	0.05	0.068	0.44	0.59	0.30	0.98	0.78	0.72	
2-5	1	H	144	0.07	0.082	0.36	0.58	0.50	0.98	0.97	0.56	
1-5	1	H	49	0.09	0.127	0.27	0.14	0.25	0.98	0.92	0.68	
1-49	1	H	-67	0.05	0.070	0.46	0.59	0.35	0.98	0.96	0.89	
1-50	1	H	3	0.19	0.084	0.38	0.52	0.20	0.98	0.91	0.61	
1-30	1	H	179	0.08	0.075	0.37	0.49	0.15	0.96	0.92	0.46	
2-7	1	H	100	0.13	0.117	0.26	0.40	0.75	0.95	0.92	0.44	40" Offset 190 Deg.
2-21	1	H	-115	0.02	0.051	0.60	0.55	0.40	0.94	0.88	0.89	
1-61	1	H	-120	0.07	0.087	0.36	0.15	0.05	0.94	0.95	0.74	
1-7	1	H	-112	0.08	0.084	0.33	0.37	0.15	0.93	0.77	0.86	
2-20	1	H	-172	0.06	0.086	0.34	0.79	0.60	0.93	0.78	0.57	30" Offset, 33 Deg.
3-1	1	H	-179	0.06	0.079	0.33	0.37	0.25	0.93	0.89	0.92	
1-54	1	H	110	0.10	0.064	0.50	0.68	0.25	0.91	0.98	0.91	
1-27	1	H	33	0.06	0.078	0.41	0.46	0.35	0.91	0.90	0.84	Strange? Vertical Plate?
2-2	1	H	155	0.08	0.058	0.52	0.59	0.40	0.90	0.95	0.91	
3-5	1	H	-50	0.06	0.064	0.40	0.39	0.20	0.90	0.88	0.93	
3-8	1	H	17	0.08	0.058	0.46	0.26	0.10	0.88	0.86	0.82	
2-16	1	H	-140	0.06	0.088	0.35	0.37	0.30	0.87	0.77	0.51	
1-4	1	H	-40	0.06	0.069	0.41	0.46	0.30	0.86	0.92	0.76	
1-3	1	H	-65	0.15	0.092	0.35	0.12	0.10	0.85	0.78	0.67	
1-53	1	H	172	0.17	0.115	0.26	0.42	0.35	0.84	0.86	0.58	
1-55	1	H	101	0.11	0.114	0.28	0.40	0.25	0.83	0.75	0.37	
1-35	1	H	-127	0.03	0.048	0.71	0.24	0.15	0.82	0.93	0.71	
2-12	1	H	157	0.14	0.126	0.24	0.36	0.30	0.80	0.91	1.00	
2-23	1	H	-39	0.14	0.108	0.28	0.45	0.25	0.77	0.88	0.37	
1-58	1	H	-62	0.11	0.045	0.72	0.67	0.50	0.76	0.83	0.38	
1-24	1	H	41	0.08	0.084	0.37	0.39	0.25	0.75	0.72	0.53	
1-36	1	H	30	0.18	0.134	0.24	0.45	0.35	0.72	0.83	0.29	Shallow & Small
2-18	1	H	-147	0.05	0.064	0.47	0.89	0.75	0.72	0.76	0.83	
1-46	1	H	180	0.09	0.078	0.43	0.37	0.30	0.71	0.83	0.69	
2-6	1	H	-74	0.06	0.074	0.40	0.40	0.70	0.70	0.86	0.97	Incorrect True Depth
1-19	1	H	-148	0.04	0.094	0.36	0.16	0.20	0.46	0.70	0.45	
1-9	1	H	16	0.05	0.063	0.44	0.42	0.25	0.43	0.59	0.87	
1-11	1	M	-3	0.11	0.093	0.33	0.63	0.76	0.99	0.98	0.57	40" Offset 0 Deg.

Item ID	UXO	Conf.	ETO (°)	CNR (damping)	CNR (GHz)	ETL (m)	DEP(m)	True Depth	Late-Time ELF(t)	Late-Time ELF(f)	Early-Time ELF	Special Note
1-52	1	M	164	0.15	0.088	0.38	0.66	0.50	0.97	0.91	0.21	
1-16	1	M	-58	0.17	0.118	0.27	0.26	0.20	0.96	0.85	0.69	
1-33	1	M	-166	0.18	0.177	0.13	0.13	0.15	0.94	0.93	0.56	
1-13	1	M	-60	0.19	0.148	0.23	0.27	0.10	0.91	0.97	0.71	
1-17	1	M	171	0.06	0.085	0.36	0.20	0.15	0.91	0.82	0.42	
1-37	1	M	-153	0.05	0.070	0.44	0.39	0.20	0.91	0.96	0.57	
1-40	1	M	-95	0.21	0.143	0.19	0.37	0.25	0.89	0.94	0.75	35" Offset, 155 D
1-31	1	M	168	0.06	0.033	0.96	0.78	0.45	0.84	0.77	0.52	
2-22	1	M	-31	0.04	0.035	0.93	1.00	0.91	0.82	0.75	0.93	
3-3	1	M	-28	0.10	0.095	0.28	0.46	0.35	0.81	0.60	0.85	
2-8	1	M	20	0.14	0.123	0.24	0.14	0.25	0.79	0.88	0.79	Near Surface
1-8	1	M	-173	0.09	0.086	0.35	0.53	0.50	0.78	0.39	0.49	
1-45	1	M	-171	0.08	0.146	0.19	0.30	0.08	0.77	0.78	0.31	
3-2	1	M	123	0.07	0.091	0.29	0.19	0.20	0.70	0.73	0.37	
2-15	1	M	-47	0.10	0.112	0.27	0.37	0.20	0.67	0.75	0.36	
1-38	1	M	-112	0.03	0.088	0.39	0.14	0.30	0.66	0.56	0.37	
1-29	1	L	-178	0.04	0.074	0.40	0.41	0.50	0.97	0.96	0.76	
2-4	1	L	167	0.30	0.088	0.34	0.42	0.35	0.97	0.73	0.19	Shallow
2-25b	1	L	-120	0.06	0.088	0.34	1.76		0.94	0.85	0.38	
1-2b	1	L	56	0.05	0.044	0.68	0.92		0.89	0.92	0.78	!!! Aditional Deep Anomaly!!!
1-41	1	L	-8	0.07	0.032	0.92	0.57	0.50	0.86	0.69	0.27	High Clutter Level
2-14	1	L	-61	0.06	0.017	1.73	0.75	0.70	0.85	0.95	0.86	
1-42	1	L	153	0.31	0.111	0.30	0.35	0.15	0.82	0.93	0.38	
1-28	1	L	-110	0.05	0.088	0.37	0.27	0.15	0.82	0.58	0.30	
1-15	1	L	73	0.12	0.120	0.28	0.12	0.10	0.82	0.80	0.50	Small, Near Surface
1-60	1	L	-143	0.04	0.031	1.01	0.60	0.75	0.78	0.89	0.93	
1-62	1	L	-103	0.04	0.058	0.52	0.94	0.50	0.77	0.83	0.68	Deeper
2-25	1	L	-63	0.03	0.098	0.31	0.75	0.55	0.75	0.82	0.91	
2-9	1	L	32	0.27	0.172	0.18	0.14	0.20	0.71	0.62	0.47	Near Surface
1-1	1	L	-4	0.03	0.051	0.58	1.06	1.20	0.41	0.55	0.71	
3-7b	1	L	60	0.03	0.080	0.31	0.95	0.55	0.30	0.08	0.75	Offset 30", 313DEG!!!
2-24	0	L	-135	0.07	0.082	0.36	1.44	1.50	0.88	0.11	0.40	Weak or Below Clutter
3-10	0	L	-38	0.35	0.190	0.13	0.54	0.25	0.83	0.55	0.18	
1-44	0	L	136	0.11	0.073	0.47	0.36	0.20	0.59	0.43	0.47	Near Tree, Corrected Site
1-12	0	L	-97	0.10	0.041	0.72	0.71	0.40	0.41	0.18	0.18	
2-17	0	L	109	0.16	0.073	0.41	0.78	0.50	0.40	0.50	0.34	
1-56	0	L	157	0.13	0.129	0.24	0.42	0.30	0.40	0.33	0.47	
3-7	0	L	45	0.12	0.083	0.31	0.59	0.55	0.30	0.21	0.19	EMI Depth (weak response)
2-19	0	L	-149	0.14	0.215	0.14	0.27	0.20	0.22	0.52	0.12	
2-1	0	L	67	0.08	0.062	0.50	2.17	1.50	0.21	0.32	0.24	Weak
1-25	0	L	-125	0.32	0.138	0.21	0.09	0.25	0.17	0.09	0.15	
3-4	0	L	90	0.07	0.071	0.35	0.82	1.15	0.12	0.26	0.50	Weak
3-6	0	L	58	0.09	0.072	0.40	0.19	0.25	0.07	0.35	0.14	Weak or Below Clutter
1-43	0	L	-179	0.10	0.100	0.28	0.08	0.20	0.03	0.17	0.13	
1-20	0	M	136	0.05	0.064	0.48	0.39	0.25	0.26	0.32	0.19	
2-13	0	M	-167	0.13	0.122	0.26	0.11	0.25	0.25	0.39	0.33	

Item ID	UXO	Conf.	ETO (°)	CNR (damping)	CNR (GHz)	ETL (m)	DEP(m)	True Depth	Late-Time ELF(t)	Late-Time ELF(f)	Early-Time ELF	Special Note
3-9	0	M	-133	0.07	0.035	0.72	0.85	0.91	0.22	0.23	0.39	
1-22	0	M	41	0.14	0.190	0.16	0.15	0.15	0.20	0.66	0.35	
1-34	0	M	-108	0.07	0.096	0.31	0.08	0.10	0.19	0.20	0.03	
1-59	0	M	-30	0.27	0.058	0.57	0.13	0.10	0.13	0.24	0.38	
1-23	0	M	15	0.24	0.188	0.18	0.10	0.15	0.08	0.22	0.64	
1-48	0	M	93	0.02	0.067	0.47	0.40	0.70	0.03	0.10	0.38	Beside Ditch (red flag)
1-10	0	M	56	0.25	0.053	0.61	0.08	0.10	0.01	0.19	0.08	
1-14	0	H	90	0.13	0.101	0.27	0.17	0.10	0.35	0.30	0.25	
1-63	0	H	-10	0.10	0.090	0.35	0.07	0.05	0.30	0.39	0.22	
2-27	0	H	-62	0.09	0.100	0.30	0.09	0.10	0.23	0.40	0.09	Shallow Plate
1-6	0	H	132	0.20	0.104	0.28	0.64	0.10	0.20	0.23	0.08	
1-26	0	H	171	0.04	0.070	0.46	0.49	0.10	0.17	0.15	0.51	Strange Feature
1-57	0	H	137	0.18	0.125	0.26	0.09	0.25	0.11	0.23	0.38	
2-10	0	H	150	0.14	0.126	0.24	0.37	0.45	0.10	0.35	0.18	
1-2	0	H	63	0.15	0.117	0.26	0.10	0.10	0.04	0.08	0.07	
1-18	0	H	-177	0.14	0.054	0.53	0.57	0.91	0.03	0.11	0.15	plate
1-32	0	H	78	0.05	0.081	0.42	0.13	0.05	0.03	0.03	0.25	

A.2 Classification Results Compared with Ground Truth Data

This appendix contains the tables of target features extracted from GPR data compared with the ground truth data. Note that the ground truth data was provided only after these features and classifications were reported to the ESTCP.

Table 22 Color Codes Used in the Classification Tables

Correctly Classified UXO's
Missed UXO's
Clutter Classified as UXO
Clutter Classified as Clutter

Table 23 Comparison of Ground Truth and GPR UXO Classification (ROUND 1, True UXO Criteria).

AREA	ITEM #	WES ID	GPR class	True Type	Type	Conf.	ETO (o)	True Azi.	True Inc.	CNR (NP/ns)	CNR (GHz)	ETL (m)	True L	DEP (m)	True Depth	Late-Time ELF(f)	Late-Time ELF(t)	Early-Time ELF
1	39	94	1	1	81mm Mortar	H	-88	75	55	0.05	0.047	0.66	0.48	0.68	0.25	0.99	0.91	0.34
2	11	128	1	1	60mm Mortar	H	-60	95	20	0.08	0.141	0.21	0.18	0.29	0.1	0.99	0.91	0.72
1	21	152	1	1	2.75" Rocket	H	-165	30	0	0.07	0.072	0.48	0.41	0.32	0.15	0.98	0.99	0.95
1	49	90	1	1	4.2" Mortar	H	-67	270	0	0.05	0.070	0.46	0.52	0.59	0.35	0.98	0.96	0.89
1	50	100	1	1	60mm Mortar	H	3	195	30	0.19	0.084	0.38	0.52	0.52	0.2	0.98	0.91	0.61
2	7	166/76	1	1	2.75" Rocket	H	100	180	20	0.13	0.117	0.26	0.41	0.40	0.75	0.95	0.92	0.44
2	21	134	1	1	4.2" Mortar	H	-115	0	0	0.02	0.051	0.60	0.52	0.55	0.4	0.94	0.88	0.89
2	20	164	1	1	2.75" Rocket	H	-172	90	10	0.06	0.086	0.34	0.41	0.79	0.6	0.93	0.78	0.57
3	1	62/80	1	1	81mm Mortar	H	-179	0	180	0.06	0.079	0.33	0.28	0.37	0.25	0.93	0.89	0.92
1	54	115	1	1	76mm Projectile	H	110	270	30	0.10	0.064	0.50	0.50	0.68	0.25	0.91	0.98	0.91
1	27	104	1	1	81mm Mortar	H	33	180	0	0.06	0.078	0.41	0.27	0.46	0.35	0.91	0.90	0.84
3	5	50/76	1	1	81mm Mortar	H	-50	-90	--	0.06	0.064	0.40	0.28	0.39	0.2	0.90	0.88	0.93
3	8	68/6	1	1	60mm Mortar	H	17	--	--	0.08	0.058	0.46	0.18	0.26	0.1	0.88	0.86	0.82
2	16	116	1	1	81mm Mortar	H	-140	45	0	0.06	0.088	0.35	0.28	0.37	0.3	0.87	0.77	0.51
1	53	88	1	1	60mm Mortar	H	172	0	0	0.17	0.115	0.26	0.18	0.82	0.35	0.84	0.86	0.58

AREA	ITEM #	WES ID	GPR class	True Type	Type	Conf.	ETO (o)	True Azi.	True Inc.	CNR (NP/ns)	CNR (GHz)	ETL (m)	True L	DEP (m)	True Depth	Late-Time ELF(f)	Late-Time ELF(t)	Early-Time ELF
1	55	117/18	1	1	152mm Projectile	H	101	--	--	0.11	0.114	0.28	0.48	0.40	0.25	0.83	0.75	0.37
2	12	120/88	1	1	60mm Mortar	H	157	270	0	0.14	0.126	0.24	0.18	0.39	0.3	0.80	0.91	1.00
2	23	131/16	1	1	81mm Mortar	H	-39	0	0	0.14	0.108	0.28	0.28	0.45	0.25	0.77	0.88	0.37
1	58	113/2	1	1	105mm Projectile	H	-62	120	30	0.11	0.045	0.72	0.37	0.67	0.5	0.76	0.83	0.38
1	24	102	1	1	81mm Mortar	H	41	210	45	0.08	0.084	0.37	0.28	0.39	0.25	0.75	0.72	0.53
2	6	130	1	1	81mm Mortar	H	-74		0	0.06	0.074	0.40	0.28	0.40	0.7	0.70	0.86	0.97
2	22	132	1	1	5" Projectile	H	69	0	90	0.08	0.074	0.41	0.63	1.10	0.91	0.65	0.36	0.65
1	9	120	1	1	76mm Projectile	H	16	0	20	0.05	0.063	0.44	0.50	0.42	0.25	0.43	0.59	0.87
1	52	144	1	1	105mm Projectile	M	164	180	0	0.15	0.088	0.38	0.37	0.66	0.5	0.97	0.91	0.21
1	37	92	1	1	81mm Mortar	M	-153	30	20	0.05	0.070	0.44	0.41	0.39	0.2	0.91	0.96	0.57
1	31	118	1	1	5" Projectile	M	168	120	30	0.06	0.033	0.96	0.63	0.78	0.45	0.84	0.77	0.52
3	3	78	1	1	60mm Mortar	M	-28	40	330	0.10	0.095	0.28	0.18	0.46	0.35	0.81	0.60	0.85
2	8	152	1	1	57mm Projectile	M	20	90	0	0.14	0.123	0.24	0.12	0.40	0.25	0.79	0.88	0.79
1	8	121/184	1	1	155mm Projectile	M	-173	200	0	0.10	0.105	0.31	0.60	0.68	0.5	0.70	0.32	0.65
1	48	150	1	1	2.75" Rocket	L	91	275	45	0.01	0.019	1.65	0.41	0.74	0.7	0.89	0.98	0.38
2	14	140	1	1	105mm Projectile	L	-61	330	10	0.06	0.017	1.73	0.37	0.75	0.7	0.85	0.95	0.86
1	16	108	1	1	60mm Mortar	L	-59	100	45	0.20	0.117	0.28	0.18	0.69	0.2	0.73	0.60	0.52
1	34	98	1	1	60mm Mortar	L	116	275	20	0.05	0.080	0.37	0.18	0.80	0.1	0.73	0.56	0.62
2	9	124	1	1	60mm Mortar	L	32	330	10	0.27	0.172	0.18	0.18	0.39	0.2	0.71	0.62	0.47
1	41	136	1	1	155mm Projectile	L	-145	90	75	0.03	0.059	0.51	0.60	0.42	0.5	0.63	0.73	0.65
1	44	126	1	1	57mm Projectile	L	136	120	30	0.11	0.073	0.47	0.12	0.36	0.2	0.59	0.43	0.47
2	1	156	1	1	155mm Projectile	L	-156	--	90	0.02	0.063	0.47	0.12	0.80	1.5	0.54	0.70	0.38
1	30	96	1	1	81mm Mortar	L	-9	330	35	0.05	0.072	0.45	0.27	0.45	0.15	0.47	0.69	0.63
1	25	132	1	1	57mm Projectile	L	27	180	0	0.06	0.066	0.45	0.12	0.52	0.25	0.47	0.18	0.61
1	59	10	1	0	Fragment	L	153	--	--	0.01	0.048	0.63	0.08	1.08	0.1	1.00	0.82	0.40
1	32	30	1	0	Fragment	L	79	--	--	0.03	0.046	0.68	0.15	0.30	0.05	0.93	0.93	0.60
1	2	84	1	0	Fragment	L	56	--	--	0.05	0.044	0.68	0.09	0.92	0.1	0.89	0.92	0.78
1	63	16	1	0	Fragment	L	21	--	--	0.09	0.050	0.64	0.11	1.98	0.05	0.85	0.53	0.22
3	2	110	1	0	Magnetic Rock	L	123			0.06	0.064	0.41	0.21	0.20	0.2	0.81	0.80	0.33
2	17		1	-1		L	110			0.08	0.061	0.49		0.78		0.73	0.39	0.55
2	24		1	-1		L	21			0.07	0.053	0.57		0.82		0.66	0.54	0.95
1	43	154	1	0	Magnetic Rock	L	93			0.04	0.099	0.35	0.21	0.34	0.2	0.62	0.90	0.24
1	60	4	1	0	Fragment	L	-101	--	--	0.08	0.031	1.01	0.31	0.87	0.75	0.54	0.91	0.42
1	42	28	1	0	Fragment	L	154	--	--	0.13	0.178	0.17	0.12	0.36	0.15	0.38	0.73	0.39
2	19	54	1	0	Fragment	L	118	--	--	0.10	0.083	0.36	0.10	0.24	0.2	0.35	0.41	0.26

AREA	ITEM #	WES ID	GPR class	True Type	Type	Conf.	ETO (o)	True Azi.	True Inc.	CNR (NP/ns)	CNR (GHz)	ETL (m)	True L	DEP (m)	True Depth	Late-Time ELF(f)	Late-Time ELF(t)	Early-Time ELF
3	7		1	-1		L	-68			0.02	0.110	0.22		0.95		0.16	0.83	0.41
1	3	78	1	0	Fragment	M	115	--	--	0.09	0.104	0.31	0.10	0.73	0.1	1.00	0.91	0.89
1	26	164	1	0	Fragment	M	171	--	--	0.10	0.059	0.55	0.13	0.56	0.1	0.90	0.98	0.05
1	40	168	1	0	Fragment	M	-95	--	--	0.21	0.143	0.19	0.20	0.37	0.25	0.89	0.94	0.75
1	15	62	1	0	Fragment	M	73	--	--	0.12	0.120	0.28	0.15	0.38	0.1	0.82	0.80	0.50
1	45	26	1	0	Fragment	M	-171	--	--	0.08	0.146	0.19	0.20	0.30	0.075	0.77	0.78	0.31
1	38	172	1	0	Fragment	M	-112	--	--	0.04	0.087	0.37	0.21	0.57	0.3	0.70	0.61	0.35
2	15	46	1	0	Fragment	M	-47	--	--	0.10	0.112	0.27	0.24	0.37	0.2	0.67	0.75	0.36
2	4	94	1	0	Fragment	M	167	--	--	0.26	0.080	0.38	0.19	0.42	0.35	0.59	0.69	0.31
2	26		1	-1		H	-177			0.03	0.078	0.36		0.73		1.00	0.90	0.71
1	51	162	1	0	Fragment	H	-26	--	--	0.04	0.076	0.40	0.33	0.45	0.25	0.99	0.92	0.78
2	3	98	1	0	Fragment	H	-175	--	--	0.05	0.068	0.44	0.40	0.59	0.3	0.98	0.78	0.72
2	5	72	1	0	Fragment	H	144	--	--	0.07	0.082	0.36	0.27	0.58	0.5	0.98	0.97	0.56
1	7	74	1	0	Fragment	H	-112	--	--	0.08	0.084	0.33	0.38	0.37	0.15	0.93	0.77	0.86
2	2	108	1	0	Fragment	H	155	--	--	0.08	0.058	0.52	0.35	0.59	0.4	0.90	0.95	0.91
1	4	198	1	0	Fragment	H	-40	--	--	0.06	0.069	0.41	0.40	0.46	0.3	0.86	0.92	0.76
3	10		1	-1		H	-38			0.02	0.044	0.57		0.04		0.83	0.91	0.18
1	35	170	1	0	Fragment	H	-127	--	--	0.03	0.048	0.71	0.43	0.24	0.15	0.82	0.93	0.71
1	36	42	1	0	Fragment	H	30	--	--	0.18	0.134	0.24	0.15	0.45	0.35	0.72	0.83	0.29
2	18	42	1	0	Fragment	H	-147	--	--	0.05	0.064	0.47	0.33	0.89	0.75	0.72	0.76	0.83
1	46	40	1	0	Fragment	H	180	--	--	0.09	0.078	0.43	0.30	0.37	0.3	0.71	0.83	0.69
1	47	38	1	0	Fragment	H	-109	--	--	0.05	0.056	0.50	0.45	0.40	0.15	0.70	0.66	0.87
1	19	64	1	0	Fragment	H	-148	--	--	0.04	0.094	0.36	0.35	0.16	0.2	0.46	0.70	0.45
1	29	54	0	0	Fragment	L	-179	--	--	0.23	0.268	0.13	0.30	0.21	0.5	0.74	0.82	0.18
1	61	158	0	0	Fragment	L	155	--	--	0.07	0.097	0.32	0.05	1.69	0.05	0.52	0.13	0.24
3	6		0	-1		L	-100			0.05	0.082	0.32		0.74		0.43	0.61	0.58
1	56	8	0	0	Fragment	L	157	--	--	0.13	0.129	0.24	0.20	0.42	0.3	0.40	0.33	0.47
2	25		0	-1		L	-106			0.01	0.028	1.06		1.08		0.28	0.40	0.88
2	13	36	0	0	Fragment	L	-167	--	--	0.13	0.122	0.26	0.11	0.11	0.25	0.25	0.39	0.33
1	33	36	0	0	Fragment	L	-155	--	--	0.01	0.022	1.54	0.20	1.07	0.15	0.10	0.10	0.58
1	13	186	0	0	Fragment	M	-60	--	--	0.13	0.069	0.40	0.10	0.35	0.1	0.85	0.90	0.02
1	14	72	0	0	Fragment	M	90	--	--	0.16	0.068	0.50	0.05	0.15	0.1	0.60	0.46	0.20
1	17	66	0	0	Fragment	M	-42	--	--	0.07	0.099	0.35	0.05	0.48	0.15	0.39	0.41	0.15
1	10	180	0	0	Fragment	M	56	--	--	0.25	0.053	0.61	0.20	0.27	0.1	0.01	0.19	0.08
1	1	196	0	0	Fragment	M	0	--	--	0.00	0.000	0.00	0.30	0.00	1.2	0.00	0.00	0.00
1	22	176	0	0	Fragment	H	-105	--	--	0.12	0.100	0.27	0.13	0.83	0.15	0.36	0.41	0.13
1	57	6	0	0	Fragment	H	137	--	--	0.18	0.125	0.26	0.16	0.09	0.25	0.11	0.23	0.38
1	6	82	0	0	Fragment	H	132	--	--	0.18	0.096	0.33	0.03	0.67	0.1	0.01	0.31	0.19
3	4		0	-1		H	0			0.00	0.000	0.00		0.00		0.00	0.00	0.00
1	12	119	0	1	152mm Projectile	L	163	270	30	0.04	0.040	0.80	0.48	0.93	0.4	0.61	0.86	0.59
1	62	149	0	1	2.75" Rocket	L	-96	30	55	0.06	0.086	0.38	0.41	0.26	0.5	0.49	0.61	0.20
3	9	100	0	1	152mm Projectile	M	40	35	90	0.05	0.067	0.37	0.48	0.56	0.91	0.48	0.20	0.34
1	20	106	0	1	60mm Mortar	M	136	75	35	0.05	0.064	0.48	0.18	0.39	0.25	0.26	0.32	0.19
1	11	153	0	1	2.75" Rocket	M	96	0	90	0.05	0.076	0.41	0.41	0.35	0.76	0.15	0.19	0.20

AREA	ITEM #	WES ID	GPR class	True Type	Type	Conf.	ETO (o)	True Azi.	True Inc.	CNR (NP/ns)	CNR (GHz)	ETL (m)	True L	DEP (m)	True Depth	Late-Time ELF(f)	Late-Time ELF(t)	Early-Time ELF
1	23	142	0	1	57mm Projectile	M	15	265	45	0.24	0.188	0.18	0.12	0.10	0.15	0.08	0.22	0.64
1	5	147	0	1	57mm Projectile	H	48	0	0	0.07	0.060	0.56	0.12	0.69	0.25	0.24	0.02	0.20
2	27	112	0	1	81mm Mortar	H	-62	--	90	0.09	0.100	0.30	0.28	0.09	0.1	0.23	0.40	0.09
2	10	144	0	1	152mm Projectile	H	150	50	30	0.14	0.126	0.24	0.48	0.37	0.45	0.10	0.35	0.18
1	18	122	0	1	5" Projectile	H	-177	270	55	0.14	0.054	0.53	0.63	0.57	0.91	0.03	0.11	0.15
1	28	138	0	1	57mm Projectile	H	0	95	45	0.00	0.000	0.00	0.12	0.00	0.15	0.00	0.00	0.00

Table 24 Comparison of Ground Truth and GPR UXO Classification (ROUND 1, LD2 Criteria).

AREA	TAR #	WES #	GPR ID	True UXO	TYPE	Conf.	ETO (o)	True Azi.	True Inc.	CNR (NP/ns)	CNR (GHz)	ETL (m)	True L	DEP (m)	True Depth	Late-Time ELF(f)	Late-Time ELF(t)	Early-Time ELF
1	51	162	1	1	Fragment	H	-26	--	--	0.04	0.076	0.40	0.33	0.45	0.25	0.99	0.92	0.78
1	39	94	1	1	81mm Mortar	H	-88	75	55	0.05	0.047	0.66	0.48	0.68	0.25	0.99	0.91	0.34
2	11	128	1	1	60mm Mortar	H	-60	95	20	0.08	0.141	0.21	0.18	0.29	0.1	0.99	0.91	0.72
1	21	152	1	1	2.75" Rocket	H	-165	30	0	0.07	0.072	0.48	0.41	0.32	0.15	0.98	0.99	0.95
2	3	98	1	1	Fragment	H	-175	--	--	0.05	0.068	0.44	0.40	0.59	0.3	0.98	0.78	0.72
2	5	72	1	1	Fragment	H	144	--	--	0.07	0.082	0.36	0.27	0.58	0.5	0.98	0.97	0.56
1	49	90	1	1	4.2" Mortar	H	-67	270	0	0.05	0.070	0.46	0.52	0.59	0.35	0.98	0.96	0.89
1	50	100	1	1	60mm Mortar	H	3	195	30	0.19	0.084	0.38	0.18	0.52	0.2	0.98	0.91	0.61
2	7	166/76	1	1	2.75" Rocket	H	100	180	20	0.13	0.117	0.26	0.41	0.40	0.75	0.95	0.92	0.44
2	21	134	1	1	4.2" Mortar	H	-115	0	0	0.02	0.051	0.60	0.52	0.55	0.4	0.94	0.88	0.89
1	7	74	1	1	Fragment	H	-112	--	--	0.08	0.084	0.33	0.38	0.37	0.15	0.93	0.77	0.86
2	20	164	1	1	2.75" Rocket	H	-172	90	10	0.06	0.086	0.34	0.41	0.79	0.6	0.93	0.78	0.57
3	1	62/80	1	1	81mm Mortar	H	-179	0	180	0.06	0.079	0.33	0.28	0.37	0.25	0.93	0.89	0.92
1	54	115	1	1	76mm Projectile	H	110	270	30	0.10	0.064	0.50	0.50	0.68	0.25	0.91	0.98	0.91
1	27	104	1	1	81mm Mortar	H	33	180	0	0.06	0.078	0.41	0.27	0.46	0.35	0.91	0.90	0.84
2	2	108	1	1	Fragment	H	155	--	--	0.08	0.058	0.52	0.35	0.59	0.4	0.90	0.95	0.91
3	5	50/76	1	1	81mm Mortar	H	-50	-90	--	0.06	0.064	0.40	0.28	0.39	0.2	0.90	0.88	0.93
3	8	68/6	1	1	60mm Mortar	H	17	--	--	0.08	0.058	0.46	0.18	0.26	0.1	0.88	0.86	0.82
2	16	116	1	1	81mm Mortar	H	-140	45	0	0.06	0.088	0.35	0.28	0.37	0.3	0.87	0.77	0.51
1	4	198	1	1	Fragment	H	-40	--	--	0.06	0.069	0.41	0.40	0.46	0.3	0.86	0.92	0.76
1	53	88	1	1	60mm Mortar	H	172	0	0	0.17	0.115	0.26	0.18	0.82	0.35	0.84	0.86	0.58
1	55	117/18	1	1	152mm Projectile	H	101	--	--	0.11	0.114	0.28	0.48	0.40	0.25	0.83	0.75	0.37

AREA	TAR #	WES #	GPR ID	True UXO	TYPE	Conf.	ETO (o)	True Azi.	True Inc.	CNR (NP/ns)	CNR (GHz)	ETL (m)	True L	DEP (m)	True Depth	Late-Time ELF(f)	Late-Time ELF(t)	Early-Time ELF
1	35	170	1	1	Fragment	H	-127	--	--	0.03	0.048	0.71	0.43	0.24	0.15	0.82	0.93	0.71
2	12	120/88	1	1	60mm Mortar	H	157	270	0	0.14	0.126	0.24	0.18	0.39	0.3	0.80	0.91	1.00
2	23	131/16	1	1	81mm Mortar	H	-39	0	0	0.14	0.108	0.28	0.28	0.45	0.25	0.77	0.88	0.37
1	58	113/2	1	1	105mm Projectile	H	-62	120	30	0.11	0.045	0.72	0.37	0.67	0.5	0.76	0.83	0.38
1	24	102	1	1	81mm Mortar	H	41	210	45	0.08	0.084	0.37	0.28	0.39	0.25	0.75	0.72	0.53
2	18	42	1	1	Fragment	H	-147	--	--	0.05	0.064	0.47	0.33	0.89	0.75	0.72	0.76	0.83
1	46	40	1	1	Fragment	H	180	--	--	0.09	0.078	0.43	0.30	0.37	0.3	0.71	0.83	0.69
2	6	130	1	1	81mm Mortar	H	-74		0	0.06	0.074	0.40	0.28	0.40	0.7	0.70	0.86	0.97
1	47	38	1	1	Fragment	H	-109	--	--	0.05	0.056	0.50	0.45	0.40	0.15	0.70	0.66	0.87
2	22	132	1	1	5" Projectile	H	69	0	90	0.08	0.074	0.41	0.63	1.10	0.91	0.65	0.36	0.65
1	19	64	1	1	Fragment	H	-148	--	--	0.04	0.094	0.36	0.35	0.16	0.2	0.46	0.70	0.45
1	9	120	1	1	76mm Projectile	H	16	0	20	0.05	0.063	0.44	0.50	0.42	0.25	0.43	0.59	0.87
1	52	144	1	1	105mm Projectile	M	164	180	0	0.15	0.088	0.38	0.37	0.66	0.5	0.97	0.91	0.21
1	37	92	1	1	81mm Mortar	M	-153	30	20	0.05	0.070	0.44	0.41	0.39	0.2	0.91	0.96	0.57
1	40	168	1	1	Fragment	M	-95	--	--	0.21	0.143	0.19	0.20	0.37	0.25	0.89	0.94	0.75
1	31	118	1	1	5" Projectile	M	168	120	30	0.06	0.033	0.96	0.63	0.78	0.45	0.84	0.77	0.52
1	15	62	1	1	Fragment	M	73	--	--	0.12	0.120	0.28	0.15	0.38	0.1	0.82	0.80	0.50
3	3	78	1	1	60mm Mortar	M	-28	40	330	0.10	0.095	0.28	0.18	0.46	0.35	0.81	0.60	0.85
2	8	152	1	1	57mm Projectile	M	20	90	0	0.14	0.123	0.24	0.12	0.40	0.25	0.79	0.88	0.79
1	38	172	1	1	Fragment	M	-112	--	--	0.04	0.087	0.37	0.21	0.57	0.3	0.70	0.61	0.35
1	8	121/184	1	1	155mm Projectile	M	-173	200	0	0.10	0.105	0.31	0.60	0.68	0.5	0.70	0.32	0.65
2	4	94	1	1	Fragment	M	167	--	--	0.26	0.080	0.38	0.19	0.42	0.35	0.59	0.69	0.31
1	32	30	1	1	Fragment	L	79	--	--	0.03	0.046	0.68	0.15	0.30	0.05	0.93	0.93	0.60
1	48	150	1	1	2.75" Rocket	L	91	275	45	0.01	0.019	1.65	0.41	0.74	0.7	0.89	0.98	0.38
1	2	84	1	1	Fragment	L	56	--	--	0.05	0.044	0.68	0.09	0.92	0.1	0.89	0.92	0.78
2	14	140	1	1	105mm Projectile	L	-61	330	10	0.06	0.017	1.73	0.37	0.75	0.7	0.85	0.95	0.86
1	16	108	1	1	60mm Mortar	L	-59	100	45	0.20	0.117	0.28	0.18	0.69	0.2	0.73	0.60	0.52
1	34	98	1	1	60mm Mortar	L	116	275	20	0.05	0.080	0.37	0.18	0.80	0.1	0.73	0.56	0.62
2	9	124	1	1	60mm Mortar	L	32	330	10	0.27	0.172	0.18	0.18	0.39	0.2	0.71	0.62	0.47
1	41	136	1	1	155mm Projectile	L	-145	90	75	0.03	0.059	0.51	0.60	0.42	0.5	0.63	0.73	0.65
1	44	126	1	1	57mm Projectile	L	136	120	30	0.11	0.073	0.47	0.12	0.36	0.2	0.59	0.43	0.47
1	60	4	1	1	Fragment	L	-101	--	--	0.08	0.031	1.01	0.31	0.87	0.75	0.54	0.91	0.42
2	1	156	1	1	155mm Projectile	L	-156	--	90	0.02	0.063	0.47	0.12	0.80	1.5	0.54	0.70	0.38
1	30	96	1	1	81mm Mortar	L	-9	330	35	0.05	0.072	0.45	0.27	0.45	0.15	0.47	0.69	0.63
1	25	132	1	1	57mm Projectile	L	27	180	0	0.06	0.066	0.45	0.12	0.52	0.25	0.47	0.18	0.61

AREA	TAR #	WES #	GPR ID	True UXO	TYPE	Conf.	ETO (o)	True Azi.	True Inc.	CNR (NP/ns)	CNR (GHz)	ETL (m)	True L	DEP (m)	True Depth	Late-Time ELF(f)	Late-Time ELF(t)	Early-Time ELF
1	59	10	1	0	Fragment	L	153	--	--	0.01	0.048	0.63	0.08	1.08	0.1	1.00	0.82	0.40
1	63	16	1	0	Fragment	L	21	--	--	0.09	0.050	0.64	0.11	1.98	0.05	0.85	0.53	0.22
3	2	110	1	0	Mag rock	L	123			0.06	0.064	0.41	0.21	0.20	0.2	0.81	0.80	0.33
2	17		1	-1		L	110			0.08	0.061	0.49		0.78		0.73	0.39	0.55
2	24		1	-1		L	21			0.07	0.053	0.57		0.82		0.66	0.54	0.95
1	43	154	1	0	Mag rock	L	93			0.04	0.099	0.35	0.21	0.34	0.2	0.62	0.90	0.24
1	42	28	1	0	Fragment	L	154	--	--	0.13	0.178	0.17	0.12	0.36	0.15	0.38	0.73	0.39
2	19	54	1	0	Fragment	L	118	--	--	0.10	0.083	0.36	0.10	0.24	0.2	0.35	0.41	0.26
3	7		1	-1		L	-68			0.02	0.110	0.22		0.95		0.16	0.83	0.41
1	3	78	1	0	Fragment	M	115	--	--	0.09	0.104	0.31	0.10	0.73	0.1	1.00	0.91	0.89
1	26	164	1	0	Fragment	M	171	--	--	0.10	0.059	0.55	0.13	0.56	0.1	0.90	0.98	0.05
1	45	26	1	0	Fragment	M	-171	--	--	0.08	0.146	0.19	0.20	0.30	0.075	0.77	0.78	0.31
2	15	46	1	0	Fragment	M	-47	--	--	0.10	0.112	0.27	0.24	0.37	0.2	0.67	0.75	0.36
2	26		1	-1		H	-177			0.03	0.078	0.36		0.73		1.00	0.90	0.71
3	10		1	-1		H	-38			0.02	0.044	0.57		0.04		0.83	0.91	0.18
1	36	42	1	0	Fragment	H	30	--	--	0.18	0.134	0.24	0.15	0.45	0.35	0.72	0.83	0.29
1	61	158	0	0	Fragment	L	155	--	--	0.07	0.097	0.32	0.05	1.69	0.05	0.52	0.13	0.24
3	6		0	-1		L	-100			0.05	0.082	0.32		0.74		0.43	0.61	0.58
2	25		0	-1		L	-106			0.01	0.028	1.06		1.08		0.28	0.40	0.88
2	13	36	0	0	Fragment	L	-167	--	--	0.13	0.122	0.26	0.11	0.11	0.25	0.25	0.39	0.33
1	13	186	0	0	Fragment	M	-60	--	--	0.13	0.069	0.40	0.10	0.35	0.1	0.85	0.90	0.02
1	14	72	0	0	Fragment	M	90	--	--	0.16	0.068	0.50	0.05	0.15	0.1	0.60	0.46	0.20
1	17	66	0	0	Fragment	M	-42	--	--	0.07	0.099	0.35	0.05	0.48	0.15	0.39	0.41	0.15
1	10	180	0	0	Fragment	M	56	--	--	0.25	0.053	0.61	0.20	0.27	0.1	0.01	0.19	0.08
1	57	6	0	0	Fragment	H	137	--	--	0.18	0.125	0.26	0.16	0.09	0.25	0.11	0.23	0.38
1	6	82	0	0	Fragment	H	132	--	--	0.18	0.096	0.33	0.03	0.67	0.1	0.01	0.31	0.19
3	4		0	-1		H	0			0.00	0.000	0.00		0.00		0.00	0.00	0.00
1	29	54	0	1	Fragment	L	-179	--	--	0.23	0.268	0.13	0.30	0.21	0.5	0.74	0.82	0.18
1	12	119	0	1	152mm Projectile	L	163	270	30	0.04	0.040	0.80	0.48	0.93	0.4	0.61	0.86	0.59
1	62	149	0	1	2.75" Rocket	L	-96	30	55	0.06	0.086	0.38	0.41	0.26	0.5	0.49	0.61	0.20
1	56	8	0	1	Fragment	L	157	--	--	0.13	0.129	0.24	0.20	0.42	0.3	0.40	0.33	0.47
1	33	36	0	1	Fragment	L	-155	--	--	0.01	0.022	1.54	0.20	1.07	0.15	0.10	0.10	0.58
3	9	100	0	1	152mm Projectile	M	40	35	90	0.05	0.067	0.37	0.48	0.56	0.91	0.48	0.20	0.34
1	20	106	0	1	60mm Mortar	M	136	75	35	0.05	0.064	0.48	0.18	0.39	0.25	0.26	0.32	0.19
1	11	153	0	1	2.75" Rocket	M	96	0	90	0.05	0.076	0.41	0.41	0.35	0.76	0.15	0.19	0.20
1	23	142	0	1	57mm Projectile	M	15	265	45	0.24	0.188	0.18	0.12	0.10	0.15	0.08	0.22	0.64
1	1	196	0	1	Fragment	M	0	--	--	0.00	0.000	0.00	0.30	0.00	1.2	0.00	0.00	0.00
1	22	176	0	1	Fragment	H	-105	--	--	0.12	0.100	0.27	0.13	0.83	0.15	0.36	0.41	0.13
1	5	147	0	1	57mm Projectile	H	48	0	0	0.07	0.060	0.56	0.12	0.69	0.25	0.24	0.02	0.20
2	27	112	0	1	81mm Mortar	H	-62	--	90	0.09	0.100	0.30	0.28	0.09	0.1	0.23	0.40	0.09
2	10	144	0	1	152mm Projectile	H	150	50	30	0.14	0.126	0.24	0.48	0.37	0.45	0.10	0.35	0.18
1	18	122	0	1	5" Proj.	H	-177	270	55	0.14	0.054	0.53	0.63	0.57	0.91	0.03	0.11	0.15
1	28	138	0	1	57mm Projectile	H	0	95	45	0.00	0.000	0.00	0.12	0.00	0.15	0.00	0.00	0.00

Table 25 Comparison of Ground Truth and GPR UXO Classification (ROUND 1, LD3 Criteria).

AREA	TAR #	WES #	GPR ID	True UXO	TYPE	Conf.	ETO (o)	True Azi.	True Inc.	CNR (NP/ns)	CNR (GHz)	ETL (m)	True L	DEP (m)	True Depth	Late-Time ELF(t)	Late-Time ELF(f)	Early-Time ELF
1	21	152	1	1	2.75" Rocket	H	-165	30	0	0.07	0.072	0.48	0.41	0.32	0.15	0.99	0.98	0.95
1	54	115	1	1	76mm Projectile	H	110	270	30	0.10	0.064	0.50	0.50	0.68	0.25	0.98	0.91	0.91
1	49	90	1	1	4.2" Mortar	H	-67	270	0	0.05	0.070	0.46	0.52	0.59	0.35	0.96	0.98	0.89
2	2	108	1	1	Fragment	H	155	--	--	0.08	0.058	0.52	0.35	0.59	0.4	0.95	0.90	0.91
1	35	170	1	1	Fragment	H	-127	--	--	0.03	0.048	0.71	0.43	0.24	0.15	0.93	0.82	0.71
2	7	166/76	1	1	2.75" Rocket	H	100	180	20	0.13	0.117	0.26	0.41	0.40	0.75	0.92	0.95	0.44
1	4	198	1	1	Fragment	H	-40	--	--	0.06	0.069	0.41	0.40	0.46	0.3	0.92	0.86	0.76
1	39	94	1	1	81mm Mortar	H	-88	75	55	0.05	0.047	0.66	0.48	0.68	0.25	0.91	0.99	0.34
2	11	128	1	1	60mm Mortar	H	-60	95	20	0.08	0.141	0.21	0.18	0.29	0.1	0.91	0.99	0.72
1	50	100	1	1	60mm Mortar	H	3	195	30	0.19	0.084	0.38	0.18	0.52	0.2	0.91	0.98	0.61
2	12	120/88	1	1	60mm Mortar	H	157	270	0	0.14	0.126	0.24	0.18	0.39	0.3	0.91	0.80	1.00
1	27	104	1	1	81mm Mortar	H	33	180	0	0.06	0.078	0.41	0.27	0.46	0.35	0.90	0.91	0.84
3	1	62/80	1	1	81mm Mortar	H	-179	0	180	0.06	0.079	0.33	0.28	0.37	0.25	0.89	0.93	0.92
2	21	134	1	1	4.2" Mortar	H	-115	0	0	0.02	0.051	0.60	0.52	0.55	0.4	0.88	0.94	0.89
3	5	50/76	1	1	81mm Mortar	H	-50	-90	--	0.06	0.064	0.40	0.28	0.39	0.2	0.88	0.90	0.93
2	23	131/16	1	1	81mm Mortar	H	-39	0	0	0.14	0.108	0.28	0.28	0.45	0.25	0.88	0.77	0.37
3	8	68/6	1	1	60mm Mortar	H	17	--	--	0.08	0.058	0.46	0.18	0.26	0.1	0.86	0.88	0.82
1	53	88	1	1	60mm Mortar	H	172	0	0	0.17	0.115	0.26	0.18	0.82	0.35	0.86	0.84	0.58
2	6	130	1	1	81mm Mortar	H	-74		0	0.06	0.074	0.40	0.28	0.40	0.7	0.86	0.70	0.97
1	58	113/2	1	1	105mm Projectile	H	-62	120	30	0.11	0.045	0.72	0.37	0.67	0.5	0.83	0.76	0.38
1	46	40	1	1	Fragment	H	180	--	--	0.09	0.078	0.43	0.30	0.37	0.3	0.83	0.71	0.69
2	3	98	1	1	Fragment	H	-175	--	--	0.05	0.068	0.44	0.40	0.59	0.3	0.78	0.98	0.72
2	20	164	1	1	2.75" Rocket	H	-172	90	10	0.06	0.086	0.34	0.41	0.79	0.6	0.78	0.93	0.57
1	7	74	1	1	Fragment	H	-112	--	--	0.08	0.084	0.33	0.38	0.37	0.15	0.77	0.93	0.86
2	16	116	1	1	81mm Mortar	H	-140	45	0	0.06	0.088	0.35	0.28	0.37	0.3	0.77	0.87	0.51
2	18	42	1	1	Fragment	H	-147	--	--	0.05	0.064	0.47	0.33	0.89	0.75	0.76	0.72	0.83
1	55	117/18	1	1	152mm Projectile	H	101	--	--	0.11	0.114	0.28	0.48	0.40	0.25	0.75	0.83	0.37
1	24	102	1	1	81mm Mortar	H	41	210	45	0.08	0.084	0.37	0.28	0.39	0.25	0.72	0.75	0.53
1	19	64	1	1	Fragment	H	-148	--	--	0.04	0.094	0.36	0.35	0.16	0.2	0.70	0.46	0.45
1	47	38	1	1	Fragment	H	-109	--	--	0.05	0.056	0.50	0.45	0.40	0.15	0.66	0.70	0.87
1	9	120	1	1	76mm Projectile	H	16	0	20	0.05	0.063	0.44	0.50	0.42	0.25	0.59	0.43	0.87
2	22	132	1	1	5" Projectile	H	69	0	90	0.08	0.074	0.41	0.63	1.10	0.91	0.36	0.65	0.65
1	37	92	1	1	81mm Mortar	M	-153	30	20	0.05	0.070	0.44	0.41	0.39	0.2	0.96	0.91	0.57

AREA	TAR #	WES #	GPR ID	True UXO	TYPE	Conf.	ETO (o)	True Azi.	True Inc.	CNR (NP/ns)	CNR (GHz)	ETL (m)	True L	DEP (m)	True Depth	Late-Time ELF(t)	Late-Time ELF(f)	Early-Time ELF
1	40	168	1	1	Fragment	M	-95	--	--	0.21	0.143	0.19	0.20	0.37	0.25	0.94	0.89	0.75
1	52	144	1	1	105mm Projectile	M	164	180	0	0.15	0.088	0.38	0.37	0.66	0.5	0.91	0.97	0.21
1	15	62	1	1	Fragment	M	73	--	--	0.12	0.120	0.28	0.15	0.38	0.1	0.80	0.82	0.50
1	31	118	1	1	5" Projectile	M	168	120	30	0.06	0.033	0.96	0.63	0.78	0.45	0.77	0.84	0.52
3	3	78	1	1	60mm Mortar	M	-28	40	330	0.10	0.095	0.28	0.18	0.46	0.35	0.60	0.81	0.85
1	8	121/184	1	1	155mm Projectile	M	-173	200	0	0.10	0.105	0.31	0.60	0.68	0.5	0.32	0.70	0.65
1	48	150	1	1	2.75" Rocket	L	91	275	45	0.01	0.019	1.65	0.41	0.74	0.7	0.98	0.89	0.38
2	14	140	1	1	105mm Projectile	L	-61	330	10	0.06	0.017	1.73	0.37	0.75	0.7	0.95	0.85	0.86
1	32	30	1	1	Fragment	L	79	--	--	0.03	0.046	0.68	0.15	0.30	0.05	0.93	0.93	0.60
1	41	136	1	1	155mm Projectile	L	-145	90	75	0.03	0.059	0.51	0.60	0.42	0.5	0.73	0.63	0.65
2	1	156	1	1	155mm Projectile	L	-156	--	90	0.02	0.063	0.47	0.12	0.80	1.5	0.70	0.54	0.38
1	30	96	1	1	81mm Mortar	L	-9	330	35	0.05	0.072	0.45	0.27	0.45	0.15	0.69	0.47	0.63
2	9	124	1	1	60mm Mortar	L	32	330	10	0.27	0.172	0.18	0.18	0.39	0.2	0.62	0.71	0.47
1	16	108	1	1	60mm Mortar	L	-59	100	45	0.20	0.117	0.28	0.18	0.69	0.2	0.60	0.73	0.52
1	34	98	1	1	60mm Mortar	L	116	275	20	0.05	0.080	0.37	0.18	0.80	0.1	0.56	0.73	0.62
1	2	84	1	0	Fragment	L	56	--	--	0.05	0.044	0.68	0.09	0.92	0.1	0.92	0.89	0.78
1	60	4	1	0	Fragment	L	-101	--	--	0.08	0.031	1.01	0.31	0.87	0.75	0.91	0.54	0.42
1	43	154	1	0	Magnetic Rock	L	93			0.04	0.099	0.35	0.21	0.34	0.2	0.90	0.62	0.24
3	7		1	-1		L	-68			0.02	0.110	0.22		0.95		0.83	0.16	0.41
1	59	10	1	0	Fragment	L	153	--	--	0.01	0.048	0.63	0.08	1.08	0.1	0.82	1.00	0.40
3	2	110	1	0	Magnetic Rock	L	123			0.06	0.064	0.41	0.21	0.20	0.2	0.80	0.81	0.33
1	42	28	1	0	Fragment	L	154	--	--	0.13	0.178	0.17	0.12	0.36	0.15	0.73	0.38	0.39
2	24		1	-1		L	21			0.07	0.053	0.57		0.82		0.54	0.66	0.95
1	63	16	1	0	Fragment	L	21	--	--	0.09	0.050	0.64	0.11	1.98	0.05	0.53	0.85	0.22
1	44	126	1	0	57mm Projectile	L	136	120	30	0.11	0.073	0.47	0.12	0.36	0.2	0.43	0.59	0.47
2	19	54	1	0	Fragment	L	118	--	--	0.10	0.083	0.36	0.10	0.24	0.2	0.41	0.35	0.26
2	17		1	-1		L	110			0.08	0.061	0.49		0.78		0.39	0.73	0.55
1	25	132	1	0	57mm Projectile	L	27	180	0	0.06	0.066	0.45	0.12	0.52	0.25	0.18	0.47	0.61
1	26	164	1	0	Fragment	M	171	--	--	0.10	0.059	0.55	0.13	0.56	0.1	0.98	0.90	0.05
1	3	78	1	0	Fragment	M	115	--	--	0.09	0.104	0.31	0.10	0.73	0.1	0.91	1.00	0.89
2	8	152	1	0	57mm Projectile	M	20	90	0	0.14	0.123	0.24	0.12	0.40	0.25	0.88	0.79	0.79
1	45	26	1	0	Fragment	M	-171	--	--	0.08	0.146	0.19	0.20	0.30	0.075	0.78	0.77	0.31
2	15	46	1	0	Fragment	M	-47	--	--	0.10	0.112	0.27	0.24	0.37	0.2	0.75	0.67	0.36
2	4	94	1	0	Fragment	M	167	--	--	0.26	0.080	0.38	0.19	0.42	0.35	0.69	0.59	0.31
1	38	172	1	0	Fragment	M	-112	--	--	0.04	0.087	0.37	0.21	0.57	0.3	0.61	0.70	0.35
2	5	72	1	0	Fragment	H	144	--	--	0.07	0.082	0.36	0.27	0.58	0.5	0.97	0.98	0.56
1	51	162	1	0	Fragment	H	-26	--	--	0.04	0.076	0.40	0.33	0.45	0.25	0.92	0.99	0.78
3	10		1	-1		H	-38			0.02	0.044	0.57		0.04		0.91	0.83	0.18
2	26		1	-1		H	-177			0.03	0.078	0.36		0.73		0.90	1.00	0.71
1	36	42	1	0	Fragment	H	30	--	--	0.18	0.134	0.24	0.15	0.45	0.35	0.83	0.72	0.29

AREA	TAR #	WES #	GPR ID	True UXO	TYPE	Conf.	ETO (o)	True Azi.	True Inc.	CNR (NP/ns)	CNR (GHz)	ETL (m)	True L	DEP (m)	True Depth	Late-Time ELF(t)	Late-Time ELF(f)	Early-Time ELF
2	25		0	-1		L	-106			0.01	0.028	1.06		1.08		0.40	0.28	0.88
2	13	36	0	0	Fragment	L	-167	--	--	0.13	0.122	0.26	0.11	0.11	0.25	0.39	0.25	0.33
1	61	158	0	0	Fragment	L	155	--	--	0.07	0.097	0.32	0.05	1.69	0.05	0.13	0.52	0.24
3	6		0	-1		L	-100			0.05	0.082	0.32		0.74		0.61	0.43	0.58
1	29	54	0	0	Fragment	L	-179	--	--	0.23	0.268	0.13	0.30	0.21	0.5	0.82	0.74	0.18
1	14	72	0	0	Fragment	M	90	--	--	0.16	0.068	0.50	0.05	0.15	0.1	0.46	0.60	0.20
1	17	66	0	0	Fragment	M	-42	--	--	0.07	0.099	0.35	0.05	0.48	0.15	0.41	0.39	0.15
1	23	142	0	0	57mm Projectile	M	15	265	45	0.24	0.188	0.18	0.12	0.10	0.15	0.22	0.08	0.64
1	10	180	0	0	Fragment	M	56	--	--	0.25	0.053	0.61	0.20	0.27	0.1	0.19	0.01	0.08
1	13	186	0	0	Fragment	M	-60	--	--	0.13	0.069	0.40	0.10	0.35	0.1	0.90	0.85	0.02
1	22	176	0	0	Fragment	H	-105	--	--	0.12	0.100	0.27	0.13	0.83	0.15	0.41	0.36	0.13
1	6	82	0	0	Fragment	H	132	--	--	0.18	0.096	0.33	0.03	0.67	0.1	0.31	0.01	0.19
1	57	6	0	0	Fragment	H	137	--	--	0.18	0.125	0.26	0.16	0.09	0.25	0.23	0.11	0.38
1	5	147	0	0	57mm Projectile	H	48	0	0	0.07	0.060	0.56	0.12	0.69	0.25	0.02	0.24	0.20
3	4		0	-1		H	0			0.00	0.000	0.00		0.00		0.00	0.00	0.00
1	28	138	0	0	57mm Projectile	H	0	95	45	0.00	0.000	0.00	0.12	0.00	0.15	0.00	0.00	0.00
1	12	119	0	1	152mm Projectile	L	163	270	30	0.04	0.040	0.80	0.48	0.93	0.4	0.86	0.61	0.59
1	62	149	0	1	2.75" Rocket	L	-96	30	55	0.06	0.086	0.38	0.41	0.26	0.5	0.61	0.49	0.20
1	56	8	0	1	Fragment	L	157	--	--	0.13	0.129	0.24	0.20	0.42	0.3	0.33	0.40	0.47
1	33	36	0	1	Fragment	L	-155	--	--	0.01	0.022	1.54	0.20	1.07	0.15	0.10	0.10	0.58
1	20	106	0	1	60mm Mortar	M	136	75	35	0.05	0.064	0.48	0.18	0.39	0.25	0.32	0.26	0.19
3	9	100	0	1	152mm Projectile	M	40	35	90	0.05	0.067	0.37	0.48	0.56	0.91	0.20	0.48	0.34
1	11	153	0	1	2.75" Rocket	M	96	0	90	0.05	0.076	0.41	0.41	0.35	0.76	0.19	0.15	0.20
1	1	196	0	1	Fragment	M	0	--	--	0.00	0.000	0.00	0.30	0.00	1.2	0.00	0.00	0.00
2	27	112	0	1	81mm Mortar	H	-62	--	90	0.09	0.100	0.30	0.28	0.09	0.1	0.40	0.23	0.09
2	10	144	0	1	152mm Projectile	H	150	50	30	0.14	0.126	0.24	0.48	0.37	0.45	0.35	0.10	0.18
1	18	122	0	1	5" Projectile	H	-177	270	55	0.14	0.054	0.53	0.63	0.57	0.91	0.11	0.03	0.15

Table 26 Comparison of Ground Truth and GPR UXO Classification (ROUND 2, True UXO Criteria).

AREA	ITEM #	WES ID	GPR ID	True Type	Type	Conf.	ETO (o)	True Azi.	True Inc.	CNR (NP/ns)	CNR (GHz)	ETL (m)	True L	DEP (m)	True Depth	Late-Time ELF(t)	Late-Time ELF(f)	Early-Time ELF
1	39	94	1	1	81mm Mortar	H	-88	75	55	0.05	0.047	0.66	0.48	0.68	0.25	0.99	0.91	0.34
2	11	128	1	1	60mm Mortar	H	-60	95	20	0.08	0.141	0.21	0.18	0.29	0.1	0.99	0.91	0.72
1	21	152	1	1	2.75" Rocket	H	-165	30	0	0.07	0.072	0.48	0.41	0.32	0.15	0.98	0.99	0.95
1	5	147	1	1	57mm Projectile	H	49	0	0	0.09	0.127	0.27	0.12	0.14	0.25	0.98	0.92	0.68
1	49	90	1	1	4.2" Mortar	H	-67	270	0	0.05	0.070	0.46	0.52	0.59	0.35	0.98	0.96	0.89
1	50	100	1	1	60mm Mortar	H	3	195	30	0.19	0.084	0.38	0.52	0.52	0.2	0.98	0.91	0.61
1	30	96	1	1	81mm Mortar	H	179	330	35	0.08	0.075	0.37	0.27	0.49	0.15	0.96	0.92	0.46
2	7	166/76	1	1	2.75" Rocket	H	100	180	20	0.13	0.117	0.26	0.41	0.40	0.75	0.95	0.92	0.44
2	21	134	1	1	4.2" Mortar	H	-115	0	0	0.02	0.051	0.60	0.52	0.55	0.4	0.94	0.88	0.89
2	20	164	1	1	2.75" Rocket	H	-172	90	10	0.06	0.086	0.34	0.41	0.79	0.6	0.93	0.78	0.57
3	1	62/80	1	1	81mm Mortar	H	-179	0	180	0.06	0.079	0.33	0.28	0.37	0.25	0.93	0.89	0.92
1	54	115	1	1	76mm Projectile	H	110	270	30	0.10	0.064	0.50	0.50	0.68	0.25	0.91	0.98	0.91
1	27	104	1	1	81mm Mortar	H	33	180	0	0.06	0.078	0.41	0.27	0.46	0.35	0.91	0.90	0.84
3	5	50/76	1	1	81mm Mortar	H	-50	-90	--	0.06	0.064	0.40	0.28	0.39	0.2	0.90	0.88	0.93
3	8	68/6	1	1	60mm Mortar	H	17	--	--	0.08	0.058	0.46	0.18	0.26	0.1	0.88	0.86	0.82
2	16	116	1	1	81mm Mortar	H	-140	45	0	0.06	0.088	0.35	0.28	0.37	0.3	0.87	0.77	0.51
1	53	88	1	1	60mm Mortar	H	172	0	0	0.17	0.115	0.26	0.18	0.82	0.35	0.84	0.86	0.58
1	55	117/18	1	1	152mm Projectile	H	101	--	--	0.11	0.114	0.28	0.48	0.40	0.25	0.83	0.75	0.37
2	12	120/88	1	1	60mm Mortar	H	157	270	0	0.14	0.126	0.24	0.18	0.36	0.3	0.80	0.91	1.00
2	23	131/16	1	1	81mm Mortar	H	-39	0	0	0.14	0.108	0.28	0.28	0.45	0.25	0.77	0.88	0.37
1	58	113/2	1	1	105mm Projectile	H	-62	120	30	0.11	0.045	0.72	0.37	0.67	0.5	0.76	0.83	0.38
1	24	102	1	1	81mm Mortar	H	41	210	45	0.08	0.084	0.37	0.28	0.39	0.25	0.75	0.72	0.53
2	6	130	1	1	81mm Mortar	H	-74		0	0.06	0.074	0.40	0.28	0.40	0.7	0.70	0.86	0.97
1	9	120	1	1	76mm Projectile	H	16	0	20	0.05	0.063	0.44	0.50	0.42	0.25	0.43	0.59	0.87
1	11	153	1	1	2.75" Rocket	M	-3	0	90	0.11	0.093	0.33	0.41	0.63	0.76	0.99	0.98	0.57
1	52	144	1	1	105mm Projectile	M	164	180	0	0.15	0.088	0.38	0.37	0.66	0.5	0.97	0.91	0.21
1	37	92	1	1	81mm Mortar	M	-153	30	20	0.05	0.070	0.44	0.41	0.39	0.2	0.91	0.96	0.57
1	31	118	1	1	5" Projectile	M	168	120	30	0.06	0.033	0.96	0.63	0.78	0.45	0.84	0.77	0.52
2	22	132	1	1	5" Projectile	M	-31	0	90	0.04	0.035	0.93	0.63	1.00	0.91	0.82	0.75	0.93

AREA	ITEM #	WES ID	GPR ID	True Type	Type	Conf.	ETO (o)	True Azi.	True Inc.	CNR (NP/ns)	CNR (GHz)	ETL (m)	True L	DEP (m)	True Depth	Late-Time ELF(t)	Late-Time ELF(f)	Early-Time ELF
3	3	78	1	1	60mm Mortar	M	-28	40	330	0.10	0.095	0.28	0.18	0.46	0.35	0.81	0.60	0.85
2	8	152	1	1	57mm Projectile	M	20	90	0	0.14	0.123	0.24	0.12	0.14	0.25	0.79	0.88	0.79
1	8	121/184	1	1	155mm Projectile	M	-173	200	0	0.09	0.086	0.35	0.60	0.53	0.5	0.78	0.39	0.49
1	16	108	1	1	60mm Mortar	L	-59	100	45	0.07	0.130	0.26	0.18	0.25	0.2	0.91	0.93	0.43
1	34	98	1	1	60mm Mortar	L	160	275	20	0.18	0.143	0.22	0.18	0.33	0.1	0.87	0.95	0.28
1	41	136	1	1	155mm Projectile	L	-8	90	75	0.07	0.032	0.92	0.60	0.57	0.5	0.86	0.69	0.27
2	1	156	1	1	155mm Projectile	L	67	--	90	0.01	0.104	0.29	0.12	2.09	1.5	0.86	0.34	0.23
2	14	140	1	1	105mm Projectile	L	-61	330	10	0.06	0.017	1.73	0.37	0.75	0.7	0.85	0.95	0.86
1	28	138	1	1	57mm Projectile	L	-110	95	45	0.05	0.088	0.37	0.12	0.27	0.15	0.82	0.58	0.30
1	62	149	1	1	2.75" Rocket	L	-103	30	55	0.04	0.058	0.52	0.41	0.94	0.5	0.77	0.83	0.68
2	9	124	1	1	60mm Mortar	L	32	330	10	0.27	0.172	0.18	0.18	0.14	0.2	0.71	0.62	0.47
1	44	126	1	1	57mm Projectile	L	136	120	30	0.11	0.073	0.47	0.12	0.36	0.2	0.59	0.43	0.47
1	12	119	1	1	152mm Projectile	L	-100	270	30	0.02	0.032	0.95	0.48	0.74	0.4	0.55	0.61	0.62
1	29	54	1	0	Fragment	L	-174	--	--	0.09	0.090	0.34	0.30	0.42	0.5	0.98	0.72	0.56
1	59	10	1	0	Fragment	L	61	--	--	0.03	0.117	0.29	0.08	0.11	0.1	0.89	0.16	0.22
1	2	84	1	0	Fragment	L	39	--	--	0.03	0.101	0.30	0.09	0.60	0.1	0.84	0.14	0.65
1	15	62	1	0	Fragment	L	73	--	--	0.12	0.120	0.28	0.15	0.12	0.1	0.82	0.80	0.50
3	2	110	1	0	Magnetic Rock	L	123			0.06	0.064	0.41	0.21	0.20	0.2	0.81	0.80	0.33
1	42	28	1	0	Fragment	L	-121	--	--	0.12	0.043	0.74	0.12	2.14	0.15	0.81	0.95	0.52
2	17		1	-1		L	110			0.12	0.078	0.38		0.76		0.78	0.51	0.62
2	24		1	-1		L	21			0.07	0.053	0.57		0.82		0.66	0.54	0.95
1	63	16	1	0	Fragment	L	-10	--	--	0.06	0.069	0.44	0.11	0.17	0.05	0.63	0.64	0.19
1	43	154	1	0	Magnetic Rock	L	93			0.04	0.099	0.35	0.21	0.34	0.2	0.62	0.90	0.24
1	32	30	1	0	Fragment	L	80	--	--	0.07	0.072	0.45	0.15	0.32	0.05	0.55	0.58	0.11
1	60	4	1	0	Fragment	L	-101	--	--	0.08	0.031	1.01	0.31	0.87	0.75	0.54	0.91	0.42
2	4	94	1	0	Fragment	L	171	--	--	0.15	0.090	0.36	0.19	0.18	0.35	0.52	0.61	0.30
2	19	54	1	0	Fragment	L	118	--	--	0.10	0.083	0.36	0.10	0.24	0.2	0.35	0.41	0.26
2	25		1	-1		L	-106			0.01	0.028	1.06		1.08		0.28	0.40	0.88
1	33	36	1	0	Fragment	M	-166	--	--	0.18	0.177	0.13	0.20	0.13	0.15	0.94	0.93	0.56
1	26	164	1	0	Fragment	M	171	--	--	0.10	0.059	0.55	0.13	0.56	0.1	0.90	0.98	0.05
1	40	168	1	0	Fragment	M	-95	--	--	0.21	0.143	0.19	0.20	0.37	0.25	0.89	0.94	0.75
1	45	26	1	0	Fragment	M	-171	--	--	0.08	0.146	0.19	0.20	0.30	0.075	0.77	0.78	0.31
2	15	46	1	0	Fragment	M	-47	--	--	0.10	0.112	0.27	0.24	0.37	0.2	0.67	0.75	0.36
1	38	172	1	0	Fragment	M	-112	--	--	0.03	0.088	0.39	0.21	0.14	0.3	0.66	0.56	0.37
2	26		1	-1		H	-177			0.03	0.078	0.36		0.73		1.00	0.90	0.71
1	51	162	1	0	Fragment	H	-26	--	--	0.04	0.076	0.40	0.33	0.45	0.25	0.99	0.92	0.78
1	47	38	1	0	Fragment	H	66	--	--	0.04	0.083	0.36	0.45	0.42	0.15	0.99	1.00	0.95
2	3	98	1	0	Fragment	H	-175	--	--	0.05	0.068	0.44	0.40	0.59	0.3	0.98	0.78	0.72
2	5	72	1	0	Fragment	H	144	--	--	0.07	0.082	0.36	0.27	0.58	0.5	0.98	0.97	0.56
1	61	158	1	0	Fragment	H	-120	--	--	0.07	0.087	0.36	0.05	0.15	0.05	0.94	0.95	0.74
1	7	74	1	0	Fragment	H	-112	--	--	0.08	0.084	0.33	0.38	0.37	0.15	0.93	0.77	0.86

AREA	ITEM #	WES ID	GPR ID	True Type	Type	Conf.	ETO (o)	True Azi.	True Inc.	CNR (NP/ns)	CNR (GHz)	ETL (m)	True L	DEP (m)	True Depth	Late-Time ELF(t)	Late-Time ELF(f)	Early-Time ELF
2	2	108	1	0	Fragment	H	155	--	--	0.08	0.058	0.52	0.35	0.59	0.4	0.90	0.95	0.91
1	4	198	1	0	Fragment	H	-40	--	--	0.06	0.069	0.41	0.40	0.46	0.3	0.86	0.92	0.76
1	35	170	1	0	Fragment	H	-127	--	--	0.03	0.048	0.71	0.43	0.24	0.15	0.82	0.93	0.71
1	36	42	1	0	Fragment	H	30	--	--	0.18	0.134	0.24	0.15	0.45	0.35	0.72	0.83	0.29
1	46	40	1	0	Fragment	H	180	--	--	0.09	0.078	0.43	0.30	0.37	0.3	0.71	0.83	0.69
1	19	64	1	0	Fragment	H	-148	--	--	0.04	0.094	0.36	0.35	0.16	0.2	0.46	0.70	0.45
3	10		0	-1		L	-38			0.35	0.190	0.13		0.54		0.83	0.55	0.18
1	56	8	0	0	Fragment	L	157	--	--	0.13	0.129	0.24	0.20	0.42	0.3	0.40	0.33	0.47
1	14	72	0	0	Fragment	L	130	--	--	0.07	0.065	0.47	0.05	0.36	0.1	0.39	0.58	0.17
3	7		0	-1		L	45			0.12	0.083	0.31		0.59		0.30	0.21	0.19
1	22	176	0	0	Fragment	L	126	--	--	0.23	0.180	0.19	0.13	0.48	0.15	0.28	0.27	0.23
2	13	36	0	0	Fragment	L	-167	--	--	0.13	0.122	0.26	0.11	0.11	0.25	0.25	0.39	0.33
3	4		0	-1		L	90			0.07	0.071	0.35		0.82		0.12	0.26	0.50
3	6		0	-1		L	58			0.09	0.072	0.40		0.19		0.07	0.35	0.14
1	13	186	0	0	Fragment	M	-60	--	--	0.13	0.069	0.40	0.10	0.35	0.1	0.85	0.90	0.02
1	17	66	0	0	Fragment	M	-42	--	--	0.07	0.099	0.35	0.05	0.48	0.15	0.39	0.41	0.15
1	1	196	0	0	Fragment	M	-45	--	--	0.31	0.170	0.18	0.30	0.05	1.2	0.10	0.14	0.04
1	10	180	0	0	Fragment	M	56	--	--	0.25	0.053	0.61	0.20	0.08	0.1	0.01	0.19	0.08
1	3	78	0	0	Fragment	H	-155	--	--	0.44	0.125	0.25	0.10	0.36	0.1	0.38	0.29	0.48
2	18	42	0	0	Fragment	H	87	--	--	0.27	0.080	0.33	0.33	0.07	0.75	0.28	0.02	0.21
1	57	6	0	0	Fragment	H	137	--	--	0.18	0.125	0.26	0.16	0.09	0.25	0.11	0.23	0.38
1	6	82	0	0	Fragment	H	132	--	--	0.18	0.096	0.33	0.03	0.67	0.1	0.01	0.31	0.19
1	25	132	0	1	57mm Projectile	L	-125	180	0	0.32	0.138	0.21	0.12	0.09	0.25	0.17	0.09	0.15
3	9	100	0	1	152mm Projectile	M	40	35	90	0.05	0.067	0.37	0.48	0.56	0.91	0.48	0.20	0.34
1	20	106	0	1	60mm Mortar	M	136	75	35	0.05	0.064	0.48	0.18	0.39	0.25	0.26	0.32	0.19
1	23	142	0	1	57mm Projectile	M	15	265	45	0.24	0.188	0.18	0.12	0.10	0.15	0.08	0.22	0.64
1	48	150	0	1	2.75" Rocket	M	93	275	45	0.02	0.067	0.47	0.41	0.40	0.7	0.03	0.10	0.38
2	27	112	0	1	81mm Mortar	H	-62	--	90	0.09	0.100	0.30	0.28	0.09	0.1	0.23	0.40	0.09
2	10	144	0	1	152mm Projectile	H	150	50	30	0.14	0.126	0.24	0.48	0.37	0.45	0.10	0.35	0.18
1	18	122	0	1	5" Projectile	H	-177	270	55	0.14	0.054	0.53	0.63	0.57	0.91	0.03	0.11	0.15

Table 27 Comparison of Ground Truth and GPR UXO Classification (ROUND 2, LD2 Criteria).

AREA	TAR #	WES #	GPR ID	True UXO	Description	Conf.	ETO (o)	True Azi.	True Inc.	CNR (NP/ns)	CNR (GHz)	ETL (m)	True L	DEP (m)	True Depth	Late-Time ELF(t)	Late-Time ELF(f)	Early-Time ELF
1	51	162	1	1	Fragment	H	-26	--	--	0.04	0.076	0.40	0.33	0.45	0.25	0.99	0.92	0.78
1	47	38	1	1	Fragment	H	66	--	--	0.04	0.083	0.36	0.45	0.42	0.15	0.99	1.00	0.95
1	39	94	1	1	81mm Mortar	H	-88	75	55	0.05	0.047	0.66	0.48	0.68	0.25	0.99	0.91	0.34
2	11	128	1	1	60mm Mortar	H	-60	95	20	0.08	0.141	0.21	0.18	0.29	0.1	0.99	0.91	0.72
1	21	152	1	1	2.75" Rocket	H	-165	30	0	0.07	0.072	0.48	0.41	0.32	0.15	0.98	0.99	0.95
2	3	98	1	1	Fragment	H	-175	--	--	0.05	0.068	0.44	0.40	0.59	0.3	0.98	0.78	0.72
2	5	72	1	1	Fragment	H	144	--	--	0.07	0.082	0.36	0.27	0.58	0.5	0.98	0.97	0.56
1	5	147	1	1	57mm Projectile	H	49	0	0	0.09	0.127	0.27	0.12	0.14	0.25	0.98	0.92	0.68
1	49	90	1	1	4.2" Mortar	H	-67	270	0	0.05	0.070	0.46	0.52	0.59	0.35	0.98	0.96	0.89
1	50	100	1	1	60mm Mortar	H	3	195	30	0.19	0.084	0.38	0.18	0.52	0.2	0.98	0.91	0.61
1	30	96	1	1	81mm Mortar	H	179	330	35	0.08	0.075	0.37	0.27	0.49	0.15	0.96	0.92	0.46
2	7	166/76	1	1	2.75" Rocket	H	100	180	20	0.13	0.117	0.26	0.41	0.40	0.75	0.95	0.92	0.44
2	21	134	1	1	4.2" Mortar	H	-115	0	0	0.02	0.051	0.60	0.52	0.55	0.4	0.94	0.88	0.89
1	7	74	1	1	Fragment	H	-112	--	--	0.08	0.084	0.33	0.38	0.37	0.15	0.93	0.77	0.86
2	20	164	1	1	2.75" Rocket	H	-172	90	10	0.06	0.086	0.34	0.41	0.79	0.6	0.93	0.78	0.57
3	1	62/80	1	1	81mm Mortar	H	-179	0	180	0.06	0.079	0.33	0.28	0.37	0.25	0.93	0.89	0.92
1	54	115	1	1	76mm Projectile	H	110	270	30	0.10	0.064	0.50	0.50	0.68	0.25	0.91	0.98	0.91
1	27	104	1	1	81mm Mortar	H	33	180	0	0.06	0.078	0.41	0.27	0.46	0.35	0.91	0.90	0.84
2	2	108	1	1	Fragment	H	155	--	--	0.08	0.058	0.52	0.35	0.59	0.4	0.90	0.95	0.91
3	5	50/76	1	1	81mm Mortar	H	-50	-90	--	0.06	0.064	0.40	0.28	0.39	0.2	0.90	0.88	0.93
2	16	116	1	1	81mm Mortar	H	-140	45	0	0.06	0.088	0.35	0.28	0.37	0.3	0.87	0.77	0.51
1	4	198	1	1	Fragment	H	-40	--	--	0.06	0.069	0.41	0.40	0.46	0.3	0.86	0.92	0.76
1	53	88	1	1	60mm Mortar	H	172	0	0	0.17	0.115	0.26	0.18	0.82	0.35	0.84	0.86	0.58
1	55	117/18	1	1	152mm Projectile	H	101	--	--	0.11	0.114	0.28	0.48	0.40	0.25	0.83	0.75	0.37
1	35	170	1	1	Fragment	H	-127	--	--	0.03	0.048	0.71	0.43	0.24	0.15	0.82	0.93	0.71
2	12	120/88	1	1	60mm Mortar	H	157	270	0	0.14	0.126	0.24	0.18	0.36	0.3	0.80	0.91	1.00
2	23	131/16	1	1	81mm Mortar	H	-39	0	0	0.14	0.108	0.28	0.28	0.45	0.25	0.77	0.88	0.37
1	58	113/2	1	1	105mm Projectile	H	-62	120	30	0.11	0.045	0.72	0.37	0.67	0.5	0.76	0.83	0.38
1	24	102	1	1	81mm Mortar	H	41	210	45	0.08	0.084	0.37	0.28	0.39	0.25	0.75	0.72	0.53
1	46	40	1	1	Fragment	H	180	--	--	0.09	0.078	0.43	0.30	0.37	0.3	0.71	0.83	0.69
2	6	130	1	1	81mm Mortar	H	-74		0	0.06	0.074	0.40	0.28	0.40	0.7	0.70	0.86	0.97
1	19	64	1	1	Fragment	H	-148	--	--	0.04	0.094	0.36	0.35	0.16	0.2	0.46	0.70	0.45
1	9	120	1	1	76mm Projectile	H	16	0	20	0.05	0.063	0.44	0.50	0.42	0.25	0.43	0.59	0.87
3	8	68/6	1	1	60mm Mortar	H	17	--	--	0.08	0.058	0.46	0.18	0.26	0.1	0.88	0.86	0.82
1	11	153	1	1	2.75" Rocket	M	-3	0	90	0.11	0.093	0.33	0.41	0.63	0.76	0.99	0.98	0.57
1	52	144	1	1	105mm Projectile	M	164	180	0	0.15	0.088	0.38	0.37	0.66	0.5	0.97	0.91	0.21
1	33	36	1	1	Fragment	M	-166	--	--	0.18	0.177	0.13	0.20	0.13	0.15	0.94	0.93	0.56
1	37	92	1	1	81mm Mortar	M	-153	30	20	0.05	0.070	0.44	0.41	0.39	0.2	0.91	0.96	0.57
1	40	168	1	1	Fragment	M	-95	--	--	0.21	0.143	0.19	0.20	0.37	0.25	0.89	0.94	0.75
1	31	118	1	1	5" Projectile	M	168	120	30	0.06	0.033	0.96	0.63	0.78	0.45	0.84	0.77	0.52

AREA	TAR #	WES #	GPR ID	True UXO	Description	Conf.	ETO (o)	True Azi.	True Inc.	CNR (NP/ns)	CNR (GHz)	ETL (m)	True L	DEP (m)	True Depth	Late-Time ELF(t)	Late-Time ELF(f)	Early-Time ELF
2	22	132	1	1	5" Projectile	M	-31	0	90	0.04	0.035	0.93	0.63	1.00	0.91	0.82	0.75	0.93
3	3	78	1	1	60mm Mortar	M	-28	40	330	0.10	0.095	0.28	0.18	0.46	0.35	0.81	0.60	0.85
2	8	152	1	1	57mm Projectile	M	20	90	0	0.14	0.123	0.24	0.12	0.14	0.25	0.79	0.88	0.79
1	8	121/184	1	1	155mm Projectile	M	-173	200	0	0.09	0.086	0.35	0.60	0.53	0.5	0.78	0.39	0.49
1	38	172	1	1	Fragment	M	-112	--	--	0.03	0.088	0.39	0.21	0.14	0.3	0.66	0.56	0.37
1	29	54	1	1	Fragment	L	-174	--	--	0.09	0.090	0.34	0.30	0.42	0.5	0.98	0.72	0.56
1	16	108	1	1	60mm Mortar	L	-59	100	45	0.07	0.130	0.26	0.18	0.25	0.2	0.91	0.93	0.43
1	34	98	1	1	60mm Mortar	L	160	275	20	0.18	0.143	0.22	0.18	0.33	0.1	0.87	0.95	0.28
1	41	136	1	1	155mm Projectile	L	-8	90	75	0.07	0.032	0.92	0.60	0.57	0.5	0.86	0.69	0.27
2	1	156	1	1	155mm Projectile	L	67	--	90	0.01	0.104	0.29	0.12	2.09	1.5	0.86	0.34	0.23
2	14	140	1	1	105mm Projectile	L	-61	330	10	0.06	0.017	1.73	0.37	0.75	0.7	0.85	0.95	0.86
1	2	84	1	1	Fragment	L	39	--	--	0.03	0.101	0.30	0.09	0.60	0.1	0.84	0.14	0.65
1	28	138	1	1	57mm Projectile	L	-110	95	45	0.05	0.088	0.37	0.12	0.27	0.15	0.82	0.58	0.30
1	15	62	1	1	Fragment	L	73	--	--	0.12	0.120	0.28	0.15	0.12	0.1	0.82	0.80	0.50
1	62	149	1	1	2.75" Rocket	L	-103	30	55	0.04	0.058	0.52	0.41	0.94	0.5	0.77	0.83	0.68
2	9	124	1	1	60mm Mortar	L	32	330	10	0.27	0.172	0.18	0.18	0.14	0.2	0.71	0.62	0.47
1	44	126	1	1	57mm Projectile	L	136	120	30	0.11	0.073	0.47	0.12	0.36	0.2	0.59	0.43	0.47
1	12	119	1	1	152mm Projectile	L	-100	270	30	0.02	0.032	0.95	0.48	0.74	0.4	0.55	0.61	0.62
1	32	30	1	1	Fragment	L	80	--	--	0.07	0.072	0.45	0.15	0.32	0.05	0.55	0.58	0.11
1	60	4	1	1	Fragment	L	-101	--	--	0.08	0.031	1.01	0.31	0.87	0.75	0.54	0.91	0.42
2	4	94	1	1	Fragment	L	171	--	--	0.15	0.090	0.36	0.19	0.18	0.35	0.52	0.61	0.30
2	26		1	-1		H	-177			0.03	0.078	0.36		0.73		1.00	0.90	0.71
1	61	158	1	0	Fragment	H	-120	--	--	0.07	0.087	0.36	0.05	0.15	0.05	0.94	0.95	0.74
1	36	42	1	0	Fragment	H	30	--	--	0.18	0.134	0.24	0.15	0.45	0.35	0.72	0.83	0.29
1	26	164	1	0	Fragment	M	171	--	--	0.10	0.059	0.55	0.13	0.56	0.1	0.90	0.98	0.05
1	45	26	1	0	Fragment	M	-171	--	--	0.08	0.146	0.19	0.20	0.30	0.075	0.77	0.78	0.31
2	15	46	1	0	Fragment	M	-47	--	--	0.10	0.112	0.27	0.24	0.37	0.2	0.67	0.75	0.36
1	59	10	1	0	Fragment	L	61	--	--	0.03	0.117	0.29	0.08	0.11	0.1	0.89	0.16	0.22
3	2	110	1	0	Magnetic Rock	L	123			0.06	0.064	0.41	0.21	0.20	0.2	0.81	0.80	0.33
1	42	28	1	0	Fragment	L	-121	--	--	0.12	0.043	0.74	0.12	2.14	0.15	0.81	0.95	0.52
2	17		1	-1		L	110			0.12	0.078	0.38		0.76		0.78	0.51	0.62
2	24		1	-1		L	21			0.07	0.053	0.57		0.82		0.66	0.54	0.95
1	63	16	1	0	Fragment	L	-10	--	--	0.06	0.069	0.44	0.11	0.17	0.05	0.63	0.64	0.19
1	43	154	1	0	Magnetic Rock	L	93			0.04	0.099	0.35	0.21	0.34	0.2	0.62	0.90	0.24
2	19	54	1	0	Fragment	L	118	--	--	0.10	0.083	0.36	0.10	0.24	0.2	0.35	0.41	0.26
2	25		1	-1		L	-106			0.01	0.028	1.06		1.08		0.28	0.40	0.88
1	3	78	0	0	Fragment	H	-155	--	--	0.44	0.125	0.25	0.10	0.36	0.1	0.38	0.29	0.48
1	57	6	0	0	Fragment	H	137	--	--	0.18	0.125	0.26	0.16	0.09	0.25	0.11	0.23	0.38
1	6	82	0	0	Fragment	H	132	--	--	0.18	0.096	0.33	0.03	0.67	0.1	0.01	0.31	0.19
1	13	186	0	0	Fragment	M	-60	--	--	0.13	0.069	0.40	0.10	0.35	0.1	0.85	0.90	0.02
1	17	66	0	0	Fragment	M	-42	--	--	0.07	0.099	0.35	0.05	0.48	0.15	0.39	0.41	0.15
1	10	180	0	0	Fragment	M	56	--	--	0.25	0.053	0.61	0.20	0.08	0.1	0.01	0.19	0.08

AREA	TAR #	WES #	GPR ID	True UXO	Description	Conf.	ETO (o)	True Azi.	True Inc.	CNR (NP/ns)	CNR (GHz)	ETL (m)	True L	DEP (m)	True Depth	Late-Time ELF(t)	Late-Time ELF(f)	Early-Time ELF
3	10		0	-1		L	-38			0.35	0.190	0.13		0.54		0.83	0.55	0.18
1	14	72	0	0	Fragment	L	130	--	--	0.07	0.065	0.47	0.05	0.36	0.1	0.39	0.58	0.17
3	7		0	-1		L	45			0.12	0.083	0.31		0.59		0.30	0.21	0.19
2	13	36	0	0	Fragment	L	-167	--	--	0.13	0.122	0.26	0.11	0.11	0.25	0.25	0.39	0.33
3	4		0	-1		L	90			0.07	0.071	0.35		0.82		0.12	0.26	0.50
3	6		0	-1		L	58			0.09	0.072	0.40		0.19		0.07	0.35	0.14
2	18	42	0	1	Fragment	H	87	--	--	0.27	0.080	0.33	0.33	0.07	0.75	0.28	0.02	0.21
2	27	112	0	1	81mm Mortar	H	-62	--	90	0.09	0.100	0.30	0.28	0.09	0.1	0.23	0.40	0.09
2	10	144	0	1	152mm Projectile	H	150	50	30	0.14	0.126	0.24	0.48	0.37	0.45	0.10	0.35	0.18
1	18	122	0	1	5" Projectile	H	-177	270	55	0.14	0.054	0.53	0.63	0.57	0.91	0.03	0.11	0.15
3	9	100	0	1	152mm Projectile	M	40	35	90	0.05	0.067	0.37	0.48	0.56	0.91	0.48	0.20	0.34
1	20	106	0	1	60mm Mortar	M	136	75	35	0.05	0.064	0.48	0.18	0.39	0.25	0.26	0.32	0.19
1	1	196	0	1	Fragment	M	-45	--	--	0.31	0.170	0.18	0.30	0.05	1.2	0.10	0.14	0.04
1	23	142	0	1	57mm Projectile	M	15	265	45	0.24	0.188	0.18	0.12	0.10	0.15	0.08	0.22	0.64
1	48	150	0	1	2.75" Rocket	M	93	275	45	0.02	0.067	0.47	0.41	0.40	0.7	0.03	0.10	0.38
1	56	8	0	1	Fragment	L	157	--	--	0.13	0.129	0.24	0.20	0.42	0.3	0.40	0.33	0.47
1	22	176	0	1	Fragment	L	126	--	--	0.23	0.180	0.19	0.13	0.48	0.15	0.28	0.27	0.23
1	25	132	0	1	57mm Projectile	L	-125	180	0	0.32	0.138	0.21	0.12	0.09	0.25	0.17	0.09	0.15

Table 28 Comparison of Ground Truth and GPR UXO Classification (ROUND 2, LD3 Criteria).

AREA	TAR #	WES #	GPR ID	True UXO	Type	Conf.	ETO (o)	True Azi.	True Inc.	CNR (NP/ns)	CNR (GHz)	ETL (m)	True L	DEP (m)	True Depth	Late-Time ELF(t)	Late-Time ELF(f)	Early-Time ELF
1	47	38	1	1	Fragment	H	66	--	--	0.04	0.083	0.36	0.45	0.42	0.15	0.99	1.00	0.95
1	39	94	1	1	81mm Mortar	H	-88	75	55	0.05	0.047	0.66	0.48	0.68	0.25	0.99	0.91	0.34
2	11	128	1	1	60mm Mortar	H	-60	95	20	0.08	0.141	0.21	0.18	0.29	0.1	0.99	0.91	0.72
1	21	152	1	1	2.75" Rocket	H	-165	30	0	0.07	0.072	0.48	0.41	0.32	0.15	0.98	0.99	0.95
2	3	98	1	1	Fragment	H	-175	--	--	0.05	0.068	0.44	0.40	0.59	0.3	0.98	0.78	0.72
1	49	90	1	1	4.2" Mortar	H	-67	270	0	0.05	0.070	0.46	0.52	0.59	0.35	0.98	0.96	0.89
1	50	100	1	1	60mm Mortar	H	3	195	30	0.19	0.084	0.38	0.52	0.52	0.2	0.98	0.91	0.61
1	30	96	1	1	81mm Mortar	H	179	330	35	0.08	0.075	0.37	0.27	0.49	0.15	0.96	0.92	0.46
2	7	166/76	1	1	2.75" Rocket	H	100	180	20	0.13	0.117	0.26	0.41	0.40	0.75	0.95	0.92	0.44
2	21	134	1	1	4.2" Mortar	H	-115	0	0	0.02	0.051	0.60	0.52	0.55	0.4	0.94	0.88	0.89
1	7	74	1	1	Fragment	H	-112	--	--	0.08	0.084	0.33	0.38	0.37	0.15	0.93	0.77	0.86
2	20	164	1	1	2.75" Rocket	H	-172	90	10	0.06	0.086	0.34	0.41	0.79	0.6	0.93	0.78	0.57
3	1	62/80	1	1	81mm Mortar	H	-179	0	180	0.06	0.079	0.33	0.28	0.37	0.25	0.93	0.89	0.92
1	54	115	1	1	76mm Projectile	H	110	270	30	0.10	0.064	0.50	0.50	0.68	0.25	0.91	0.98	0.91
1	27	104	1	1	81mm Mortar	H	33	180	0	0.06	0.078	0.41	0.27	0.46	0.35	0.91	0.90	0.84
2	2	108	1	1	Fragment	H	155	--	--	0.08	0.058	0.52	0.35	0.59	0.4	0.90	0.95	0.91
3	5	50/76	1	1	81mm Mortar	H	-50	-90	--	0.06	0.064	0.40	0.28	0.39	0.2	0.90	0.88	0.93
3	8	68/6	1	1	60mm Mortar	H	17	--	--	0.08	0.058	0.46	0.18	0.26	0.1	0.88	0.86	0.82
2	16	116	1	1	81mm Mortar	H	-140	45	0	0.06	0.088	0.35	0.28	0.37	0.3	0.87	0.77	0.51
1	4	198	1	1	Fragment	H	-40	--	--	0.06	0.069	0.41	0.40	0.46	0.3	0.86	0.92	0.76
1	53	88	1	1	60mm Mortar	H	172	0	0	0.17	0.115	0.26	0.18	0.82	0.35	0.84	0.86	0.58
1	55	117/18	1	1	152mm Projectile	H	101	--	--	0.11	0.114	0.28	0.48	0.40	0.25	0.83	0.75	0.37
1	35	170	1	1	Fragment	H	-127	--	--	0.03	0.048	0.71	0.43	0.24	0.15	0.82	0.93	0.71
2	12	120/88	1	1	60mm Mortar	H	157	270	0	0.14	0.126	0.24	0.18	0.36	0.3	0.80	0.91	1.00
2	23	131/16	1	1	81mm Mortar	H	-39	0	0	0.14	0.108	0.28	0.28	0.45	0.25	0.77	0.88	0.37
1	58	113/2	1	1	105mm Projectile	H	-62	120	30	0.11	0.045	0.72	0.37	0.67	0.5	0.76	0.83	0.38
1	24	102	1	1	81mm Mortar	H	41	210	45	0.08	0.084	0.37	0.28	0.39	0.25	0.75	0.72	0.53
1	46	40	1	1	Fragment	H	180	--	--	0.09	0.078	0.43	0.30	0.37	0.3	0.71	0.83	0.69
2	6	130	1	1	81mm Mortar	H	-74		0	0.06	0.074	0.40	0.28	0.40	0.7	0.70	0.86	0.97
1	19	64	1	1	Fragment	H	-148	--	--	0.04	0.094	0.36	0.35	0.16	0.2	0.46	0.70	0.45
1	9	120	1	1	76mm Projectile	H	16	0	20	0.05	0.063	0.44	0.50	0.42	0.25	0.43	0.59	0.87
1	11	153	1	1	2.75" Rocket	M	-3	0	90	0.11	0.093	0.33	0.41	0.63	0.76	0.99	0.98	0.57
1	52	144	1	1	105mm Projectile	M	164	180	0	0.15	0.088	0.38	0.37	0.66	0.5	0.97	0.91	0.21

AREA	TAR #	WES #	GPR ID	True UXO	Type	Conf.	ETO (o)	True Azi.	True Inc.	CNR (NP/ns)	CNR (GHz)	ETL (m)	True L	DEP (m)	True Depth	Late-Time ELF(t)	Late-Time ELF(f)	Early-Time ELF
1	33	36	1	1	Fragment	M	-166	--	--	0.18	0.177	0.13	0.20	0.13	0.15	0.94	0.93	0.56
1	37	92	1	1	81mm Mortar	M	-153	30	20	0.05	0.070	0.44	0.41	0.39	0.2	0.91	0.96	0.57
1	40	168	1	1	Fragment	M	-95	--	--	0.21	0.143	0.19	0.20	0.37	0.25	0.89	0.94	0.75
1	31	118	1	1	5" Projectile	M	168	120	30	0.06	0.033	0.96	0.63	0.78	0.45	0.84	0.77	0.52
2	22	132	1	1	5" Projectile	M	-31	0	90	0.04	0.035	0.93	0.63	1.00	0.91	0.82	0.75	0.93
3	3	78	1	1	60mm Mortar	M	-28	40	330	0.10	0.095	0.28	0.18	0.46	0.35	0.81	0.60	0.85
1	8	121/184	1	1	155mm Projectile	M	-173	200	0	0.09	0.086	0.35	0.60	0.53	0.5	0.78	0.39	0.49
1	16	108	1	1	60mm Mortar	L	-59	100	45	0.07	0.130	0.26	0.18	0.25	0.2	0.91	0.93	0.43
1	34	98	1	1	60mm Mortar	L	160	275	20	0.18	0.143	0.22	0.18	0.33	0.1	0.87	0.95	0.28
1	41	136	1	1	155mm Projectile	L	-8	90	75	0.07	0.032	0.92	0.60	0.57	0.5	0.86	0.69	0.27
2	1	156	1	1	155mm Projectile	L	67	--	90	0.01	0.104	0.29	0.12	2.09	1.5	0.86	0.34	0.23
2	14	140	1	1	105mm Projectile	L	-61	330	10	0.06	0.017	1.73	0.37	0.75	0.7	0.85	0.95	0.86
1	15	62	1	1	Fragment	L	73	--	--	0.12	0.120	0.28	0.15	0.12	0.1	0.82	0.80	0.50
1	62	149	1	1	2.75" Rocket	L	-103	30	55	0.04	0.058	0.52	0.41	0.94	0.5	0.77	0.83	0.68
2	9	124	1	1	60mm Mortar	L	32	330	10	0.27	0.172	0.18	0.18	0.14	0.2	0.71	0.62	0.47
1	12	119	1	1	152mm Projectile	L	-100	270	30	0.02	0.032	0.95	0.48	0.74	0.4	0.55	0.61	0.62
1	32	30	1	1	Fragment	L	80	--	--	0.07	0.072	0.45	0.15	0.32	0.05	0.55	0.58	0.11
1	29	54	1	0	Fragment	L	-174	--	--	0.09	0.090	0.34	0.30	0.42	0.5	0.98	0.72	0.56
1	59	10	1	0	Fragment	L	61	--	--	0.03	0.117	0.29	0.08	0.11	0.1	0.89	0.16	0.22
1	2	84	1	0	Fragment	L	39	--	--	0.03	0.101	0.30	0.09	0.60	0.1	0.84	0.14	0.65
1	28	138	1	0	57mm Projectile	L	-110	95	45	0.05	0.088	0.37	0.12	0.27	0.15	0.82	0.58	0.30
3	2	110	1	0	Magnetic Rock	L	123			0.06	0.064	0.41	0.21	0.20	0.2	0.81	0.80	0.33
1	42	28	1	0	Fragment	L	-121	--	--	0.12	0.043	0.74	0.12	2.14	0.15	0.81	0.95	0.52
2	17		1	-1		L	110			0.12	0.078	0.38		0.76		0.78	0.51	0.62
2	24		1	-1		L	21			0.07	0.053	0.57		0.82		0.66	0.54	0.95
1	63	16	1	0	Fragment	L	-10	--	--	0.06	0.069	0.44	0.11	0.17	0.05	0.63	0.64	0.19
1	43	154	1	0	Magnetic Rock	L	93			0.04	0.099	0.35	0.21	0.34	0.2	0.62	0.90	0.24
1	44	126	1	0	57mm Projectile	L	136	120	30	0.11	0.073	0.47	0.12	0.36	0.2	0.59	0.43	0.47
1	60	4	1	0	Fragment	L	-101	--	--	0.08	0.031	1.01	0.31	0.87	0.75	0.54	0.91	0.42
2	4	94	1	0	Fragment	L	171	--	--	0.15	0.090	0.36	0.19	0.18	0.35	0.52	0.61	0.30
2	19	54	1	0	Fragment	L	118	--	--	0.10	0.083	0.36	0.10	0.24	0.2	0.35	0.41	0.26
2	25		1	-1		L	-106			0.01	0.028	1.06		1.08		0.28	0.40	0.88
1	26	164	1	0	Fragment	M	171	--	--	0.10	0.059	0.55	0.13	0.56	0.1	0.90	0.98	0.05
2	8	152	1	0	57mm Projectile	M	20	90	0	0.14	0.123	0.24	0.12	0.14	0.25	0.79	0.88	0.79
1	45	26	1	0	Fragment	M	-171	--	--	0.08	0.146	0.19	0.20	0.30	0.075	0.77	0.78	0.31
2	15	46	1	0	Fragment	M	-47	--	--	0.10	0.112	0.27	0.24	0.37	0.2	0.67	0.75	0.36
1	38	172	1	0	Fragment	M	-112	--	--	0.03	0.088	0.39	0.21	0.14	0.3	0.66	0.56	0.37
2	26		1	-1		H	-177			0.03	0.078	0.36		0.73		1.00	0.90	0.71
1	51	162	1	0	Fragment	H	-26	--	--	0.04	0.076	0.40	0.33	0.45	0.25	0.99	0.92	0.78
2	5	72	1	0	Fragment	H	144	--	--	0.07	0.082	0.36	0.27	0.58	0.5	0.98	0.97	0.56

AREA	TAR #	WES #	GPR ID	True UXO	Type	Conf.	ETO (o)	True Azi.	True Inc.	CNR (NP/ns)	CNR (GHz)	ETL (m)	True L	DEP (m)	True Depth	Late-Time ELF(t)	Late-Time ELF(f)	Early-Time ELF
1	5	147	1	0	57mm Projectile	H	49	0	0	0.09	0.127	0.27	0.12	0.14	0.25	0.98	0.92	0.68
1	61	158	1	0	Fragment	H	-120	--	--	0.07	0.087	0.36	0.05	0.15	0.05	0.94	0.95	0.74
1	36	42	1	0	Fragment	H	30	--	--	0.18	0.134	0.24	0.15	0.45	0.35	0.72	0.83	0.29
3	10		0	-1		L	-38			0.35	0.190	0.13		0.54		0.83	0.55	0.18
1	14	72	0	0	Fragment	L	130	--	--	0.07	0.065	0.47	0.05	0.36	0.1	0.39	0.58	0.17
3	7		0	-1		L	45			0.12	0.083	0.31		0.59		0.30	0.21	0.19
1	22	176	0	0	Fragment	L	126	--	--	0.23	0.180	0.19	0.13	0.48	0.15	0.28	0.27	0.23
2	13	36	0	0	Fragment	L	-167	--	--	0.13	0.122	0.26	0.11	0.11	0.25	0.25	0.39	0.33
1	25	132	0	0	57mm Projectile	L	-125	180	0	0.32	0.138	0.21	0.12	0.09	0.25	0.17	0.09	0.15
3	4		0	-1		L	90			0.07	0.071	0.35		0.82		0.12	0.26	0.50
3	6		0	-1		L	58			0.09	0.072	0.40		0.19		0.07	0.35	0.14
1	13	186	0	0	Fragment	M	-60	--	--	0.13	0.069	0.40	0.10	0.35	0.1	0.85	0.90	0.02
1	17	66	0	0	Fragment	M	-42	--	--	0.07	0.099	0.35	0.05	0.48	0.15	0.39	0.41	0.15
1	23	142	0	0	57mm Projectile	M	15	265	45	0.24	0.188	0.18	0.12	0.10	0.15	0.08	0.22	0.64
1	10	180	0	0	Fragment	M	56	--	--	0.25	0.053	0.61	0.20	0.08	0.1	0.01	0.19	0.08
1	3	78	0	0	Fragment	H	-155	--	--	0.44	0.125	0.25	0.10	0.36	0.1	0.38	0.29	0.48
1	57	6	0	0	Fragment	H	137	--	--	0.18	0.125	0.26	0.16	0.09	0.25	0.11	0.23	0.38
1	6	82	0	0	Fragment	H	132	--	--	0.18	0.096	0.33	0.03	0.67	0.1	0.01	0.31	0.19
1	56	8	0	1	Fragment	L	157	--	--	0.13	0.129	0.24	0.20	0.42	0.3	0.40	0.33	0.47
3	9	100	0	1	152mm Projectile	M	40	35	90	0.05	0.067	0.37	0.48	0.56	0.91	0.48	0.20	0.34
1	20	106	0	1	60mm Mortar	M	136	75	35	0.05	0.064	0.48	0.18	0.39	0.25	0.26	0.32	0.19
1	1	196	0	1	Fragment	M	-45	--	--	0.31	0.170	0.18	0.30	0.05	1.2	0.10	0.14	0.04
1	48	150	0	1	2.75" Rocket	M	93	275	45	0.02	0.067	0.47	0.41	0.40	0.7	0.03	0.10	0.38
2	18	42	0	1	Fragment	H	87	--	--	0.27	0.080	0.33	0.33	0.07	0.75	0.28	0.02	0.21
2	27	112	0	1	81mm Mortar	H	-62	--	90	0.09	0.100	0.30	0.28	0.09	0.1	0.23	0.40	0.09
2	10	144	0	1	152mm Projectile	H	150	50	30	0.14	0.126	0.24	0.48	0.37	0.45	0.10	0.35	0.18
1	18	122	0	1	5" Projectile	H	-177	270	55	0.14	0.054	0.53	0.63	0.57	0.91	0.03	0.11	0.15

Table 29 Comparison of Ground Truth and GPR UXO Classification (ROUND 3, True UXO Criteria).

AREA	TAR #	WES #	GPR ID	True UXO	Type	Conf.	ETO (o)	T. Azi. (o)	T. Inc. (o)	CNR (NP/ns)	CNR (GHz)	ETL (m)	True L	DEP (m)	True Depth (m)	Late-Time ELF(t)	Late-Time ELF(f)	Early-Time ELF
1	39	94	1	1	81mm Mortar	H	-88	O75	55	0.05	0.047	0.66	0.48	0.68	0.25	0.99	0.91	0.34
2	11	128	1	1	60mm Mortar	H	-60	O95	20	0.08	0.141	0.21	0.18	0.29	0.10	0.99	0.91	0.72
1	21	152	1	1	2.75" Rocket	H	-165	30	0	0.07	0.072	0.48	0.41	0.32	0.15	0.98	0.99	0.95
1	5	147	1	1	57mm Projectile	H	49	0	0	0.09	0.127	0.27	0.12	0.14	0.25	0.98	0.92	0.68
1	49	90	1	1	4.2" Mortar	H	-67	270	0	0.05	0.070	0.46	0.52	0.59	0.35	0.98	0.96	0.89
1	50	100	1	1	60mm Mortar	H	3	195	30	0.19	0.084	0.38	0.52	0.52	0.20	0.98	0.91	0.61
1	30	96	1	1	81mm Mortar	H	179	330	35	0.08	0.075	0.37	0.27	0.49	0.15	0.96	0.92	0.46
2	7	166/76	1	1	2.75" Rocket	H	100	180	20	0.13	0.117	0.26	0.41	0.40	0.75	0.95	0.92	0.44
2	21	134	1	1	4.2" Mortar	H	-115	0	0	0.02	0.051	0.60	0.52	0.55	0.40	0.94	0.88	0.89
2	20	164	1	1	2.75" Rocket	H	-172	O90	10	0.06	0.086	0.34	0.41	0.79	0.60	0.93	0.78	0.57
3	1	62/80	1	1	81mm Mortar	H	-179	0	180	0.06	0.079	0.33	0.28	0.37	0.25	0.93	0.89	0.92
1	54	115	1	1	76mm Projectile	H	110	270	30	0.10	0.064	0.50	0.50	0.68	0.25	0.91	0.98	0.91
1	27	104	1	1	81mm Mortar	H	33	180	0	0.06	0.078	0.41	0.27	0.46	0.35	0.91	0.90	0.84
3	5	50/76	1	1	81mm Mortar	H	-50	-90	--	0.06	0.064	0.40	0.28	0.39	0.20	0.90	0.88	0.93
3	8	68/6	1	1	60mm Mortar	H	17	--	--	0.08	0.058	0.46	0.18	0.26	0.10	0.88	0.86	0.82
2	16	116	1	1	81mm Mortar	H	-140	O45	0	0.06	0.088	0.35	0.28	0.37	0.30	0.87	0.77	0.51
1	53	88	1	1	60mm Mortar	H	172	0	0	0.17	0.115	0.26	0.18	0.42	0.35	0.84	0.86	0.58
1	55	117/18	1	1	152mm Projectile	H	101	--	--	0.11	0.114	0.28	0.48	0.40	0.25	0.83	0.75	0.37
2	12	120/88	1	1	60mm Mortar	H	157	270	0	0.14	0.126	0.24	0.18	0.36	0.30	0.80	0.91	1.00
2	23	131/16	1	1	81mm Mortar	H	-39	0	0	0.14	0.108	0.28	0.28	0.45	0.25	0.77	0.88	0.37
1	58	113/2	1	1	105mm Projectile	H	-62	120	30	0.11	0.045	0.72	0.37	0.67	0.50	0.76	0.83	0.38
1	24	102	1	1	81mm Mortar	H	41	210	45	0.08	0.084	0.37	0.28	0.39	0.25	0.75	0.72	0.53
2	6	130	1	1	81mm Mortar	H	-74		0	0.06	0.074	0.40	0.28	0.40	0.70	0.70	0.86	0.97
1	9	120	1	1	76mm Projectile	H	16	0	20	0.05	0.063	0.44	0.50	0.42	0.25	0.43	0.59	0.87
1	11	153	1	1	2.75" Rocket	M	-3	0	90	0.11	0.093	0.33	0.41	0.63	0.76	0.99	0.98	0.57
1	52	144	1	1	105mm Projectile	M	164	180	0	0.15	0.088	0.38	0.37	0.66	0.50	0.97	0.91	0.21
1	16	108	1	1	60mm Mortar	M	-58	100	45	0.17	0.118	0.27	0.18	0.26	0.20	0.96	0.85	0.69
1	37	92	1	1	81mm Mortar	M	-153	O30	20	0.05	0.070	0.44	0.41	0.39	0.20	0.91	0.96	0.57
1	31	118	1	1	5" Projectile	M	168	120	30	0.06	0.033	0.96	0.63	0.78	0.45	0.84	0.77	0.52

AREA	TAR #	WES #	GPR ID	True UXO	Type	Conf.	ETO (o)	T. Azi. (o)	T. Inc. (o)	CNR (NP/ns)	CNR (GHz)	ETL (m)	True L	DEP (m)	True Depth (m)	Late-Time ELF(t)	Late-Time ELF(f)	Early-Time ELF
2	22	132	1	1	5" Projectile	M	-31	0	O90	0.04	0.035	0.93	0.63	1.00	0.91	0.82	0.75	0.93
3	3	78	1	1	60mm Mortar	M	-28	40	330	0.10	0.095	0.28	0.18	0.46	0.35	0.81	0.60	0.85
2	8	152	1	1	57mm Projectile	M	20	O90	0	0.14	0.123	0.24	0.12	0.14	0.25	0.79	0.88	0.79
1	8	121/184	1	1	155mm Projectile	M	-173	200	0	0.09	0.086	0.35	0.60	0.53	0.50	0.78	0.39	0.49
1	41	136	1	1	155mm Projectile	L	-8	O90	75	0.07	0.032	0.92	0.60	0.57	0.50	0.86	0.69	0.27
2	14	140	1	1	105mm Projectile	L	-61	330	10	0.06	0.017	1.73	0.37	0.75	0.70	0.85	0.95	0.86
1	28	138	1	1	57mm Projectile	L	-110	O95	45	0.05	0.088	0.37	0.12	0.27	0.15	0.82	0.58	0.30
1	62	149	1	1	2.75" Rocket	L	-103	O30	55	0.04	0.058	0.52	0.41	0.94	0.50	0.77	0.83	0.68
2	9	124	1	1	60mm Mortar	L	32	330	10	0.27	0.172	0.18	0.18	0.14	0.20	0.71	0.62	0.47
2	4	94	1	0	Fragment	L	167	--	--	0.30	0.088	0.34	0.19	0.42	0.35	0.97	0.73	0.19
1	29	54	1	0	Fragment	L	-178	--	--	0.04	0.074	0.40	0.30	0.41	0.50	0.97	0.96	0.76
1	42	28	1	0	Fragment	L	153	--	--	0.31	0.111	0.30	0.12	0.35	0.15	0.82	0.93	0.38
1	15	62	1	0	Fragment	L	73	--	--	0.12	0.120	0.28	0.15	0.12	0.10	0.82	0.80	0.50
1	60	4	1	0	Fragment	L	-143	--	--	0.04	0.031	1.01	0.31	0.60	0.75	0.78	0.89	0.93
2	25		1	-1		L	-63			0.03	0.098	0.31		0.75	0.55	0.75	0.82	0.91
1	1	196	1	0	Fragment	L	-4	0	--	0.03	0.051	0.58	0.30	1.06	1.20	0.41	0.55	0.71
1	33	36	1	0	Fragment	M	-166	--	--	0.18	0.177	0.13	0.20	0.13	0.15	0.94	0.93	0.56
1	17	66	1	0	Fragment	M	171	--	--	0.06	0.085	0.36	0.05	0.20	0.15	0.91	0.82	0.42
1	13	186	1	0	Fragment	M	-60	--	--	0.19	0.148	0.23	0.10	0.27	0.10	0.91	0.97	0.71
1	40	168	1	0	Fragment	M	-95	--	--	0.21	0.143	0.19	0.20	0.37	0.25	0.89	0.94	0.75
1	45	26	1	0	Fragment	M	-171	--	--	0.08	0.146	0.19	0.20	0.30	0.08	0.77	0.78	0.31
3	2	110	1	0	Magnetic Rock	M	123			0.07	0.091	0.29	0.21	0.19	0.20	0.70	0.73	0.37
2	15	46	1	0	Fragment	M	-47	--	--	0.10	0.112	0.27	0.24	0.37	0.20	0.67	0.75	0.36
1	38	172	1	0	Fragment	M	-112	--	--	0.03	0.088	0.39	0.21	0.14	0.30	0.66	0.56	0.37
2	26		1	-1		H	-177			0.03	0.078	0.36		0.73	0.35	1.00	0.90	0.71
1	51	162	1	0	Fragment	H	-26	--	--	0.04	0.076	0.40	0.33	0.45	0.25	0.99	0.92	0.78
1	47	38	1	0	Fragment	H	66	--	--	0.04	0.083	0.36	0.45	0.42	0.15	0.99	1.00	0.95
2	3	98	1	0	Fragment	H	-175	--	--	0.05	0.068	0.44	0.40	0.59	0.30	0.98	0.78	0.72
2	5	72	1	0	Fragment	H	144	--	--	0.07	0.082	0.36	0.27	0.58	0.50	0.98	0.97	0.56
1	61	158	1	0	Fragment	H	-120	--	--	0.07	0.087	0.36	0.05	0.15	0.05	0.94	0.95	0.74
1	7	74	1	0	Fragment	H	-112	--	--	0.08	0.084	0.33	0.38	0.37	0.15	0.93	0.77	0.86
2	2	108	1	0	Fragment	H	155	--	--	0.08	0.058	0.52	0.35	0.59	0.40	0.90	0.95	0.91
1	4	198	1	0	Fragment	H	-40	--	--	0.06	0.069	0.41	0.40	0.46	0.30	0.86	0.92	0.76
1	3	78	1	0	Fragment	H	-65	--	--	0.15	0.092	0.35	0.10	0.12	0.10	0.85	0.78	0.67
1	35	170	1	0	Fragment	H	-127	--	--	0.03	0.048	0.71	0.43	0.24	0.15	0.82	0.93	0.71
1	36	42	1	0	Fragment	H	30	--	--	0.18	0.134	0.24	0.15	0.45	0.35	0.72	0.83	0.29
2	18	42	1	0	Fragment	H	-147	--	--	0.05	0.064	0.47	0.33	0.89	0.75	0.72	0.76	0.83
1	46	40	1	0	Fragment	H	180	--	--	0.09	0.078	0.43	0.30	0.37	0.30	0.71	0.83	0.69
1	19	64	1	0	Fragment	H	-148	--	--	0.04	0.094	0.36	0.35	0.16	0.20	0.46	0.70	0.45
2	24		0	-1		L	-135			0.07	0.082	0.36		1.44	1.50	0.88	0.11	0.40
3	10		0	-1		L	-38			0.35	0.190	0.13		0.54	0.25	0.83	0.55	0.18
2	17		0	-1		L	109			0.16	0.073	0.41		0.78	0.50	0.40	0.50	0.34

AREA	TAR #	WES #	GPR ID	True UXO	Type	Conf.	ETO (o)	T. Azi. (o)	T. Inc. (o)	CNR (NP/ns)	CNR (GHz)	ETL (m)	True L	DEP (m)	True Depth (m)	Late-Time ELF(t)	Late-Time ELF(f)	Early-Time ELF
1	56	8	0	0	Fragment	L	157	--	--	0.13	0.129	0.24	0.20	0.42	0.30	0.40	0.33	0.47
3	7		0	-1		L	45			0.12	0.083	0.31		0.59	0.55	0.30	0.21	0.19
2	19	54	0	0	Fragment	L	-149	--	--	0.14	0.215	0.14	0.10	0.27	0.20	0.22	0.52	0.12
3	4		0	-1		L	90			0.07	0.071	0.35		0.82	1.15	0.12	0.26	0.50
3	6		0	-1		L	58			0.09	0.072	0.40		0.19	0.25	0.07	0.35	0.14
1	43	154	0	0	Magnetic Rock	L	-179			0.10	0.100	0.28	0.21	0.08	0.20	0.03	0.17	0.13
2	13	36	0	0	Fragment	M	-167	--	--	0.13	0.122	0.26	0.11	0.11	0.25	0.25	0.39	0.33
1	22	176	0	0	Fragment	M	41	--	--	0.14	0.190	0.16	0.13	0.15	0.15	0.20	0.66	0.35
1	59	10	0	0	Fragment	M	-30	--	--	0.27	0.058	0.57	0.08	0.13	0.10	0.13	0.24	0.38
1	10	180	0	0	Fragment	M	56	--	--	0.25	0.053	0.61	0.20	0.08	0.10	0.01	0.19	0.08
1	14	72	0	0	Fragment	H	90	--	--	0.13	0.101	0.27	0.05	0.17	0.10	0.35	0.30	0.25
1	63	16	0	0	Fragment	H	-10	--	--	0.10	0.090	0.35	0.11	0.07	0.05	0.30	0.39	0.22
1	6	82	0	0	Fragment	H	132	--	--	0.20	0.104	0.28	0.03	0.64	0.10	0.20	0.23	0.08
1	26	164	0	0	Fragment	H	171	--	--	0.04	0.070	0.46	0.13	0.49	0.10	0.17	0.15	0.51
1	57	6	0	0	Fragment	H	137	--	--	0.18	0.125	0.26	0.16	0.09	0.25	0.11	0.23	0.38
1	2	84	0	0	Fragment	H	63	--	--	0.15	0.117	0.26	0.09	0.10	0.10	0.04	0.08	0.07
1	32	30	0	0	Fragment	H	78	--	--	0.05	0.081	0.42	0.15	0.13	0.05	0.03	0.03	0.25
1	44	126	0	1	57mm Projectile	L	136	120	30	0.11	0.073	0.47	0.12	0.36	0.20	0.59	0.43	0.47
1	12	119	0	1	152mm Projectile	L	-97	270	30	0.10	0.041	0.72	0.48	0.71	0.40	0.41	0.18	0.18
2	1	156	0	1	155mm Projectile	L	67	--	90	0.08	0.062	0.50	0.12	2.17	1.50	0.21	0.32	0.24
1	25	132	0	1	57mm Projectile	L	-125	180	0	0.32	0.138	0.21	0.12	0.09	0.25	0.17	0.09	0.15
1	20	106	0	1	60mm Mortar	M	136	O75	35	0.05	0.064	0.48	0.18	0.39	0.25	0.26	0.32	0.19
3	9	100	0	1	152mm Projectile	M	-133	35	90	0.07	0.035	0.72	0.48	0.85	0.91	0.22	0.23	0.39
1	34	98	0	1	60mm Mortar	M	-108	275	20	0.07	0.096	0.31	0.18	0.08	0.10	0.19	0.20	0.03
1	23	142	0	1	57mm Projectile	M	15	265	45	0.24	0.188	0.18	0.12	0.10	0.15	0.08	0.22	0.64
1	48	150	0	1	2.75" Rocket	M	93	275	45	0.02	0.067	0.47	0.41	0.40	0.70	0.03	0.10	0.38
2	27	112	0	1	81mm Mortar	H	-62	--	90	0.09	0.100	0.30	0.28	0.09	0.10	0.23	0.40	0.09
2	10	144	0	1	152mm Projectile	H	150	O50	30	0.14	0.126	0.24	0.48	0.37	0.45	0.10	0.35	0.18
1	18	122	0	1	5" Projectile	H	-177	270	55	0.14	0.054	0.53	0.63	0.57	0.91	0.03	0.11	0.15

Table 30 Comparison of Ground Truth and GPR UXO Classification (ROUND 3, LD2 Criteria).

AREA	TAR #	WES ID	GPR ID	True UXO	Type	Conf.	ETO (o)	T. Azi. (o)	T. Inc. (o)	CNR (NP/ns)	CNR (GHz)	ETL (m)	True L	DEP (m)	True Depth	Late-Time ELF(t)	Late-Time ELF(f)	Early-Time ELF
1	51	162	1	1	Fragment	H	-26	--	--	0.04	0.076	0.40	0.33	0.45	0.25	0.99	0.92	0.78
1	47	38	1	1	Fragment	H	66	--	--	0.04	0.083	0.36	0.45	0.42	0.15	0.99	1.00	0.95
1	39	94	1	1	81mm Mortar	H	-88	O75	55	0.05	0.047	0.66	0.48	0.68	0.25	0.99	0.91	0.34
2	11	128	1	1	60mm Mortar	H	-60	O95	20	0.08	0.141	0.21	0.18	0.29	0.10	0.99	0.91	0.72
1	21	152	1	1	2.75" Rocket	H	-165	30	0	0.07	0.072	0.48	0.41	0.32	0.15	0.98	0.99	0.95
2	3	98	1	1	Fragment	H	-175	--	--	0.05	0.068	0.44	0.40	0.59	0.30	0.98	0.78	0.72
2	5	72	1	1	Fragment	H	144	--	--	0.07	0.082	0.36	0.27	0.58	0.50	0.98	0.97	0.56
1	5	147	1	1	57mm Projectile	H	49	0	0	0.09	0.127	0.27	0.12	0.14	0.25	0.98	0.92	0.68
1	49	90	1	1	4.2" Mortar	H	-67	270	0	0.05	0.070	0.46	0.52	0.59	0.35	0.98	0.96	0.89
1	50	100	1	1	60mm Mortar	H	3	195	30	0.19	0.084	0.38	0.18	0.52	0.20	0.98	0.91	0.61
1	30	96	1	1	81mm Mortar	H	179	330	35	0.08	0.075	0.37	0.27	0.49	0.15	0.96	0.92	0.46
2	7	166/76	1	1	2.75" Rocket	H	100	180	20	0.13	0.117	0.26	0.41	0.40	0.75	0.95	0.92	0.44
2	21	134	1	1	4.2" Mortar	H	-115	0	0	0.02	0.051	0.60	0.52	0.55	0.40	0.94	0.88	0.89
1	7	74	1	1	Fragment	H	-112	--	--	0.08	0.084	0.33	0.38	0.37	0.15	0.93	0.77	0.86
2	20	164	1	1	2.75" Rocket	H	-172	O90	10	0.06	0.086	0.34	0.41	0.79	0.60	0.93	0.78	0.57
3	1	62/80	1	1	81mm Mortar	H	-179	0	180	0.06	0.079	0.33	0.28	0.37	0.25	0.93	0.89	0.92
1	54	115	1	1	76mm Projectile	H	110	270	30	0.10	0.064	0.50	0.50	0.68	0.25	0.91	0.98	0.91
1	27	104	1	1	81mm Mortar	H	33	180	0	0.06	0.078	0.41	0.27	0.46	0.35	0.91	0.90	0.84
2	2	108	1	1	Fragment	H	155	--	--	0.08	0.058	0.52	0.35	0.59	0.40	0.90	0.95	0.91
3	5	50/76	1	1	81mm Mortar	H	-50	-90	--	0.06	0.064	0.40	0.28	0.39	0.20	0.90	0.88	0.93
3	8	68/6	1	1	60mm Mortar	H	17	--	--	0.08	0.058	0.46	0.18	0.26	0.10	0.88	0.86	0.82
2	16	116	1	1	81mm Mortar	H	-140	O45	0	0.06	0.088	0.35	0.28	0.37	0.30	0.87	0.77	0.51
1	4	198	1	1	Fragment	H	-40	--	--	0.06	0.069	0.41	0.40	0.46	0.30	0.86	0.92	0.76
1	53	88	1	1	60mm Mortar	H	172	0	0	0.17	0.115	0.26	0.18	0.42	0.35	0.84	0.86	0.58
1	55	117/18	1	1	152mm Projectile	H	101	--	--	0.11	0.114	0.28	0.48	0.40	0.25	0.83	0.75	0.37
1	35	170	1	1	Fragment	H	-127	--	--	0.03	0.048	0.71	0.43	0.24	0.15	0.82	0.93	0.71
2	12	120/88	1	1	60mm Mortar	H	157	270	0	0.14	0.126	0.24	0.18	0.36	0.30	0.80	0.91	1.00
2	23	131/16	1	1	81mm Mortar	H	-39	0	0	0.14	0.108	0.28	0.28	0.45	0.25	0.77	0.88	0.37
1	58	113/2	1	1	105mm Projectile	H	-62	120	30	0.11	0.045	0.72	0.37	0.67	0.50	0.76	0.83	0.38
1	24	102	1	1	81mm Mortar	H	41	210	45	0.08	0.084	0.37	0.28	0.39	0.25	0.75	0.72	0.53
2	18	42	1	1	Fragment	H	-147	--	--	0.05	0.064	0.47	0.33	0.89	0.75	0.72	0.76	0.83
1	46	40	1	1	Fragment	H	180	--	--	0.09	0.078	0.43	0.30	0.37	0.30	0.71	0.83	0.69
2	6	130	1	1	81mm Mortar	H	-74		0	0.06	0.074	0.40	0.28	0.40	0.70	0.70	0.86	0.97
1	19	64	1	1	Fragment	H	-148	--	--	0.04	0.094	0.36	0.35	0.16	0.20	0.46	0.70	0.45

AREA	TAR #	WES ID	GPR ID	True UXO	Type	Conf.	ETO (o)	T. Azi. (o)	T. Inc. (o)	CNR (NP/ns)	CNR (GHz)	ETL (m)	True L	DEP (m)	True Depth	Late-Time ELF(t)	Late-Time ELF(f)	Early-Time ELF
1	9	120	1	1	76mm Projectile	H	16	0	20	0.05	0.063	0.44	0.50	0.42	0.25	0.43	0.59	0.87
1	11	153	1	1	2.75" Rocket	M	-3	0	90	0.11	0.093	0.33	0.41	0.63	0.76	0.99	0.98	0.57
1	52	144	1	1	105mm Projectile	M	164	180	0	0.15	0.088	0.38	0.37	0.66	0.50	0.97	0.91	0.21
1	16	108	1	1	60mm Mortar	M	-58	100	45	0.17	0.118	0.27	0.18	0.26	0.20	0.96	0.85	0.69
1	33	36	1	1	Fragment	M	-166	--	--	0.18	0.177	0.13	0.20	0.13	0.15	0.94	0.93	0.56
1	37	92	1	1	81mm Mortar	M	-153	O30	20	0.05	0.070	0.44	0.41	0.39	0.20	0.91	0.96	0.57
1	40	168	1	1	Fragment	M	-95	--	--	0.21	0.143	0.19	0.20	0.37	0.25	0.89	0.94	0.75
1	31	118	1	1	5" Projectile	M	168	120	30	0.06	0.033	0.96	0.63	0.78	0.45	0.84	0.77	0.52
2	22	132	1	1	5" Projectile	M	-31	0	O90	0.04	0.035	0.93	0.63	1.00	0.91	0.82	0.75	0.93
3	3	78	1	1	60mm Mortar	M	-28	40	330	0.10	0.095	0.28	0.18	0.46	0.35	0.81	0.60	0.85
2	8	152	1	1	57mm Projectile	M	20	O90	0	0.14	0.123	0.24	0.12	0.14	0.25	0.79	0.88	0.79
1	8	121/184	1	1	155mm Projectile	M	-173	200	0	0.09	0.086	0.35	0.60	0.53	0.50	0.78	0.39	0.49
1	38	172	1	1	Fragment	M	-112	--	--	0.03	0.088	0.39	0.21	0.14	0.30	0.66	0.56	0.37
1	29	54	1	1	Fragment	L	-178	--	--	0.04	0.074	0.40	0.30	0.41	0.50	0.97	0.96	0.76
1	41	136	1	1	155mm Projectile	L	-8	O90	75	0.07	0.032	0.92	0.60	0.57	0.50	0.86	0.69	0.27
2	14	140	1	1	105mm Projectile	L	-61	330	10	0.06	0.017	1.73	0.37	0.75	0.70	0.85	0.95	0.86
1	28	138	1	1	57mm Projectile	L	-110	O95	45	0.05	0.088	0.37	0.12	0.27	0.15	0.82	0.58	0.30
1	15	62	1	1	Fragment	L	73	--	--	0.12	0.120	0.28	0.15	0.12	0.10	0.82	0.80	0.50
1	60	4	1	1	Fragment	L	-143	--	--	0.04	0.031	1.01	0.31	0.60	0.75	0.78	0.89	0.93
1	62	149	1	1	2.75" Rocket	L	-103	O30	55	0.04	0.058	0.52	0.41	0.94	0.50	0.77	0.83	0.68
2	9	124	1	1	60mm Mortar	L	32	330	10	0.27	0.172	0.18	0.18	0.14	0.20	0.71	0.62	0.47
1	1	196	1	1	Fragment	L	-4	0	--	0.03	0.051	0.58	0.30	1.06	1.20	0.41	0.55	0.71
2	4	94	1	0	Fragment	L	167	--	--	0.30	0.088	0.34	0.19	0.42	0.35	0.97	0.73	0.19
1	42	28	1	0	Fragment	L	153	--	--	0.31	0.111	0.30	0.12	0.35	0.15	0.82	0.93	0.38
2	25		1	-1		L	-63			0.03	0.098	0.31		0.75		0.75	0.82	0.91
1	13	186	1	0	Fragment	M	-60	--	--	0.19	0.148	0.23	0.10	0.27	0.10	0.91	0.97	0.71
1	17	66	1	0	Fragment	M	171	--	--	0.06	0.085	0.36	0.05	0.20	0.15	0.91	0.82	0.42
1	45	26	1	0	Fragment	M	-171	--	--	0.08	0.146	0.19	0.20	0.30	0.08	0.77	0.78	0.31
3	2	110	1	0	Magnetic Rock	M	123			0.07	0.091	0.29	0.21	0.19	0.20	0.70	0.73	0.37
2	15	46	1	0	Fragment	M	-47	--	--	0.10	0.112	0.27	0.24	0.37	0.20	0.67	0.75	0.36
2	26		1	-1		H	-177			0.03	0.078	0.36		0.73		1.00	0.90	0.71
1	61	158	1	0	Fragment	H	-120	--	--	0.07	0.087	0.36	0.05	0.15	0.05	0.94	0.95	0.74
1	3	78	1	0	Fragment	H	-65	--	--	0.15	0.092	0.35	0.10	0.12	0.10	0.85	0.78	0.67
1	36	42	1	0	Fragment	H	30	--	--	0.18	0.134	0.24	0.15	0.45	0.35	0.72	0.83	0.29
2	24		0	-1		L	-135			0.07	0.082	0.36		1.44		0.88	0.11	0.40
3	10		0	-1		L	-38			0.35	0.190	0.13		0.54		0.83	0.55	0.18
2	17		0	-1		L	109			0.16	0.073	0.41		0.78		0.40	0.50	0.34
3	7		0	-1		L	45			0.12	0.083	0.31		0.59		0.30	0.21	0.19
2	19	54	0	0	Fragment	L	-149	--	--	0.14	0.215	0.14	0.10	0.27	0.20	0.22	0.52	0.12
3	4		0	-1		L	90			0.07	0.071	0.35		0.82		0.12	0.26	0.50
3	6		0	-1		L	58			0.09	0.072	0.40		0.19		0.07	0.35	0.14

AREA	TAR #	WES ID	GPR ID	True UXO	Type	Conf.	ETO (o)	T. Azi. (o)	T. Inc. (o)	CNR (NP/ns)	CNR (GHz)	ETL (m)	True L	DEP (m)	True Depth	Late-Time ELF(t)	Late-Time ELF(f)	Early-Time ELF
1	43	154	0	0	Magnetic Rock	L	-179			0.10	0.100	0.28	0.21	0.08	0.20	0.03	0.17	0.13
2	13	36	0	0	Fragment	M	-167	--	--	0.13	0.122	0.26	0.11	0.11	0.25	0.25	0.39	0.33
1	59	10	0	0	Fragment	M	-30	--	--	0.27	0.058	0.57	0.08	0.13	0.10	0.13	0.24	0.38
1	10	180	0	0	Fragment	M	56	--	--	0.25	0.053	0.61	0.20	0.08	0.10	0.01	0.19	0.08
1	14	72	0	0	Fragment	H	90	--	--	0.13	0.101	0.27	0.05	0.17	0.10	0.35	0.30	0.25
1	63	16	0	0	Fragment	H	-10	--	--	0.10	0.090	0.35	0.11	0.07	0.05	0.30	0.39	0.22
1	6	82	0	0	Fragment	H	132	--	--	0.20	0.104	0.28	0.03	0.64	0.10	0.20	0.23	0.08
1	26	164	0	0	Fragment	H	171	--	--	0.04	0.070	0.46	0.13	0.49	0.10	0.17	0.15	0.51
1	57	6	0	0	Fragment	H	137	--	--	0.18	0.125	0.26	0.16	0.09	0.25	0.11	0.23	0.38
1	44	126	0	1	57mm Projectile	L	136	120	30	0.11	0.073	0.47	0.12	0.36	0.20	0.59	0.43	0.47
1	12	119	0	1	152mm Projectile	L	-97	270	30	0.10	0.041	0.72	0.48	0.71	0.40	0.41	0.18	0.18
1	56	8	0	1	Fragment	L	157	--	--	0.13	0.129	0.24	0.20	0.42	0.30	0.40	0.33	0.47
2	1	156	0	1	155mm Projectile	L	67	--	90	0.08	0.062	0.50	0.12	2.17	1.50	0.21	0.32	0.24
1	25	132	0	1	57mm Projectile	L	-125	180	0	0.32	0.138	0.21	0.12	0.09	0.25	0.17	0.09	0.15
1	20	106	0	1	60mm Mortar	M	136	O75	35	0.05	0.064	0.48	0.18	0.39	0.25	0.26	0.32	0.19
3	9	100	0	1	152mm Projectile	M	-133	35	90	0.07	0.035	0.72	0.48	0.85	0.91	0.22	0.23	0.39
1	22	176	0	1	Fragment	M	41	--	--	0.14	0.190	0.16	0.13	0.15	0.15	0.20	0.66	0.35
1	34	98	0	1	60mm Mortar	M	-108	275	20	0.07	0.096	0.31	0.18	0.08	0.10	0.19	0.20	0.03
1	23	142	0	1	57mm Projectile	M	15	265	45	0.24	0.188	0.18	0.12	0.10	0.15	0.08	0.22	0.64
1	48	150	0	1	2.75" Rocket	M	93	275	45	0.02	0.067	0.47	0.41	0.40	0.70	0.03	0.10	0.38
2	27	112	0	1	81mm Mortar	H	-62	--	90	0.09	0.100	0.30	0.28	0.09	0.10	0.23	0.40	0.09
2	10	144	0	1	152mm Projectile	H	150	O50	30	0.14	0.126	0.24	0.48	0.37	0.45	0.10	0.35	0.18
1	2	84	0	1	Fragment	H	63	--	--	0.15	0.117	0.26	0.09	0.10	0.10	0.04	0.08	0.07
1	18	122	0	1	5" Projectile	H	-177	270	55	0.14	0.054	0.53	0.63	0.57	0.91	0.03	0.11	0.15
1	32	30	0	1	Fragment	H	78	--	--	0.05	0.081	0.42	0.15	0.13	0.05	0.03	0.03	0.25

Table 31 Comparison of Ground Truth and GPR UXO Classification (ROUND 3, LD3 Criteria).

AREA	GPR #	WES #	GPR ID	True UXO	Type	Conf.	ETO (o)	T. Azi. (o)	T. Inc. (o)	CNR (NP/ns)	CNR (GHz)	ETL (m)	True L	DEP (m)	True Depth (m)	Late-Time ELF(t)	Late-Time ELF(f)	Early-Time ELF
1	47	38	1	1	Fragment	H	66	--	--	0.04	0.083	0.36	0.45	0.42	0.15	0.99	1.00	0.95
1	39	94	1	1	81mm Mortar	H	-88	O75	55	0.05	0.047	0.66	0.48	0.68	0.25	0.99	0.91	0.34
2	11	128	1	1	60mm Mortar	H	-60	O95	20	0.08	0.141	0.21	0.18	0.29	0.10	0.99	0.91	0.72
1	21	152	1	1	2.75" Rocket	H	-165	30	0	0.07	0.072	0.48	0.41	0.32	0.15	0.98	0.99	0.95
2	3	98	1	1	Fragment	H	-175	--	--	0.05	0.068	0.44	0.40	0.59	0.30	0.98	0.78	0.72
1	49	90	1	1	4.2" Mortar	H	-67	270	0	0.05	0.070	0.46	0.52	0.59	0.35	0.98	0.96	0.89
1	50	100	1	1	60mm Mortar	H	3	195	30	0.19	0.084	0.38	0.18	0.52	0.20	0.98	0.91	0.61
1	30	96	1	1	81mm Mortar	H	179	330	35	0.08	0.075	0.37	0.27	0.49	0.15	0.96	0.92	0.46
2	7	166/76	1	1	2.75" Rocket	H	100	180	20	0.13	0.117	0.26	0.41	0.40	0.75	0.95	0.92	0.44
2	21	134	1	1	4.2" Mortar	H	-115	0	0	0.02	0.051	0.60	0.52	0.55	0.40	0.94	0.88	0.89
1	7	74	1	1	Fragment	H	-112	--	--	0.08	0.084	0.33	0.38	0.37	0.15	0.93	0.77	0.86
2	20	164	1	1	2.75" Rocket	H	-172	O90	10	0.06	0.086	0.34	0.41	0.79	0.60	0.93	0.78	0.57
3	1	62/80	1	1	81mm Mortar	H	-179	0	180	0.06	0.079	0.33	0.28	0.37	0.25	0.93	0.89	0.92
1	54	115	1	1	76mm Projectile	H	110	270	30	0.10	0.064	0.50	0.50	0.68	0.25	0.91	0.98	0.91
1	27	104	1	1	81mm Mortar	H	33	180	0	0.06	0.078	0.41	0.27	0.46	0.35	0.91	0.90	0.84
2	2	108	1	1	Fragment	H	155	--	--	0.08	0.058	0.52	0.35	0.59	0.40	0.90	0.95	0.91
3	5	50/76	1	1	81mm Mortar	H	-50	-90	--	0.06	0.064	0.40	0.28	0.39	0.20	0.90	0.88	0.93
3	8	68/6	1	1	60mm Mortar	H	17	--	--	0.08	0.058	0.46	0.18	0.26	0.10	0.88	0.86	0.82
2	16	116	1	1	81mm Mortar	H	-140	O45	0	0.06	0.088	0.35	0.28	0.37	0.30	0.87	0.77	0.51
1	4	198	1	1	Fragment	H	-40	--	--	0.06	0.069	0.41	0.40	0.46	0.30	0.86	0.92	0.76
1	53	88	1	1	60mm Mortar	H	172	0	0	0.17	0.115	0.26	0.18	0.42	0.35	0.84	0.86	0.58
1	55	117/18	1	1	152mm Projectile	H	101	--	--	0.11	0.114	0.28	0.48	0.40	0.25	0.83	0.75	0.37
1	35	170	1	1	Fragment	H	-127	--	--	0.03	0.048	0.71	0.43	0.24	0.15	0.82	0.93	0.71
2	12	120/88	1	1	60mm Mortar	H	157	270	0	0.14	0.126	0.24	0.18	0.36	0.30	0.80	0.91	1.00
2	23	131/16	1	1	81mm Mortar	H	-39	0	0	0.14	0.108	0.28	0.28	0.45	0.25	0.77	0.88	0.37
1	58	113/2	1	1	105mm Projectile	H	-62	120	30	0.11	0.045	0.72	0.37	0.67	0.50	0.76	0.83	0.38
1	24	102	1	1	81mm Mortar	H	41	210	45	0.08	0.084	0.37	0.28	0.39	0.25	0.75	0.72	0.53
2	18	42	1	1	Fragment	H	-147	--	--	0.05	0.064	0.47	0.33	0.89	0.75	0.72	0.76	0.83
1	46	40	1	1	Fragment	H	180	--	--	0.09	0.078	0.43	0.30	0.37	0.30	0.71	0.83	0.69
2	6	130	1	1	81mm Mortar	H	-74		0	0.06	0.074	0.40	0.28	0.40	0.70	0.70	0.86	0.97
1	19	64	1	1	Fragment	H	-148	--	--	0.04	0.094	0.36	0.35	0.16	0.20	0.46	0.70	0.45
1	9	120	1	1	76mm Projectile	H	16	0	20	0.05	0.063	0.44	0.50	0.42	0.25	0.43	0.59	0.87
1	11	153	1	1	2.75" Rocket	M	-3	0	90	0.11	0.093	0.33	0.41	0.63	0.76	0.99	0.98	0.57

AREA	GPR #	WES #	GPR ID	True UXO	Type	Conf.	ETO (o)	T. Azi. (o)	T. Inc. (o)	CNR (NP/ns)	CNR (GHz)	ETL (m)	True L	DEP (m)	True Depth (m)	Late-Time ELF(t)	Late-Time ELF(f)	Early-Time ELF
1	52	144	1	1	105mm Projectile	M	164	180	0	0.15	0.088	0.38	0.37	0.66	0.50	0.97	0.91	0.21
1	16	108	1	1	60mm Mortar	M	-58	100	45	0.17	0.118	0.27	0.18	0.26	0.20	0.96	0.85	0.69
1	33	36	1	1	Fragment	M	-166	--	--	0.18	0.177	0.13	0.20	0.13	0.15	0.94	0.93	0.56
1	37	92	1	1	81mm Mortar	M	-153	O30	20	0.05	0.070	0.44	0.41	0.39	0.20	0.91	0.96	0.57
1	40	168	1	1	Fragment	M	-95	--	--	0.21	0.143	0.19	0.20	0.37	0.25	0.89	0.94	0.75
1	31	118	1	1	5" Projectile	M	168	120	30	0.06	0.033	0.96	0.63	0.78	0.45	0.84	0.77	0.52
2	22	132	1	1	5" Projectile	M	-31	0	O90	0.04	0.035	0.93	0.63	1.00	0.91	0.82	0.75	0.93
3	3	78	1	1	60mm Mortar	M	-28	40	330	0.10	0.095	0.28	0.18	0.46	0.35	0.81	0.60	0.85
1	8	121/184	1	1	155mm Projectile	M	-173	200	0	0.09	0.086	0.35	0.60	0.53	0.50	0.78	0.39	0.49
1	41	136	1	1	155mm Projectile	L	-8	O90	75	0.07	0.032	0.92	0.60	0.57	0.50	0.86	0.69	0.27
2	14	140	1	1	105mm Projectile	L	-61	330	10	0.06	0.017	1.73	0.37	0.75	0.70	0.85	0.95	0.86
1	15	62	1	1	Fragment	L	73	--	--	0.12	0.120	0.28	0.15	0.12	0.10	0.82	0.80	0.50
1	62	149	1	1	2.75" Rocket	L	-103	O30	55	0.04	0.058	0.52	0.41	0.94	0.50	0.77	0.83	0.68
2	9	124	1	1	60mm Mortar	L	32	330	10	0.27	0.172	0.18	0.18	0.14	0.20	0.71	0.62	0.47
1	1	196	1	1	Fragment	L	-4	0	--	0.03	0.051	0.58	0.30	1.06	1.20	0.41	0.55	0.71
2	26		1	-1		H	-177			0.03	0.078	0.36		0.73	0.35	1.00	0.90	0.71
1	51	162	1	0	Fragment	H	-26	--	--	0.04	0.076	0.40	0.33	0.45	0.25	0.99	0.92	0.78
2	5	72	1	0	Fragment	H	144	--	--	0.07	0.082	0.36	0.27	0.58	0.50	0.98	0.97	0.56
1	5	147	1	0	57mm Projectile	H	49	0	0	0.09	0.127	0.27	0.12	0.14	0.25	0.98	0.92	0.68
1	61	158	1	0	Fragment	H	-120	--	--	0.07	0.087	0.36	0.05	0.15	0.05	0.94	0.95	0.74
1	3	78	1	0	Fragment	H	-65	--	--	0.15	0.092	0.35	0.10	0.12	0.10	0.85	0.78	0.67
1	36	42	1	0	Fragment	H	30	--	--	0.18	0.134	0.24	0.15	0.45	0.35	0.72	0.83	0.29
1	13	186	1	0	Fragment	M	-60	--	--	0.19	0.148	0.23	0.10	0.27	0.10	0.91	0.97	0.71
1	17	66	1	0	Fragment	M	171	--	--	0.06	0.085	0.36	0.05	0.20	0.15	0.91	0.82	0.42
2	8	152	1	0	57mm Projectile	M	20	O90	0	0.14	0.123	0.24	0.12	0.14	0.25	0.79	0.88	0.79
1	45	26	1	0	Fragment	M	-171	--	--	0.08	0.146	0.19	0.20	0.30	0.08	0.77	0.78	0.31
3	2	110	1	0	Magnetic Rock	M	123			0.07	0.091	0.29	0.21	0.19	0.20	0.70	0.73	0.37
2	15	46	1	0	Fragment	M	-47	--	--	0.10	0.112	0.27	0.24	0.37	0.20	0.67	0.75	0.36
1	38	172	1	0	Fragment	M	-112	--	--	0.03	0.088	0.39	0.21	0.14	0.30	0.66	0.56	0.37
1	29	54	1	0	Fragment	L	-178	--	--	0.04	0.074	0.40	0.30	0.41	0.50	0.97	0.96	0.76
2	4	94	1	0	Fragment	L	167	--	--	0.30	0.088	0.34	0.19	0.42	0.35	0.97	0.73	0.19
1	42	28	1	0	Fragment	L	153	--	--	0.31	0.111	0.30	0.12	0.35	0.15	0.82	0.93	0.38
1	28	138	1	0	57mm Projectile	L	-110	O95	45	0.05	0.088	0.37	0.12	0.27	0.15	0.82	0.58	0.30
1	60	4	1	0	Fragment	L	-143	--	--	0.04	0.031	1.01	0.31	0.60	0.75	0.78	0.89	0.93
2	25		1	-1		L	-63			0.03	0.098	0.31		0.75	0.55	0.75	0.82	0.91
2	24		0	-1		L	-135			0.07	0.082	0.36		1.44	1.50	0.88	0.11	0.40
3	10		0	-1		L	-38			0.35	0.190	0.13		0.54	0.25	0.83	0.55	0.18
1	44	126	0	0	57mm Projectile	L	136	120	30	0.11	0.073	0.47	0.12	0.36	0.20	0.59	0.43	0.47
2	17		0	-1		L	109			0.16	0.073	0.41		0.78	0.50	0.40	0.50	0.34
3	7		0	-1		L	45			0.12	0.083	0.31		0.59	0.55	0.30	0.21	0.19
2	19	54	0	0	Fragment	L	-149	--	--	0.14	0.215	0.14	0.10	0.27	0.20	0.22	0.52	0.12

AREA	GPR #	WES #	GPR ID	True UXO	Type	Conf.	ETO (o)	T. Azi. (o)	T. Inc. (o)	CNR (NP/ns)	CNR (GHz)	ETL (m)	True L	DEP (m)	True Depth (m)	Late-Time ELF(t)	Late-Time ELF(f)	Early-Time ELF
1	25	132	0	0	57mm Projectile	L	-125	180	0	0.32	0.138	0.21	0.12	0.09	0.25	0.17	0.09	0.15
3	4		0	-1		L	90			0.07	0.071	0.35		0.82	1.15	0.12	0.26	0.50
3	6		0	-1		L	58			0.09	0.072	0.40		0.19	0.25	0.07	0.35	0.14
1	43	154	0	0	Magnetic Rock	L	-179			0.10	0.100	0.28	0.21	0.08	0.20	0.03	0.17	0.13
2	13	36	0	0	Fragment	M	-167	--	--	0.13	0.122	0.26	0.11	0.11	0.25	0.25	0.39	0.33
1	22	176	0	0	Fragment	M	41	--	--	0.14	0.190	0.16	0.13	0.15	0.15	0.20	0.66	0.35
1	59	10	0	0	Fragment	M	-30	--	--	0.27	0.058	0.57	0.08	0.13	0.10	0.13	0.24	0.38
1	23	142	0	0	57mm Projectile	M	15	265	45	0.24	0.188	0.18	0.12	0.10	0.15	0.08	0.22	0.64
1	10	180	0	0	Fragment	M	56	--	--	0.25	0.053	0.61	0.20	0.08	0.10	0.01	0.19	0.08
1	14	72	0	0	Fragment	H	90	--	--	0.13	0.101	0.27	0.05	0.17	0.10	0.35	0.30	0.25
1	63	16	0	0	Fragment	H	-10	--	--	0.10	0.090	0.35	0.11	0.07	0.05	0.30	0.39	0.22
1	6	82	0	0	Fragment	H	132	--	--	0.20	0.104	0.28	0.03	0.64	0.10	0.20	0.23	0.08
1	26	164	0	0	Fragment	H	171	--	--	0.04	0.070	0.46	0.13	0.49	0.10	0.17	0.15	0.51
1	57	6	0	0	Fragment	H	137	--	--	0.18	0.125	0.26	0.16	0.09	0.25	0.11	0.23	0.38
1	2	84	0	0	Fragment	H	63	--	--	0.15	0.117	0.26	0.09	0.10	0.10	0.04	0.08	0.07
1	12	119	0	1	152mm Projectile	L	-97	270	30	0.10	0.041	0.72	0.48	0.71	0.40	0.41	0.18	0.18
1	56	8	0	1	Fragment	L	157	--	--	0.13	0.129	0.24	0.20	0.42	0.30	0.40	0.33	0.47
2	1	156	0	1	155mm Projectile	L	67	--	90	0.08	0.062	0.50	0.12	2.17	1.50	0.21	0.32	0.24
1	20	106	0	1	60mm Mortar	M	136	O75	35	0.05	0.064	0.48	0.18	0.39	0.25	0.26	0.32	0.19
3	9	100	0	1	152mm Projectile	M	-133	35	90	0.07	0.035	0.72	0.48	0.85	0.91	0.22	0.23	0.39
1	34	98	0	1	60mm Mortar	M	-108	275	20	0.07	0.096	0.31	0.18	0.08	0.10	0.19	0.20	0.03
1	48	150	0	1	2.75" Rocket	M	93	275	45	0.02	0.067	0.47	0.41	0.40	0.70	0.03	0.10	0.38
2	27	112	0	1	81mm Mortar	H	-62	--	90	0.09	0.100	0.30	0.28	0.09	0.10	0.23	0.40	0.09
2	10	144	0	1	152mm Projectile	H	150	O50	30	0.14	0.126	0.24	0.48	0.37	0.45	0.10	0.35	0.18
1	18	122	0	1	5" Projectile	H	-177	270	55	0.14	0.054	0.53	0.63	0.57	0.91	0.03	0.11	0.15
1	32	30	0	1	Fragment	H	78	--	--	0.05	0.081	0.42	0.15	0.13	0.05	0.03	0.03	0.25

Appendix B Archiving

GPR Data Files – *.cdt

The data for system-calibrated frequency-domain radar data was stored in ASCII-format files called "**aydddaa.cdt**", where "a" is from A to Z for file ordering. The letter "y" indicates the last digit of the year. For example, "0" means the year of 2000. The three-digit number, "ddd" , indicates the Julian date when the data was stored. Each file contains data taken at a single target location. The first frequency (10 MHz) data was stored in the first row, the second frequency (12 MHz) data was stored in the second row, etc. The columns contain the frequency, co-polarization and cross-polarization data in a format shown below. For each radar file, '*.cdt", there is an associated comment file called "*.txt" to store the system information, comments and processed results. All of these files will be available in a CD-ROM after this submission of this report.

Frequency (MHz)	Re(S_{11})	Im(S_{11})	Re(S_{21})	Im(S_{21})	Re(S_{22})	Im(S_{22})

"Re()" and "Im()" indicate the real and imaginary parts, respectively (combined, these provide the amplitude and phase).

Comment Text Files - *.txt

The comment text files contain information about measurement conditions (i.e. position, direction, etc.) and any comments the user entered during the measurements. Comment files with an extra letter on the end of the names are the processed comment files. These files contain all the information about measurement, as before, but also contain information about the processing of the file. For example, the comment file a0014gbu.txt is printed below:

14-Jan-2000/Target #: 101/No Target File: a0014fz.cdt/Antenna Orientation: 194/Antenna Position: xoffset: 0.0000/yoffset: 10.0000/Relative Permittivity: 4/User Comments: UE3@@@********/$ETO/3/ -1.0000/ 179.0000/ 0.7471/ELF/2/ 0.7726/ 0.0213/CNR/2/ 0.0913/ 0.2046/ETL/1/ 0.3666/SNR/1/ 49.7574/TCP/2/ 12.3932/ 0.5861/timerange1/ 17.3146/timerange2/ 24.4088/timepeakmax/ 12.3932/waveformselection/ 3.0000/FELF/ 0.8443/$$**

This is a typical comment file after processing. The letter 'u' on the end of the file name denotes that a user specified center frequency band-pass filter was used before the processing of the file. A letter 'f' on the end would denote that the full 800 MHz bandwidth was used in processing that file, while a letter 'l' and 'h' denotes that a low-pass and a high-pass filter was used, respectively.

One can see that all of the processed parameters (i.e. ETO, ETL, ELF, etc.) for this target are stored in the file. There are also four other parameters (timerange1, timerange2, timepeakmax, and waveformselection) stored in the file which provide information about the late-time region selected for processing. These parameters allow for the automatic re-processing of the data, if necessary.

Processed Files -*.mat Files

The processed data is saved in *.mat format (a Matlab file fomat), in which the following variables are saved.

Variables for Processed Data Results

ELF – Estimated Linear Factor vs. position
fELF – Frequency Estimated Linear Factor vs. position
melf – Mean of ELF and fELF
ETO – Estimated Target Orientation vs. position
CNR – Complex Natural Resonance and Damping vs. position
ETL – Estimated Target Length vs. position
Y1a – Position vector
SNR – Estimated Signal to Noise Ratio vs. position
SCR – Estimated Signal to Clutter Ratio vs. position
ATV – Antenna Orientation

Variables for How Data was Processed

SELECTION –Data Channel used for CNR extraction
ftype – Type of frequency domain filter
ucfreq2 – User Centered frequency for the adaptive bandpass filter
npoint – Number of points in the adaptive bandpass filter
nx – Position vector for late-time region selection
ntmax – First Time position for late-time region vs. x-position
numTdiff – Number of points in late-time region vs. x-postion
T0 – Variable for slope gain
TM – Variable for slope gain
gainfac – Variable for slope gain
imgT – Variable for adaptive smoothing
imgindT - Variable for adaptive smoothing
imgindx - Variable for adaptive smoothing
imgN - Variable for adaptive smoothing
SIDE - Variable for adaptive smoothing

Appendix C Electrical Properties of the JPG V Soil

The soil electrical properties – permittivity and conductivity at 40 MHz and 60 MHz - were measured at different depths using the OSU/ESL soil probe as shown in Figure 55. Subsequent figures show the values obtained for the properties in the course of the demo.

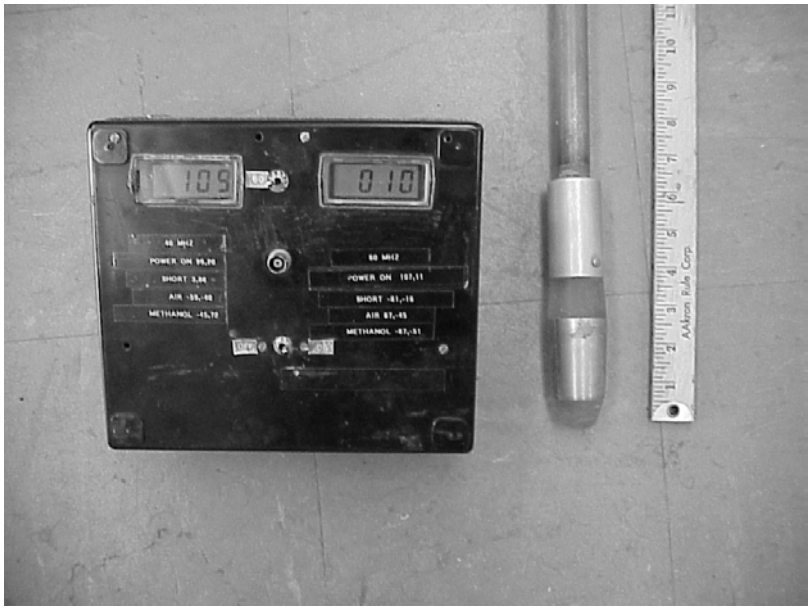

Figure 55 OSU/ESL soil probe for permittivity and conductivity measurement at 40 MHz and 60 MHz.

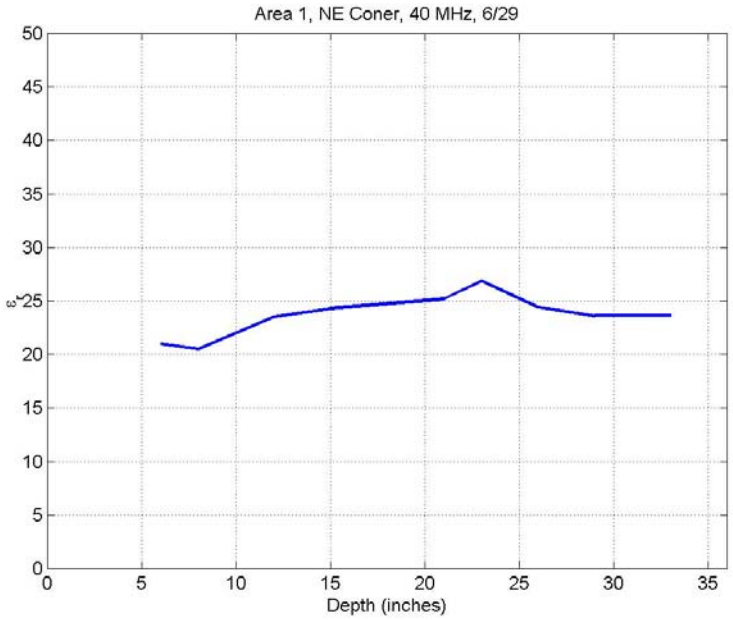

Figure 56 Soil dielectric constant of Area 1 measured on 6/29/2001 at 40 MHz.

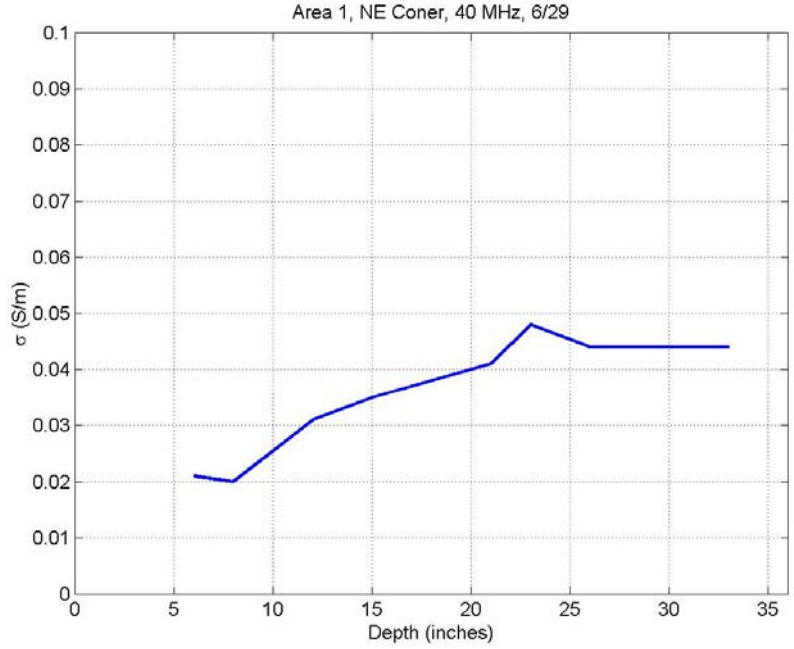

Figure 57 Soil conductivity of Area 1 measured on 6/29/2001 at 40 MHz.

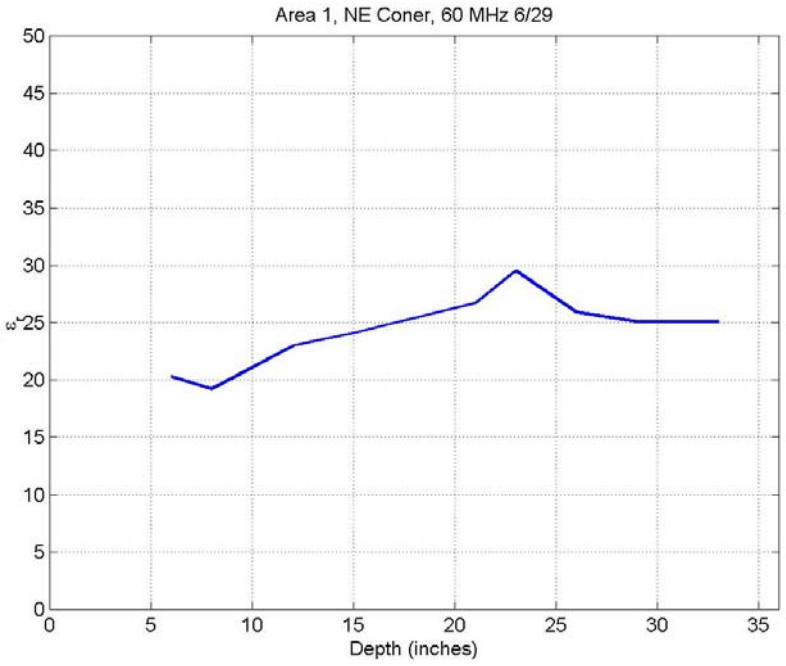

Figure 58 Soil dielectric constant of Area 1 measured on 6/29/2001 at 60 MHz.

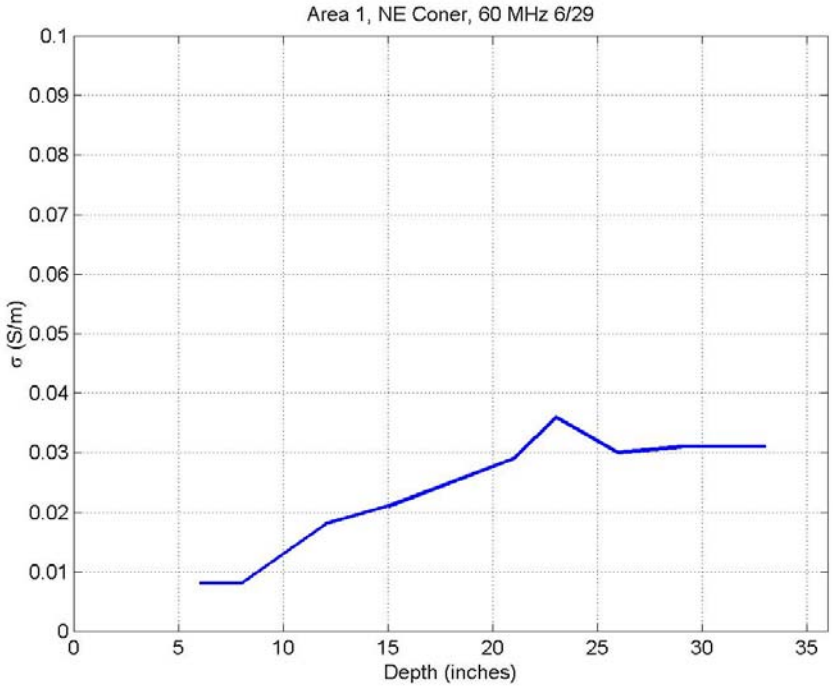

Figure 59 Soil conductivity of Area 1 measured on 6/29/2001 at 60 MHz.

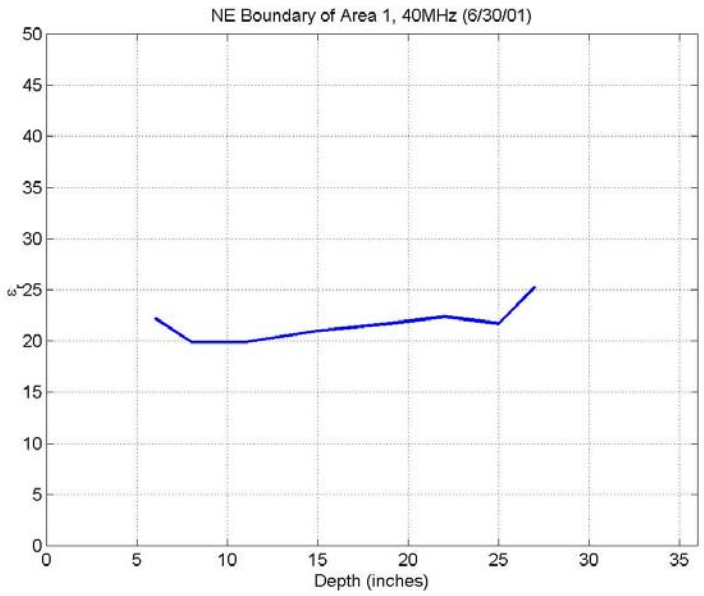

Figure 60 Soil dielectric constant of Area 1 measured on 6/30/2001 at 40 MHz.

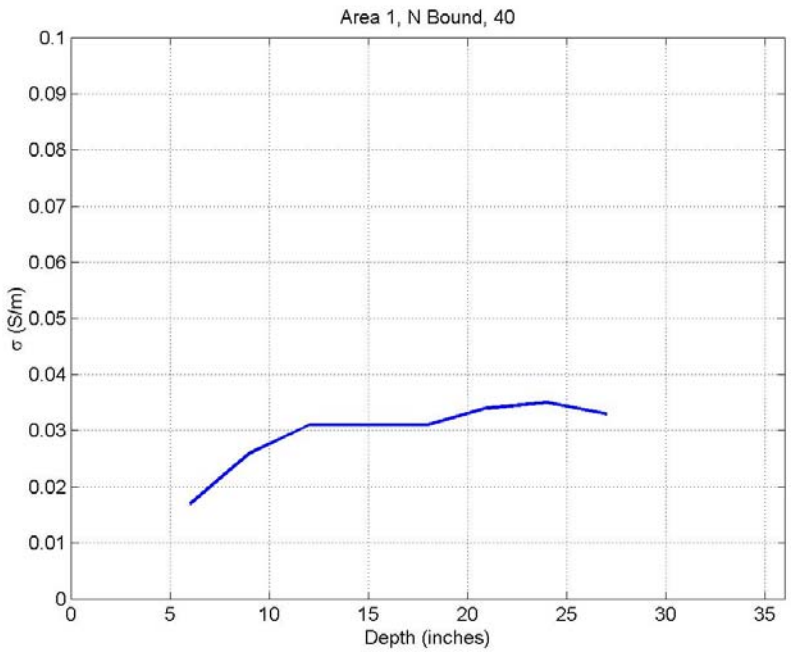

Figure 61 Soil conductivity of Area 1 measured on 6/30/2001 at 40 MHz.

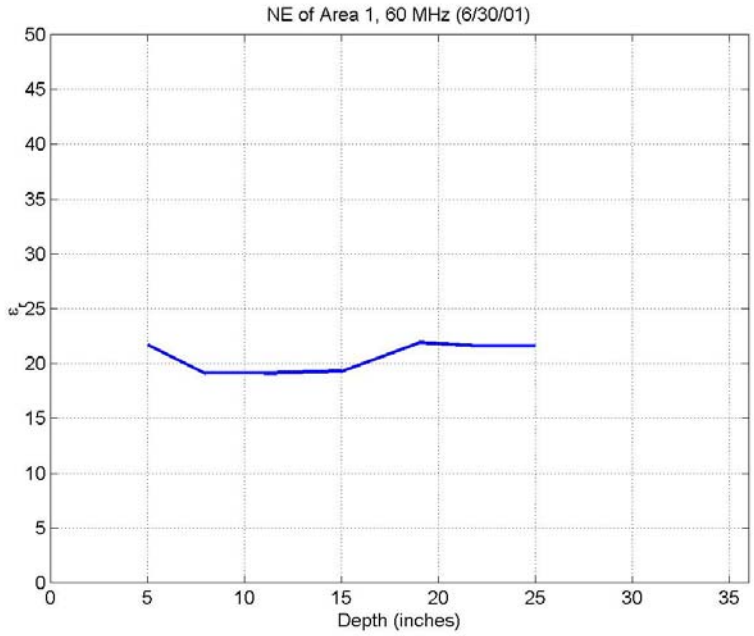

Figure 62 Soil dielectric constant of Area 1 measured on 6/30/2001 at 60 MHz.

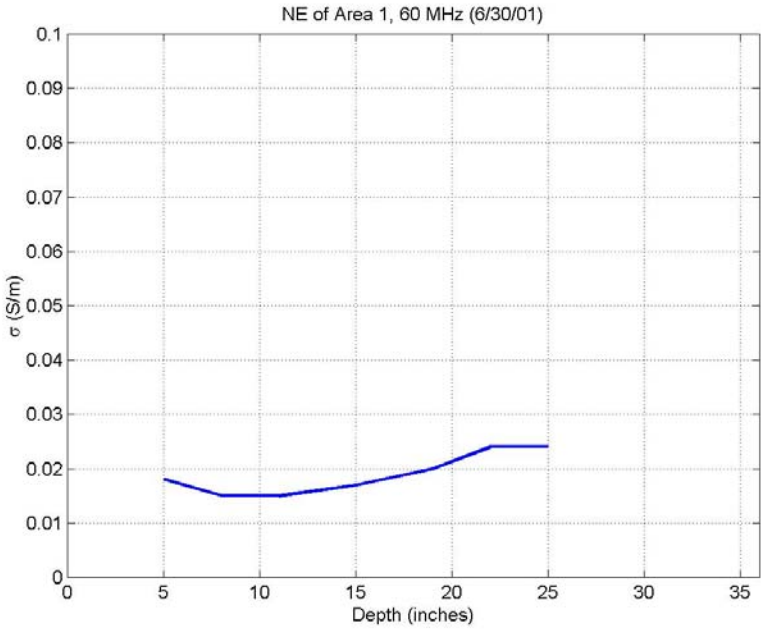

Figure 63 Soil conductivity of Area 1 measured on 6/30/2001 at 60 MHz.

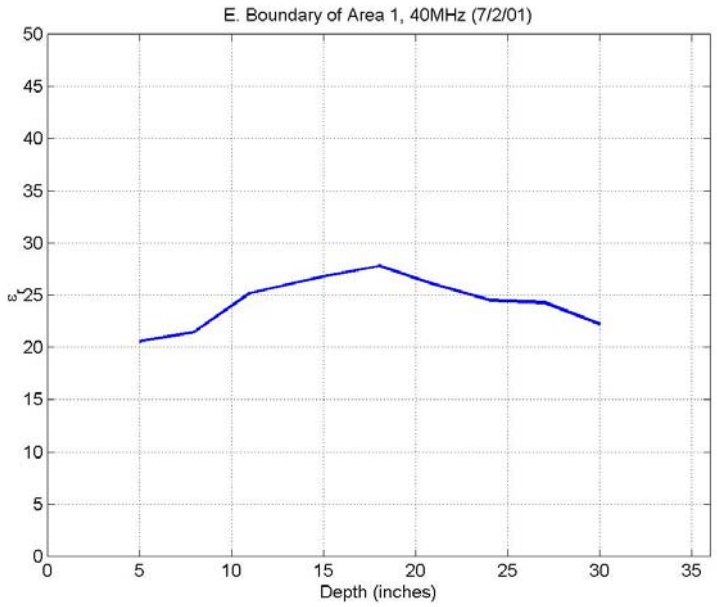

Figure 64 Soil dielectric constant of Area 1 measured on 7/1/2001 at 40 MHz.

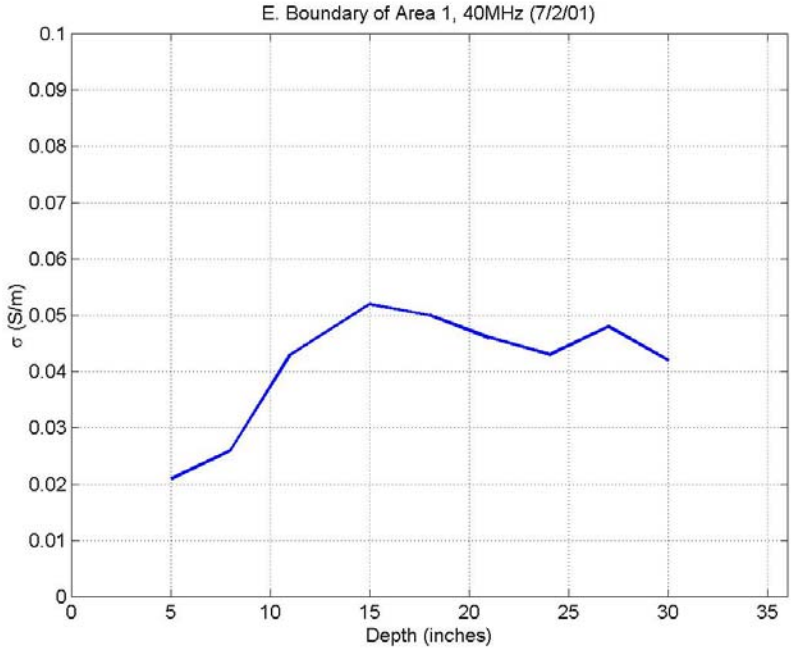

Figure 65 Soil conductivity of Area 1 measured on 7/1/2001 at 40 MHz.

Appendix D Field Log

Table 32 The offset and orientation of each pass for each target.

Area 1							
Item No.	Pass 1Orient	Pass 2 Offset	Pass 2 Orient	Pass 3 Offset	Pass 3 Orient	Pass 4 Orient	Comment
1-1	0	0	105		X	45	empty
1-2	68	10	120		300 (repeat)	35 & 80	Non-UXO
1-3	205	0	130		85	x	empty
1-4	20	-30	114	-10 from Pass 1	120	50 (0 offset from Pass 3 Center)	UXO-like
1-5	317	10	65		332	110 (offset 10 from Pass 1 center)	
1-6	133	-10	38	Centered at flag	40	88 (center at flag)	
1-7	40	0	330	0	260	x	
1-8	225	10	200	0	0	90 (centered at flag)	
1-9	16	10	310	15 from Pass1	285	60 (centered at pass 3)	
1-10	56	0	150		x	105	
1-11	0	0	108		x	225	
1-12	170	10	259		x	125	
1-13	20	0	270		x	45	
1-14	40	-10	324		x	0	
1-15	90	0	213		x	78	
1-16	302	0	278		x	55	
1-17	172	-10	318		48	93	
1-18	270	-15	186		x	141	Hole 6’ S. of Target
1-19	134	10	120		50	95	
1-20	138	0	246	15 from Pass 2 center	x	273	
1-21	203	5	111		x	246	
1-22	310	-10	30		x	255	
1-23	277	15	320	30 from Pass 2	275	52 (centered at Flag)	
1-24	309	0	40		x	x	
1-25	288	-5	27		x	252	empty
1-26	0	0	70	-10 from Pass 2 Center	110	30 (centered at Pass 3 center)	
1-27	16	-5	302	10 from Pass 2 Center	218	100 (centered at Flag)	
1-28	333	0	265		x	0	
1-29	90	0	160		x	25	

Area 1 Item No.	Pass 1Orient	Pass 2 Offset	Pass 2 Orient	Pass 3 Offset	Pass 3 Orient	Pass 4 Orient	Comment
1-30	180	0	250	15 from pass2 center	150	45 (Centered at Pass 3)	
1-31	123	0	280	20 from pass 2 center	10	50 (offset 15 from Pass 3 center)	
1-32	351	10	80		X	45	
1-33	104	10	0		X	45	empty
1-34	162	5	70		X	25	
1-35	233	10	143	Center at Pass 1	X	185	
1-36	30	20	300		X	75	
1-37	207	-10	120	Center at Pass 1	X	75	
1-38	247	10	157	-10 Pass 1 center	X	112	
1-39	153	0	63	-10 Pass2 Center	X	288	
1-40	95	0	0	30 from Pass 2 center	270	45 (Pass 3 center)	Additional Pass at Offset
1-41	235	30	325		235	110 (15 offset in Pass 1)	
1-42	154	20	60	Pass 1 Center	x	110	
1-43	90	0	0		x	225	
1-44	100	0	x		x	45	Near Tree
1-45	68	0	0	10 from Pass 2	90	45 (centered at flag)	
1-46	36	10	180		90	X	
1-47	335	-10	65	-30 form Pass 1 Center	65	155 & 110(-30 offset in Pass 1)	Offset Confirmed By Mag.
1-48	94	0	0				Near Ditch
1-49	112	-10	200		x	155	
1-50	4	-10	30	20 from Pass 2 Center	120	75 Pass 3 Center	Mag. At 10” form Pass 2
1-51	235	20	180		x	X	
1-52	174	15	70	Pass 1 Center	x	130	
1-53	173	10	90		315	X	
1-54	27	20	110		x	255	
1-55	3	0	90	10 from Pass 2 center	x	45	
1-56	63	0	330	Pass 1 center	x	288	
1-57	138	0	230		x	93	
1-58	207	10	120		x	75	
1-59	330	0	60		x	105	
1-60	170	0	260		x	125	
1-61	150	10	60		x	105	
1-62	264	20	330	Pass1 Center	X	39	
1-63	335	20	80	Pass1 Center	x	110	

Area 2							
Item No.	Pass 1 Orient	Pass 2 Offset	Pass 2 Orient	Pass 3 Offset	Pass 3 Orient	Pass 4 Orient	Comment
2-1	113	0	203	0	x	68	empty
2-2	62	-10	160	Pass1 Center	x	107	
2-3	68	0	40		68 (repeat)	23	
2-4	76	-10	165	10 from Pass 2 center	x	210	
2-5	194	0	150		230	x	UXO
2-6	295	10	15		30	x	UXO
2-7	60	-10	10	-40 Pass 2 Center	100	x	Offset Confirmed By Mag.
2-8	290	0	20		x	65	
2-9	206	-5	300	-5 from Pass 2 Center	30	75	
2-10	240	15	150		60	15	
2-11	39	15	130		X	X	
2-12	218	-5	140	Pass 2 center	50	X	
2-13	103	-10	13	Flag center	13 (Repeat)	58 (Flag center)	
2-14	300	0	30		x	75	
2-15	316	-10	260		Repeat Pass 2	0 (centered at pass 2)	
2-16	14	-15	120		40	x	
2-17	22	0	112		x	67	
2-18	347	10	100	20 from Pass 2 Center	10	55	
2-19	165	0	75		x	120	
2-20	213	-30	120	Pass2 center	60	x	
2-21	245	0	120		x	X	
2-22	297	-20	10	-20 from Pass 2	x	55	
2-23	335	-10	250		x	x	
2-24	40	0	130		x	85	empty
2-25	256	0	166	20 from pass1	121	x	metal
2-26	190	0	90		45	x	Deep or empty
2-27	117	0	27		72	x	empty

Area 3					
Item No.	Pass 1 Orient	Pass 2 Offset	Pass 2 Orient	Pass 3 Orient	Pass 4 Orient
3-1	182	0	90	x	X
3-2	123	10	33	x	X
3-3	276	0	0	160	70
3-4	0	0	90	x	45
3-5	215	0	305	100 (offset –15 from Pass 2 center)	10
3-6	148	0	58	x	X
3-7	313	0	223	x	X
3-8	30	0	110	x	X
3-9	45	0	135	x	X
3-10	232	10	142	x	X

Table 33 Manual Magnetometer Survey Note

Item ID	Height	Flag Loc.	Rader Loc.	Strongest Loc.	Comments
1-1	9	Y	Y	F	
1-2	8	W	W	R	strongest:P1 center
1-3	7	W	Y	R	
1-4	2	Y	Y	F	No response at P2 center
1-5	N.A.	N	Y	N.A.	
1-6	3	Y	Y	F	
1-7	N.A.	W	W	N.A.	
1-8	14	Y	Y	E	strongest: 20" offset to SW from flag through Pass 4 line
1-9	5	N	Y	R	strongest: P2 center
1-10	5	W	Y	R	
1-11	8	Y	Y	R	
1-12	9	Y	W	W	
1-13	4	Y	Y	R	
1-14	4	Y	W	F	
1-15	7	W	W	E	strongest: 7" offset to S from P3 center through Pass 3 line
1-16	7	Y	Y	F	
1-17	4	Y	Y	R	
1-18	7	Y	N	F	
1-19	4	Y	Y	R	
1-20	10	Y	N	F	
1-21	5	Y	Y	F	
1-22	4	N	Y	R	
1-23	6	Y	N	F	

Item ID	Height	Flag Loc.	Rader Loc.	Strongest Loc.	Comments
1-24	7	Y	Y	F	
1-25	6	Y	Y	R	
1-26	4	Y	W	F	No response at P4 center
1-27	1	Y	Y	F	
1-28	6	Y	W	F	
1-29	9	Y	Y	E	strongest: 15" offset to East from flag through Pass 1 line
1-30	7	N	Y	R	
1-31	7	Y	N	F	
1-32	13	N	N	R	
1-33	10	N	W	E	strongest: 15" offset to SW from P3 center through Pass 3 line
1-34	3	N	W	E	strongest: 10" offset to E from P3 center through Pass 3 line
1-35	7	W	Y	R	
1-36	12	Y	W	F	
1-37	9	W	W	R	strongest: P3 center
1-38	6	W	N	R	
1-39	5	Y	Y	R	weaker response at P3 Center than at flag
1-40	N.A.	N	N	E	strongest: 40" offset to N from flag
1-41	10	Y	N	F	
1-42	5	N	Y	R	
1-43	4	Y	Y	F	
1-44	14	W	W	F	
1-45	5	W	Y	R	strongest: P3 center
1-46	6	W	Y	R	
1-47	6	N	Y	R	strongest: P3 center
1-48	14	W	W	F	
1-49	7	Y	Y	F	
1-50	10	W	W	E	strongest: 10" offset From P2 center through Pass 2 line
1-51	5	Y	W	F	
1-52	7	N	Y	R	
1-53	11	Y	Y	R	
1-54	13	W	W	R	
1-55	3	W	Y	R	
1-56	N.A.	N	N	N.A.	
1-57	5	Y	Y	F	
1-58	6	Y	Y	F	
1-59	10	W	W	E	strongest: 10" offset to NW from P1 center through Pass 1 line
1-60	9	Y	Y	R	
1-61	7	Y	Y	R	
1-62	5	Y	Y	F	
1-63	12	W	W	F	
2-1	10	Y	Y	F	
2-2	10	Y	Y	F	

Item ID	Height	Flag Loc.	Rader Loc.	Strongest Loc.	Comments
2-3	12	Y	Y	F	
2-4	5	Y	Y	R	
2-5	10	Y	Y	F	
2-6	8	Y	Y	R	
2-7	N.A.	N	N	E	strongest: 40" offset to S from P2 center through Pass 2 line
2-8	7	W	W	F	
2-9	16	Y	Y	R	
2-10	13	Y	Y	R	
2-11	9	Y	Y	R	
2-12	4	Y	Y	R	
2-13	2	W	Y	R	strongest: P1 center
2-14	13	W	W	F	
2-15	11	N	Y	R	
2-16	7	Y	Y	R	
2-17	N.A.	N	N	N.A.	
2-18	16	W	W	R	
2-19	4	W	W	F	
2-20	8	Y	Y	E	strongest: 30" offset to NE from P1 center through Pass1 line
2-21	9	Y	Y	F	
2-22	11	Y	N	F	
2-23	15	Y	Y	R	
2-24	15	W	W	F	
2-25	16	W	W	E	strongest: 20" offset to W from P1 center through Pass1 line
2-26	15	W	W	F	
2-27	2	Y	Y	F	
3-1	8	W	Y	R	
3-2	5	Y	Y	R	
3-3	12	W	W	E	strongest: 15" offset to W from P1 center through Pass1 line
3-4	N.A.	W	W	N.A.	
3-5	4	Y	Y	E	strongest: 9" offset to SW from P1 center through Pass1 line
3-6	14	W	W	R	
3-7	14	W	W	F	
3-8	5	Y	Y	F	
3-9	12	Y	Y	R	
3-10	14	W	W	R	

Appendix E Photos of "UXO-Like" Clutter Items Using LD2 Criteria

(1-1)

(1-2)

(1-4)

(1-7)

(1-15)

(1-19)

(1-22)

(1-29)

(1-32)

(1-33)

(1-35)

(1-38)

(1-40)

(1-46)

(1-47)

(1-51)

(1-55b)

(1-56)

(1-60)

(2-2)

(2-3)

(2-5)


2-42
2-42
Fragment
(large)

(2-18)


2-16
2-16
Fragment
(medium)


3-62
Fragment
(medium)


3-6
Fragment
(medium)

(3-8b)

(3-5b)

(3-8b)

References

[1] C-C. Chen, M.B. Higgins, K. O'Neill and R. Detsch, "UWB Fully-polarimetric GPR Classification of Subsurface Unexploded Ordnance", *IEEE Transactions on Geoscience and Remote Sensing,* Vol. 39, No.6, pp.1221-1230.

[2] M.B. Higgins, C.-C. Chen and K. O'Neill, "Improvement of UXO Classification Based on Fully-Polarimetric GPR Data," *USA UXO/Countermine Forum*, New Oleans, April, 2001.

[3] C-C. Chen and L. Peters Jr., "Buried Unexploded Ordnance Identification via Complex Natural Resonances",*IEEE Transaction on Antennas and Propagation* , vol. AP-42, pp. 1645-1654, Nov. 1997.

[4] Tyndall AFB Final ESTCP Report

[5] Blossom Point Final ESTCP Report

[6] J. L. Salvati,C-C. Chen and J. T. Johnson "Theoretical Study of a Surface Clutter Reduction Algorithm", *Proceeding of IGARSS*, July, 1998.

[7] Inder J. Gupta, Andria van der Merwe and C.-C. Chen, " Extraction of Complex Resonances Associated with Buried Targets", *Proceeding of SPIE* 1998.

[8] J.D. Young, "Target Imaging from Multiple Frequency Radar Returns," Ph.D. Dissertation, The Ohio State University, Columbus, June 1971.

[9] J.D. Young, K.A. Shubert and D.L. Moffatt, "Synthetic Radar Imaginery," *IEEE Transaction on Antennas and Propagation* , vol. AP-24, May. 1976.

[10] S. Nag and L. Peters Jr., "Radar Image of Penetrable Targets Generated from Ramp Profile Functions," *IEEE Transaction on Antennas and Propagation* , vol. AP-49, pp. 32-40, Jan. 2001.

[11] See numerous classic treatments of scattering from a long cylindrical reflector, e.g. R.F. Harrington, "Time-harmonic Electromagnetic Fields," Chapter 5, McGraw-Hill, Inc. 1961